

Regional Profiling of Abnormal Protein Expression & Post Translational Modifications in Glioblastoma

By Artur Kocon

Supervisors: Dr Wayne Carter, Dr Ruman Rahman, Dr Stuart Smith

UNIVERSITY OF NOTTINGHAM

Abstract

Glioblastoma is one of the most common brain tumours that is associated with poor prognosis and median survival of 12 to 15 months. Classed as WHO grade IV, glioblastomas are highly aggressive tumours that quickly proliferate and diffusely infiltrate surrounding brain tissue. Current treatments of glioblastoma are often ineffective and even with total resection, tumours recur with more aggressive sub-clonal populations of malignant cells. One of the main characteristics of glioblastoma is its highly heterogeneous nature and acquirement of somatic mutations advantageous to tumour growth and suppression of apoptotic pathways. Pathogenesis of malignant brain tumours as well as mode of its transformation to a more aggressive phenotype is still largely unknown. Although genomic studies in brain tumours have elucidated a plethora of genetic markers associated with the subtypes of the disease and identified key gene regulators, only a few have been utilised in a clinical setting. One of the emerging approaches to study glioblastomas is by investigation of the active proteome that drives the disease and contributes to its aggressive nature. Genomic and proteomic studies have suggested that genes and proteins are both selectively up and down regulated in various tumour regions. Furthermore, through activation of specific pathways via post translational modifications of proteins such as phosphorylation, glioblastomas create an intricate network of signalling pathways which favour tumour growth and proliferation. In this study, we aimed to investigate abnormal signalling across distinct tumour sites which include tumour core, tumour rim and invasive margin of glioblastoma. Using glioblastoma tumour tissue, we utilised a number of proteomic techniques to investigate abnormal protein expression and post translational modifications. We found that protein expression was highly variable and distinct amongst tumour regions with some key regulatory proteins such as cytosolic superoxide dismutase, microtubule associated protein two and protein-L-isoaspartyl methyltransferase being heavily downregulated. We have also observed significant changes in activation of transcription factors and kinases that could drive malignant progression of glioblastoma tumour. Furthermore, we have evaluated efficacy of cannabidiol and s-adenosylmethionine as therapeutic agents in inhibition of proliferation. Our findings indicate that cannabidiol could act via G-protein-coupled receptor 55 and serotonin receptor type 1A to elicit its antiproliferative effects. However, further studies are required to clarify efficacy and targets of these compounds.

Table of Contents

| | |
|--|----|
| Abstract | 1 |
| Table of Contents | 3 |
| List of Abbreviations | 6 |
| 1 Introduction | 10 |
| 1.1 Post Translational Modifications | 12 |
| 1.1.1 Phosphorylation..... | 13 |
| 1.1.2 Methylation..... | 15 |
| 1.1.3 Acetylation | 16 |
| 1.2 Tumours of the Central Nervous System | 17 |
| 1.2.1 Glioblastoma..... | 18 |
| 1.3 Glioblastoma Heterogeneity | 18 |
| 1.4 GBM Pathology | 21 |
| 1.4.1 Hypoxia..... | 21 |
| 1.4.2 Angiogenesis | 24 |
| 1.4.3 Reactive Oxygen Species & Oxidative Stress Response | 26 |
| 1.5 GBM Signalling Pathways..... | 27 |
| 1.5.1 Growth Factors..... | 27 |
| 1.5.2 Epidermal Growth Factor Receptor | 29 |
| 1.5.3 Platelet Derived Growth Factor Receptor..... | 30 |
| 1.5.4 PI3K/Akt signalling | 31 |
| 1.5.5 Ras/Raf/MAPK..... | 32 |
| 1.5.6 P53 mutations..... | 33 |
| 1.5.7 Prognostic Mutations of IDH & MGMT | 33 |
| 1.6 Alternative Treatments of GBM..... | 34 |
| 1.6.1 Endocannabinoid System in Glioblastoma | 35 |
| 1.6.2 S-adenosyl Methionine Methyl Donor & Homocysteine/Methionine Cycle in Cancer & Possible Treatment Options | 36 |
| 1.7 Aims of the Study | 41 |
| 2 Methods | 42 |
| 2.1 Preparation of Buffers & Other Reagents | 42 |

| | | |
|--------|--|----|
| 2.2 | Samples | 44 |
| 2.3 | Sample Homogenisation..... | 46 |
| 2.4 | Cellular Fractionation..... | 46 |
| 2.5 | Protein Quantification..... | 47 |
| 2.6 | Protein Precipitation with Acetone..... | 48 |
| 2.7 | SDS-PAGE | 48 |
| 2.7.1 | Sample Preparation for 1D SDS-PAGE | 48 |
| 2.7.2 | Preparation of Pre-cast Gels..... | 49 |
| 2.7.3 | Hand-casting Polyacrylamide Gels for 1D- & 2D-PAGE..... | 49 |
| 2.7.4 | Running 1D-PAGE | 51 |
| 2.8 | 2D-PAGE | 51 |
| 2.8.1 | Protein Solubilisation & Isoelectric Focusing..... | 51 |
| 2.8.2 | Running 2D-PAGE Gels..... | 52 |
| 2.9 | Gel Staining..... | 53 |
| 2.9.1 | Pro-Q Diamond Staining | 53 |
| 2.9.2 | Colloidal Blue Staining..... | 54 |
| 2.9.3 | Silver Staining..... | 54 |
| 2.10 | Mass Spectrometric Analysis | 55 |
| 2.11 | Western Blotting..... | 55 |
| 2.12 | Staining PVDF membranes..... | 57 |
| 2.13 | Immuno-Detection of Proteins..... | 57 |
| 2.14 | Detection of Oxidative Stress with OxyBlot™ Kit..... | 58 |
| 2.15 | Quantification of Proteins on Gels & PVDF membranes..... | 59 |
| 2.16 | Normalisation of Protein Expression..... | 59 |
| 2.17 | Milliplex MAP Assays..... | 60 |
| 2.18 | Cell Culture | 62 |
| 2.18.1 | Media Preparation & Cell Maintenance | 62 |
| 2.18.2 | Seeding Cells from Frozen | 62 |
| 2.18.3 | Passaging Cells | 63 |
| 2.18.4 | Counting Cells..... | 63 |
| 2.18.5 | Treating Cells..... | 63 |
| 2.18.6 | Cell Proliferation Assay with MTT..... | 65 |
| 2.19 | Statistical analysis | 65 |
| 3 | Results | 66 |

| | | |
|-------|---|-----|
| 3.1 | 1D-SDS PAGE | 66 |
| 3.1.1 | 1D-PAGE Analysis of Proteins with Colloidal Blue Total Protein Staining | 67 |
| 3.1.2 | 1D-PAGE Analysis of Proteins with Pro-Q Diamond Total Phosphorylation Staining..... | 72 |
| 3.2 | 2D-PAGE | 78 |
| 3.3 | Mass Spectrometry analysis | 84 |
| 3.4 | Western Blotting | 87 |
| 3.5 | Redox Regulation & Oxidative damage..... | 96 |
| 3.6 | Milliplex Phosphorylation Assay..... | 102 |
| 3.7 | U87 Cell Line Study | 108 |
| 4 | Discussion | 118 |
| 4.1 | Assessment & Evaluation of Proteomic Methods Used..... | 118 |
| 4.2 | Role of Energy Metabolism Enzyme & Use of Housekeeping Protein GAPDH in GBM | 121 |
| 4.3 | Cytoskeletal Associated Proteins in GBM | 125 |
| 4.4 | Redox Response & Repair Enzymes | 126 |
| 4.5 | Transcription Factors..... | 129 |
| 4.6 | CBD Treatment..... | 131 |
| 5 | Conclusion..... | 132 |
| 6 | References..... | 134 |
| 7 | Appendix | 161 |

List of Abbreviations

1D-PAGE – One Dimension Poly-acrylamide Gel Electrophoresis
2D-PAGE - Two Dimension Poly-acrylamide Gel Electrophoresis
2DE – Two-dimensional electrophoresis
5-ALA – δ -Aminolaevulinic Acid
5-HT(1A) – Serotonin Receptor (Type 1A)
ADAM – α -disintegrating and Metalloprotease
ADP – Adenosine Diphosphate
AEA – Anandamide
AG – Arachidonoylglycerol
ANOVA – Analysis of Variance
APS – Ammonium Persulphate
ATP – Adenosine Triphosphate
Bcl-2 – B-cell Lymphoma 2
Bcl-x_L – B-cell Lymphoma-extra Large
BHMT - Betaine-homocysteine Methyltransferase
BSA – Bovine Serum Albumin
cAMP – Cyclic Adenosine Monophosphate
CAT – Catalase
CB1/2 – Cannabinoid Receptor Type 1 and 2
CBD – Cannabidiol
CBS - Cystathionine Beta-Synthase
CBTRC – Children Brain Tumour Research
CHAPS – 3-[(3-cholamidopropyl)dimethylammonio]-1-propanesulfonate
CNS – Central Nervous System
CpG – Cytosine-Phosphate-guanine
CREB – cAMP Response Element Binding
CSF – Cerebrospinal Fluid
DGL- α – Diacylglycerol Lipase Alpha
DNA – Deoxyribonucleic Acid
DNPH – 2,4-Dinitrophenylhydrazine
DTT - Dithiothreitol

EDTA – Ethylenediaminetetraacetic Acid
EGF – Epidermal Growth Factor
EGFR – Epidermal Growth Factor Receptor
FAAH – Fatty Acid Amide Hydrolase
FGF – Fibroblast Growth Factor
FGFR – Fibroblast Growth Factor Receptor
G3P – Glyceraldehyde-3-phosphate
GAPDH – Glyceraldehyde 3-phosphate Dehydrogenase
GBM – Glioblastoma Multiforme
GPR55 – G Protein-coupled Receptor 55
GPx – Glutathione Peroxidase
GTP – Guanosine Triphosphate
HAT – Histone Acetyltransferases
HBSS – Hanks' Balanced Salt Solution
HCL – Hydrochloric Acid
HDAC - Histone Deacetylases
HGP – Human Genome Project
HIF – Hypoxia Inducible Factor
HKP – Housekeeping Protein
HRP – Horseradish Peroxide
IDH – Isocitrate Dehydrogenase 1
IEF – Isoelectric Focusing
IGF – Insulin-like Growth Factor
IGFR – Insulin-like Growth Factor Receptor
IPG – Immobilised pH Gradient
JAK – Janus Kinase
JNK – c-Jun N-terminal Kinases
KO – Knock Out
LDS – Lithium Dodecyl Sulphate
MAGL – Monoacylglycerol Lipase
MAP – Microtubule Associated Protein
MAPK – Mitogen Activated Protein Kinase
MAT – Methionine Adenosyltransferase

MEK - Mitogen Activated Protein Kinase Kinase
 MGMT – O⁶-methylguanine DNA Methyltransferase
 MOPS – 3-(N-morpholino)propane-sulfonic Acid
 MS/MS – Tandem Mass Spectrometry
 MTT – 3-(4,5-dimethylthiazol-2-yl)-2,5-diphenyltetrazolium Bromide
 mRNA – Messenger Ribonucleic Acid
 ncRNA – Non-coding Ribonucleic Acid
 NF1 – Neurofibromatosis type 1
 NFκB – Nuclear Factor Kappa-light-chain-enhancer-of-activated B cells
 OEA – Oleoylethanolamide
 PAGE – Polyacrylamide Gel Electrophoresis
 PBS – Phosphate Buffer Saline
 PD – Parkinson’s Disease
 PDGF – Platelet Derived Growth Factor
 PDGFR – Platelet Derived Growth Factor Receptor
 PFC – Pre-frontal Cortex
 PI3K – Phosphatidylinositol-4,5-bisphosphate 3-kinase
 PIMT – Protein-L-Isoaspartyl Methyltransferase
 PPAR-γ – Peroxisome Proliferator-activated Receptor
 PRMT – Protein Arginine Methyltransferases
 PTEN – Phosphatase and Tensin Homolog
 PTM – Post Translational Modifications
 PVDF – Polyvinylidene Fluoride
 RNA – Ribonucleic Acid
 ROS – Reactive Oxygen Species
 RTK – Receptor Tyrosine Kinase
 SAH – S-adenosyl-L-homocysteine
 SAM – S-adenosylmethionine
 SAPE – Streptavidin Phycoerythrin
 SDS – Sodium Dodecyl Sulphate
 SEM – Standard Error of the Mean
 siRNA – Short Interfering Ribonucleic Acid
 SOD – Superoxide Dismutase

STAT – Signal Transducers and Activators of Transcription

TEMED – Tetramethylethylenediamine

TMZ – Temozolomide

TSC2 – Tuberous Sclerosis Complex Two

VEGF – Vascular Endothelial Growth Factor

VEGFR – Vascular Endothelial Growth Factor Receptor

1 Introduction

Cancer is one of the leading causes of mortality and morbidity worldwide. Term cancer encompasses a broad group of diseases which can be characterised by abnormal cell division and invasion into neighbouring tissue. Uncontrollable division of abnormal cells leads to formation of tumorous tissue which can alter and destroy surrounding healthy tissue. Cancer remains as one of the major health concerns in today's world.

Investment in research has steadily paved a way for improvement in cancer management and treatment. The trends in cancer survival have been slowly increasing including lung, breast, colon or prostate cancer (National Cancer Institute, 2018). There are now multiple cancers that can effectively be treated and eliminated. However, some of the most malignant and deadly cancers including highly malignant brain tumours remain untreatable with poor prognosis and short survival. Despite their clinical importance and constantly developing research, cancer pathogenesis and progression is still very poorly understood. There is a great requirement to fill the gaps of knowledge with regards to cancer which could thereafter provide a more effective solution for cancer treatment.

In the past decade, one of key milestones in the field of biomedicine was the accomplishment of sequencing the human genome. Deciphering of the genetic sequence that creates the building blocks of life revolutionised our approach to science and served as a catalyst for more personalised medicine. Yet, in the early years of genomics, human genome project (HGP) has been met with some scepticism, arguing that it would not be feasible and mapping the whole genome would mostly yield 'junk' data that would be of no use. On the other hand, a scientist such as Renato Dulbecco firmly stood behind the idea stating that knowledge of the genome and availability of genetic information is crucial in progress of human physiology and a turning point for understanding pathology of cancer (Dulbecco, 1986). Now almost two decades later, the impact of HGP has been immeasurable leading to vast developments in medicine and technology.

Our understanding of the underpinnings of the genetic basis of disease and treatment response has become considerably more sophisticated, because of, to name a few, emerging disciplines; epigenetics, non-coding RNAs, microRNAs, transcriptomics and proteomics. Discovery of biological markers (biomarkers) of disease has had a tremendous impact on classification and treatment of disease. This has led to a new era where characterisation of the active human proteome and biomarker discovery has become one of the principal challenges in our understanding health and disease (Hibbert et al., 2018).

The term proteomics refers to large scale characterisation of proteins encoded by the genome whereas proteome can be defined as the complete protein content of a cell or a tissue. It serves as a complementary system to genomics where gaps of genetic research, such as defining physiological outcome of genes, can be succeeded and further decoded. As a result, transcribed proteins provide a more informative medium for cellular function (Hood and Rowen, 2013). Examination of the proteome also provides an insight into the cell-type expression patterns, protein localization, protein abundance, various protein isoforms, post-translational modifications (PTMs) and protein-protein interaction. Because proteins are subject to constant environmental and structural changes by various substrates they often harbour significant functional changes in their lifespan, and so, the extent of the proteome is considerably larger than that of the genome (Srivastava and Creek, 2018). This could be also considered as one of the downsides of proteomics as the sheer number of protein species and families that are involved in functionality of the cell makes it difficult to establish the cause and effect of various protein-protein interactions and all-encompassing studies are necessary to delineate functionality of a protein. Functional proteomics focuses on protein-protein interactions and interpretation of biological function of unknown proteins at the molecular level. Understanding protein functions and following the molecular mechanisms within cells are one of the key ways by which cell's dynamic environment and intracellular hierarchy can be defined. Many proteins are in nature pleiotropic and often have several allocated functions in cellular pathways. Henceforth, characterisation of the entire proteome would be a cumbersome task that is almost certainly unattainable with current technology.

Nevertheless, similarly to the HGP, several projects have been established in order to catalogue and map the human proteome such as Human Proteome Project, Human Protein Atlas and ProteomeXchange consortium, which facilitates sharing of proteomic data (Karmali et al., 2010; Kim et al., 2014; Wilhelm et al., 2014). Compiling an extensive map of the proteome could enable and initiate a more efficient path for proteomic research and understanding of various cancers and other diseases. Ideally, through utilizing both, genomic and proteomic information, a more comprehensive picture of human physiology as well as pathology can be achieved to offer more personalised medicine.

1.1 Post Translational Modifications

The majority of proteins are actively modified through enzymes, other proteins or various substrates. Post-translational modifications (PTMs) are a carefully orchestrated events that influence protein structure as well as activity and coordinate localisation and interactions with other proteins thereby maintaining cellular homeostasis. Intracellular modification of proteins is one of the major ways by which signals for protein transcription, cell division, growth and many more functions are controlled. PTMs, through binding to a specific amino acids and sites, are able to change the properties of proteins to elicit effect and change their localisation and function. There is a plethora of signal transduction effectors which are responsible for such modifications to generate complex signalling circuitry that is necessary for quick cellular responses. There are many types of PTMs in humans but some of the most common ones include phosphorylation, methylation, acetylation, ubiquitination, glycosylation and sumoylation though there is an excess of many more. With the wide range of possible PTMs, the proteins and further down, DNA expression, can be affected in a number of ways to elicit a specific response and alter cells' behaviours. While crucial in normal cell homeostasis, studies on PTMs have also elucidated the importance of protein modifications as one of the hallmark features in a tumours' ability to adapt and enhance proliferation (Martín-Bernabé et al., 2017). Aberrations of PTMs are highly implicated in cancer pathogenesis, progression

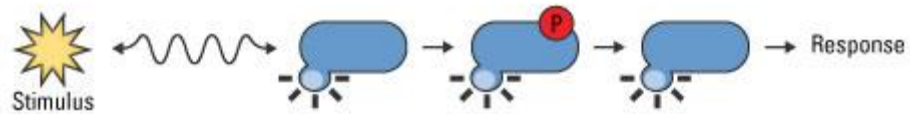
and response to treatment therefore it is of high importance to understand the links between target proteins and their regulation in the cellular environment.

1.1.1 Phosphorylation

The most abundant modification in eukaryotic cells is the addition of phosphoryl group to other substrates. This process is termed phosphorylation and is responsible for activation/inactivation of many important proteins within a cell. The transfer of phosphoryl from high energy molecule to a lower energy group is catalysed by kinases, one of the largest groups of catalytic enzymes in eukaryotic cells and is a common source of cancer-promoting mutations in brain tumours such as GBM (Wagih and Bader, 2013). The reversible process of phosphorylation primarily affects serine, threonine or tyrosine residues of proteins. This is a reversible process which can be 'switched on and off' when necessary by specific enzymes. While kinases attach the phosphoryl groups, phosphatases are required for de-phosphorylation of proteins. Phosphorylation is mostly facilitated by transfer of γ -phosphoryl group from an ATP molecule to a nucleophilic side chain of the protein, though transfer of phosphoryl group from GTP by GTPases in a similar manner is also possible.

Phosphorylation of substrates is a major way by which signal transduction pathways are activated in response to intracellular and extracellular stimuli. Binding of a ligand to a substrate or its cleavage often act as a cue for phosphorylation to take place which in turn activates downstream targets or other kinases leading to linear signal transduction or a transduction cascade to elicit specific response (Figure 1-1).

Linear signal transduction



Signal transduction cascade

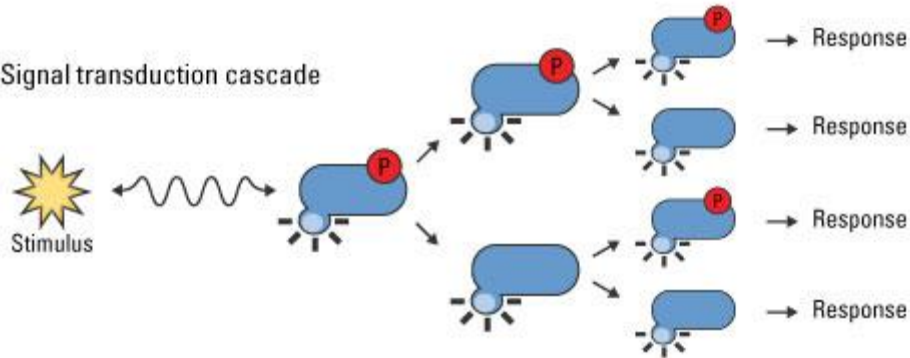


Figure 1-1 | Signal transduction acts in response to external or internal stimuli to elicit a given response in either linear signal transduction or transduction cascade. In linear transduction only specific downstream effectors are activated whereas signal transduction pathway can yield a much larger global cellular response by amplification of the initial stimuli through activation of many various kinases. Image by: ThermoFisher Scientific.

The importance of protein phosphorylation in human physiology and pathology is well established and it has been shown that various cellular events including cell division, movement, survival and apoptosis are regulated by phosphorylation (Shchemelinin et al., 2006). Tight regulation of protein phosphorylation by protein kinases and phosphatases allows cells to properly function and progress through the cell cycle. Interaction between proteins via cellular phosphorylation creates an intricate circuitry signalling network governing cellular homeostasis. Disruption of these networks by means of extra-cellular events, substrates and genetic mutations is a common feature of cancer and other diseases (Olow et al., 2016).

1.1.2 Methylation

The progress and expansion of epigenetics has led to a lot of interest dedicated to methylation and its importance in genetic expression. There is much emphasis put on DNA methylation which serves as an epigenetic signalling tool able to turn specific genes 'on' or 'off'. Methylation of DNA is facilitated by a family of enzymes called DNA methyltransferases (DNMTs) which transfer the methyl group from a primary methyl donor S-adenosyl methionine (SAM) to the cytosine residues, dominantly at cytosine-phosphate-guanine (CpG) sites (Etcheverry et al., 2010). DNA sequences rich in guanine and cytosine (G-C) and CpG, referred to as CpG islands, are dispersed throughout the genome and are often located next to gene promoting regions (Deaton and Bird, 2011). These regions are generally not methylated in healthy tissue, however it has been postulated that DNA methylation commonly occurs in ageing and could serve as a biomarker for senescence that is associated with neurodegenerative and functional decline (Bocklandt et al., 2011; Horvath and Ritz, 2015; Marioni et al., 2015). It is possible that reduced gene expression and decrease in certain proteins in ageing is associated with increased methylation of CpG islands. In addition, methylation patterns, responsible for silencing of certain tumour-suppressor genes, have been associated with cancer development and progression (Easwaran et al., 2012; Estécio and Issa, 2011). Abnormal methylation patterns of CpG islands can be generally associated with loss of function of various genes therefore leading to altered expression and abnormal signalling of major protein pathways. This mechanism often allows the tumour to escape apoptosis which in turn leads to more malignant phenotype. The role of epigenetic mechanisms and their deviations from norm is closely linked to tumour development and progression. The landscape of epigenetic changes in cancer is vast and greatly contributes to heterogeneity of the disease.

1.1.3 Acetylation

Acetylation, defined as the covalent addition of an acetyl group to the ϵ -amino groups of lysine residues has gained recent recognition as an important post-translational modification in modulating protein function (Carrozza et al., 2003). It is a reversible process that is catalysed by the histone acetyltransferase (HAT) family of enzymes utilising acetyl-coenzyme A as a donor of the acetyl group (Soeda et al., 2015). Accordingly, the reverse process is catalysed by enzymes within the histone deacetylase (HDAC) family (Soeda et al., 2015). Classically, lysine acetylation is considered to be a PTM that acts at histone proteins and additional nuclear targets, regulating gene transcription. However, recent studies have identified a variety of targets within the cytosol that are acetylated (Choudhary et al., 2009). These non-histone targets are implicated in a variety of cellular responses many of which are implicated in cancer (Kim et al., 2006).

The capacity of a tumour cell to migrate and degrade extracellular matrix is a critical property in describing invasive potential of the disease (Demuth and Berens, 2004). Reorganisation of the cytoskeleton is vital in forming of organised cell protrusions at the cell-front known as invadopodia (Fife et al., 2014) and the modification and polymerisation of microtubule associated proteins such as α -tubulin and cortactin. Recent evidence has suggested that the de-acetylation of α -tubulin and cortactin by HDAC6 confers both, a non-transformed and cancer cells with an increased migratory capacity in a metastatic breast cancer model (Castro-Castro et al., 2012). Furthermore, inhibition of HDAC6 reduced tumour migration and invasive capacity.

Limited data exists on the role of acetylation in GBM and the invasive phenotype, however a recent study has shown increased expression of HDAC6 in the stem-like subpopulation of GBM; cells that possess a much greater migratory capacity than their more differentiated counterparts (Yang et al., 2018).

1.2 Tumours of the Central Nervous System

Tumours of the central nervous system (CNS) encompass a wide range of brain and spinal cord neoplasms that arise from a variety of cell lineages. Collectively, CNS tumours represent approximately 1.6% of all cancer diagnoses and contribute to 2.5% of cancer deaths worldwide (Bray et al., 2018). Though relatively rare, mortality and morbidity associated with CNS tumours is disproportionately high. In UK alone, tumours of the CNS are the leading causes of cancer death in children and young adults below the age of 25 (Cancer Research UK, 2018).

CNS tumours are classified depending on their aggressiveness and behaviour, from benign tumours, WHO grade I – II, to malignant tumours, WHO grade III – IV (Louis et al., 2016). Historically, diagnosis and classification of head and neck tumours was principally based on histopathological features of the tumour and on cell of origin of these cancers. Nomenclature of most CNS tumours has been derived from presumed histogenesis of the tumour i.e. astrocytomas arising from astrocytes, ependymoma from ependymal cells, glioma from glial cells. However, advances in human genomics and epigenetics have led to identifications of genetic alterations involved in tumorigenesis and cancer pathophysiology. This allowed for further, more detailed classification of CNS tumours and improved, more tailored way of treatment for patients with brain tumours highlighting the importance of multi-layered approach to characterisation of the disease (Louis, 2012).

With the continuous development in human genomics and molecular diagnostics, the paradigm of diagnosis has shifted from identification of tumours based on their histopathology towards a more phenotypic approach. This is not to say that histological diagnosis has been replaced but rather enriched by incorporation of molecular characteristics into brain tumour diagnostics. For example, status of methylation of MGMT promoter gene in glioma patients serves as a prognostic marker for efficacy of TMZ treatment and patient survival (Hegi et al., 2005). Similarly, studies into lower grade brain tumours harbouring *BRAF-V600* mutations suggest prospective clinical benefit for treatment of brain

tumours with BRAF and other kinase inhibitors (Preusser et al., 2016). The identification of molecular changes in those tumours is therefore crucial for better targeted treatment.

1.2.1 Glioblastoma

Gliomas are the most frequent of the CNS malignancies, representing over 70% of all malignant brain tumours. Of those, glioblastomas (GBM) are the most common and deadliest type of gliomas (Verma, 2009). Classified as WHO grade IV astrocytomas, GBMs are neuroepithelial tumours that are highly heterogeneous and rapidly evolving. They pose one of the greatest challenges for patients and clinicians in terms of treatment and management. The prognosis of patients diagnosed with GBM is very bleak as the median survival for the disease approximates at 12 – 15 months, even after neurosurgical resection and rigorous treatment with radio- and chemo-therapy (Villanueva-Meyer et al., 2017). The lethality of GBM tumours is increased by their versatility and aggressive microvascular proliferation leading to its poor prognosis and high mortality rate. Complete eradication of the tumour is highly unlikely as GBM tumour often spreads into surrounding brain tissue. As a result, recurrence is often inevitable and the neoplasms usually relapse within 2 cm of the primary tumour site (De Bonis et al., 2013). The recurrence of the tumour tends to be more aggressive with higher resistance to treatment posing greater risk to patients (Huang et al., 2008).

1.3 Glioblastoma Heterogeneity

GBMs remain as one of the most complex of brain neoplasms in terms of histology and classification. There is no single feature that differentiates high grade gliomas from lower grade malignancies and initial diagnosis relies on fulfilment of WHO histological feature criteria. GBM's can be defined by several

features such as high cellular pleomorphism, nuclear atypia, necrosis and endothelial proliferation (Louis et al., 2007). This however classes GBMs as single entity disease and overlooks the distinct molecular features that play a major part in GBM pathology. The vastly evolving nature of GBMs and versatility to adapt to changing microenvironment is what drives its fast growth and diffuse proliferation into neighbouring tissue (Sottoriva et al., 2013; Stratton et al., 2009; Q. Wang et al., 2017b). Acquisition of somatic mutations with time and across various tumour sites makes it difficult to define a single biomarker that is specific to GBM. Identification of specific therapeutic targets is often more viable but due to GBMs high heterogeneity, sub-clonal populations with advantageous mutations conferred by chemotherapy or radiotherapy emerge and predominate the tumour with higher resistance to therapeutic agents.

Fast growth of tumour typically results in spontaneous necrosis and quickly develops into a necrotic tumour core. Somatic mutations, suppression of cell cycle regulating genes and proteins are common events in GBM that lead to progressive pathological transformation and survival of abnormal cell populations. As an effort to improve patients outcome and survival, research has mainly focused on identifying molecular and cellular elements which contribute to GBM evolution and progression (Liu et al., 2006).

GBM can develop in one of two ways either from pre-existing low-grade astrocytoma or *de novo* without prior malignant precursors. Primary GBM are the most frequent accounting for approximately 90% of all GBM cases. Secondary GBM are quite rare and usually develop from low grade astrocytomas, mostly affecting patients below age of 45 (Ohgaki and Kleihues, 2013). Both tumours are morphologically indistinguishable but have the same devastating outcome. However, genomic analysis of gliomas and advancements in molecular technology have highlighted unique development of these tumours and differences in their acquired molecular mutations.

Microarray profiling and next generation sequencing has provided a further delineation of GBM subtypes expanding the classical histology/grade based glioma diagnosis, (Phillips et al., 2006). In their study, Philips et al. (2006) investigated grade II and grade IV gliomas and identified expression of genes associated with proneural, mesenchymal and proliferative markers. These

markers are a useful tool in identifying tumour aggressiveness and provide a valuable indicator of the prognostic outcome of the disease. Expression of angiogenic and wound healing markers in mesenchymal and proliferative tumours has been associated with poor prognosis whereas proneural subtype had gene expression that was more similar to normal brain gene expression which is associated with better prognosis.

Amplifications of genes associated with growth factor signalling pathways such as EGF (epidermal growth factor), PDGF (platelet derived growth factor), FGF (fibroblast growth factor) are commonly found in GBM and are associated with more aggressive disease (Dunn et al., 2000). Expression of those markers is highly implicated with many signalling cascade events that influence angiogenesis, cell proliferation and endothelial cell migration and are pivotal for cellular processes. Mutations of genes related to cell cycle control pathways such as CDK4, MDM2 and P53 have also been frequently observed in GBMs and alteration of those often leads to disruption of cell arrest cycle and enhancing survival (Biernat et al., 1997; Lubanska and Porter, 2017; McDonald et al., 2002).

Several studies have reported altered protein regulation between different grades of gliomas using proteomics-based technologies. Ren Tong et al. (2016) conducted an iTRAQ based quantitative proteomics study to compare the proteomic profile of different grades of astrocytoma and reported that several proteins such as metalloproteinase 9 and metalloproteinase inhibitor 1 were upregulated in GBMs. Other proteins including fibulin 2 and fibulin 5 were downregulated in higher grades which was associated with advanced clinical stage (Ren et al., 2016). Studies using label based quantitative proteomics identified heat shock protein 27 (HSB1/HSP27) as a probable predictive factor of poor GBM prognosis with high expression observed in GBM with relatively short survival, in addition to proteins that were found to be dysregulated between different grades of glioma (Gimenez et al., 2015). Other studies have suggested upregulation of proteins in major pathways such as glycolysis, lactate metabolism, oxidative phosphorylation, apoptosis and cell cycle. These reports suggest that proteomics is a valuable genome-wide platform to study differential

protein regulation and that this plays an important role in GBM pathophysiology of key cellular pathways.

1.4 GBM Pathology

Delineation of GBM with regards to protein expressions is still poorly understood. Highly heterogeneous tumours, such as GBM, have very distinctive progression with numerous molecular alterations, yet histologically they are often classed as one entity disease. Many studies of GBM suggest that the abnormal signalling from different sites of the tumour greatly contributes to its ability to evade apoptosis, proliferate, spread and resist treatment. Many signalling molecules involved in GBM are pleiotropic and play an important role in various cellular and pathological functions (Mao et al., 2013). Investigation of abnormal protein activities can lead to better therapeutic targets and more defined diagnosis of the disease. It is therefore important to address how the signalling networks across GBM tumour contribute to the cellular response. Identifying major signalling pathways in different tumour regions and knowing the intricate processes in which proteins are activated can provide clues regarding tumour invasion but also define targets for novel, combined personalised treatments.

1.4.1 Hypoxia

Deprivation of oxygen in highly cellular regions of a tumour is a common feature among many solid cancers. Lack of adequate oxygen supply to cells caused by quick tumour expansion and consequent poor diffusion of oxygen leads to severe hypoxic conditions. Adequate oxygen supply to cells is crucial for production of ATP required for normal metabolic function. Oxidative phosphorylation required in cellular respiration is a powerful tool for cells to produce energy required for most cellular processes. Aerobic oxidation is a more

efficient and preferred system of a healthy cell to produce ATP from available oxygen. However, the lack of oxygen in cancers leads to high rates of anaerobic glycolysis especially in the hypoxic areas of the tumour and leads to cellular shift to glycolytic phenotype and preferential use of glycolytic pathway (Liberti and Locasale, 2016; Warburg, 1956). Anaerobic glycolysis utilises glucose to produce lactate and fewer ATPs are produced. Glycolysis is able to produce ATPs at a faster rate which could explain why cancer cells prefer an anaerobic respiration over oxidative phosphorylation even in the presence of oxygen (Zheng, 2012).

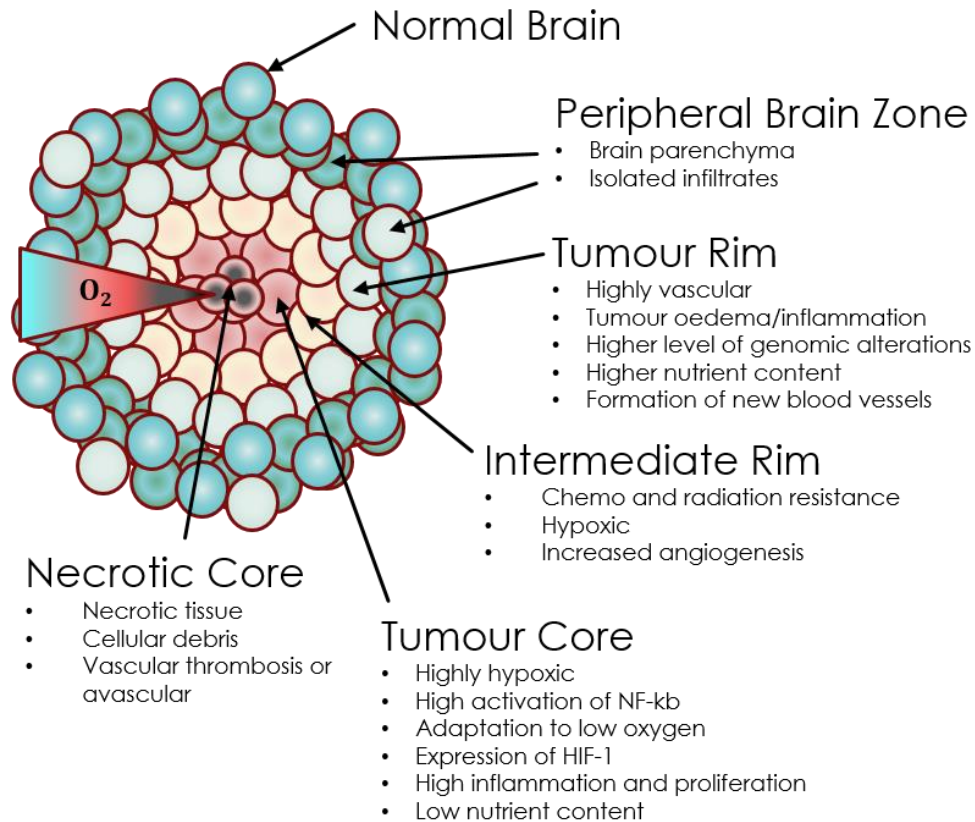


Figure 1-2/ Distribution of tumour cells in GBM and pathological features associated with distinct tumour areas caused by hypoxic states and decrease of oxygen content across the tissue
 Formation of necrotic core in the centre of a tumour leads to low oxygen supply. The consequent lack of nutrients leads to cells branching out and proliferating towards less hypoxic areas and more oxygenated areas. In GBM 'pseudopalisading' of cells is often observed where cells position themselves away from the tumour core. Increased expression of transcription factors such as HIF-1 and increased levels of VEGF lead to high vascularisation of tumour at the tumour rim. Additionally, the oxidative stress resulting from hypoxic conditions and dysregulation of redox proteins are one of the possible ways by which GBM cells acquire somatic mutations that allow them to survive and evade apoptosis. Image adapted from *The Three-Layer Concentric Model of Glioblastoma: Cancer Stem Cells, Microenvironmental Regulation and, Therapeutic Implications* by Persano L., et al., 2011 *The Scientific World Journal*, 11(18):1829-41,

Change of oxygen levels can induce a variety of responses in expression or suppression of homeostasis regulatory genes that promote cell survival. Molecular markers of hypoxia such as HIF and VEGF are key regulators of the adaptive response to low oxygen supply (Ziello et al., 2007). Expression of HIF-1 gene triggered by hypoxic states is one of the key pathway regulators required for formation of new blood vessels and supply of oxygen to surrounding tumour tissue and proliferation of cancer tissue (Rong et al., 2006). As shown in Figure

1-2, the lack of oxygen inside of the tumour leads to clonal expansion of cells into more oxygenated areas where more nutrients are available. This often leads to opportunistic mutations that are generally different from the hypoxic core cells and results in higher differentiation of the oncogenic cells in tumour periphery and in more vascularised areas (Persano et al., 2011a). Additionally, areas of necrosis are a common feature of GBM in the avascular low-oxygenated areas surrounded by “pseudopalisading” hyper-cellular regions.

In hypoxic regions of the tumour HIF-1 is triggered, successively stimulating VEGF expression. HIF-1 complex composed of HIF-1 α and HIF-1 β can bind to DNA and initiate gene transcription. Several gene targets are upregulated by HIF-1 and promote transcriptional activity. Furthermore, increased transcription of VEGF through HIF-1 α can be achieved through PI3K/Akt and/or Ras/Raf pathway. Studies show that inhibiting PI3K/Akt and Ras/Raf pathway decreases HIF-1 binding to DNA although the exact processes by which Akt is able to initiate HIF-1 α binding is unknown (Kaur et al., 2005).

1.4.2 Angiogenesis

What distinguishes GBM from lower grade tumour is its ability to infiltrate the surrounding tissue. Areas of increased diffuse proliferation at the infiltrating edge and presence of necrotic core surrounded by microvascular hyperplasia of cells are key defining structures in the histopathological diagnosis of glioblastoma (Rong et al., 2006). The feature described as ‘pseudopalisading’, where necrotic core is surrounded by neoplastic cells, seems to be unique to malignant gliomas and carries a grim prognosis for patients. The highly compact regions are associated with low oxygen levels and increased levels of vascular endothelial growth factors (VEGF) (Kaur et al., 2005). Expression of VEGF is suggested to be one of the adaptive features of malignant tumour to the hypoxic regions. Oxygen supply must be maintained for normal cellular function. However, through lack of adequate supply of oxygen, the neoplastic tissue can

signal the surrounding tissue to form new blood vessels. This leads to a cascade of events in the cell and surrounding environment leading to angiogenesis, formation of new blood vessels. Angiogenesis is a key complex biological step in the vascular proliferation of GBM and is tightly regulated. Nonetheless, the accelerated proliferation of GBM suggests that it is able to evade the regulation of angiogenesis to favour tumour growth. Hypoxia mediated through Hypoxia-inducible factor-1 (HIF-1) is thought to be the main mediator of angiogenesis in GBM (Krock et al., 2011).

Paracrine interactions between cells and interactions of succeeding extracellular matrix molecules with endothelial cells can create cellular response such as angiogenesis. Angiogenesis is a complex process which relies on proteomic and mitogenic signals. The hypoxic state of necrotic regions of the tumour results in increased transcription of growth factor such as VEGF. VEGF consists of seven different homologues, with VEGF-A being the most prominent serving as mitogenic, anti-apoptotic and survival signal for endothelial cells (Reardon et al., 2008). VEGF-A binding to its receptor results in intracellular signalling transduction cascade and activation of many enzymes. This activation through many pathways, including PI3K/Akt can promote cell proliferation and survival. Moreover, activation of proteins through VEGF can lead to synthesis of enzymes responsible for extracellular matrix degradation, increased vascular permeability, and proangiogenic factors synthesis (Kowanetz and Ferrara, 2006). Raised VEGF-A expression has been commonly reported in gliomas and it correlates directly to high vascularization of the tumour and its inherent survival. This represents the means by which distinct tumour areas can influence signalling from one end to another. By cross talk between highly hypoxic regions, tumour is able to provoke formation of blood vessels around the tumour peripheral rim and augment the spread of glioma cells.

1.4.3 Reactive Oxygen Species & Oxidative Stress Response

Prolonged and acute exposure to hypoxic conditions are considered as a triggering mechanism for disruption of redox balance leading to severe oxidative damage by ROS and free radicals (Debevec et al., 2017). ROS such as peroxides, superoxides and hydroxyl radicals are a common by-product of oxygen metabolism and are produced intracellularly through multiple mechanisms. Although ROS play a vital role in mediating many physiological processes such as cell signalling and immune pathways, they are highly cytotoxic when accumulated at high concentration (Dasuri et al., 2013). Redox regulation in the brain is carefully balanced by enzymatic and non-enzymatic antioxidants which prevent oxidation of proteins and DNA. Non-enzymatic antioxidants include molecules such as glutathione, Vitamin C and E and lipoic acid and other. Enzymatic antioxidants are part of a defence system that safeguards the cells from accumulation of ROS and include SOD, CAT, GPX. Regulation of several of the antioxidant enzymes including SOD, CAT and GPX was shown to be decreased in malignant brain tumours suggesting their role in tumour pathogenesis and increased oxidative stress (Khan et al., 2010). SOD is responsible for removing superoxide radicals and consists of three isoforms, cytosolic Cu/Zn SOD1, mitochondrial SOD2 and extracellular SOD3. SOD catalyses removal of superoxide (O_2^-) by binding either to copper or zinc molecules of O_2^- and breaking it down to less reactive O_2 and H_2O_2 . Though SOD has been shown to be decreased in primary tumour it has also been suggested that increased mitochondrial SOD2 is present in recurring glioblastoma contributing to its radio-therapy resistance (Hardiany et al., 2017; Shwetha et al., 2016). The expression of mitochondrial SOD2 in recurrent GBM could therefore serve as a prognostic marker and potential therapeutic target. SOD catalyse superoxides into hydrogen peroxides, which in turn are catalysed by CAT into water and oxygen. Overexpression of certain antioxidant enzymes such as CAT can have a protective function from oxidative injury and enhance apoptotic evasion for cancer sustaining its progression (Bai et al., 1999). Co-operation between various redox molecules and enzymes maintains a carefully orchestrated balance keeping ROS in check.

The imbalance caused by substantial increase of ROS or changes in regulation of key redox enzymes can lead to pro-oncogenic factors and increase of somatic mutations in a cell. The maintenance of this system is important and dysregulations of it are commonly reported in various cancers (Alfadda and Sallam, 2012; Huo et al., 2009).

1.5 GBM Signalling Pathways

The molecular biology of GBM has been extensively studied; yet because of a high degree of both intra- and inter-tumour heterogeneity and unique development of each tumour, the active signalling archetype is still largely unknown with respect to this heterogeneity. Though genetic alterations are well known with regards to GBM, the proteome is still largely undefined. Studies in proteomics have an advantage over genomic studies as they can explore the more dynamic cell biology including its post-translational modifications which can both modify the structure and function of proteins. Moreover, many of mutated genes may not be transcribed due to epi-genetic factors and ncRNAs. Several biomarkers involved in cell signalling have been discovered and further investigation of specific protein modifications and signalling transduction is necessary to better describe GBM and begin to rationalise multiple targets for next-generation patient-tailored pharmacology. Below are some of the key mechanisms and signalling pathways mentioned in recent GBM literature considered to be a major factor in GBM malignant nature.

1.5.1 Growth Factors

Cells maintain an incessant crosstalk between each other through extracellular signals which contain biological cues about growth and cellular progression. This communication network is sustained through small

extracellular polypeptides called growth factors and mitogens. Mitogens stimulate progression of cells into G1 phase of the cell cycle and initiate subsequent division. However, cell division cannot increase the cell mass alone and growth factors are needed to initiate growth through activation of intracellular signals and control of protein synthesis, accumulation and degradation. Integration of these signals by complex circuits within cells is a vital part of tissue homeostasis and growth factors are involved in regulation of variety of cellular processes including proliferation, migration, differentiation and survival. In normal cell homeostasis, extracellular signals are attentively orchestrated to maintain the welfare of a tissue or an organism. Decisions regarding growth are therefore made through synchronisation of cells via extracellular signals and paracrine, autocrine, juxtacrine or endocrine mechanisms. Receptors on plasma membrane specific to their target growth factors are generally composed of an extracellular domain designed for ligand binding and intracellular domain capable of activating cytoplasmic targets. The initial high-affinity binding of the signalling polypeptide to a specific transmembrane receptor commences a cascade of intracellular signals resulting in an activation or repression of various subtypes of genes.

Involvement of growth factors in tumour progression has been well documented and even though aberrations of cellular homeostasis in cancer are principally instigated through somatic and germ line mutations, growth factors play a major part in oncogenic progression and clonal expansion (Witsch et al., 2010). Somatic mutations involved in selective expression and over-expression of interrelated growth factors and growth factor receptors enable cancer cells to form autocrine signalling loops (Heldin, 2012a) and lead to constitutive pathway activation (Gan et al., 2013). Research on brain tumours suggests that development of such mutations might be an early event which further facilitates propensity for somatic mutations and permits fixation of already established ones (Del Vecchio et al., 2013; Paugh et al., 2013; Uhrbom et al., 1998).

Because of their role in early tumour development and further tumour progression, growth factor receptors have been considered as a promising drug target. One of the largest family of growth factor receptors are receptor tyrosine

kinases (RTKs) such as Epidermal Growth Factor Receptors (EGFR), Platelet Derived Growth Factor Receptors (PDGFR), Vascular-Endothelial Growth Factor Receptors (VEGFR), Insulin Growth Factor Receptors (IGFR) and other.

1.5.2 Epidermal Growth Factor Receptor

EGFR is part of receptor tyrosine kinase (RTK) family. EGFR amplification is frequently observed in primary GBM and has an important role in activation of many intracellular signals. The most common EGFR variation is *EGFRvIII* that is present in over 50% of primary GBM with overexpressed EGFR (Hatanpaa et al., 2010). Deletion of exon 2-7 in this mutation causes the receptor to be truncated/shortened and results in ligand independent activity. The constant activation of the receptor leads to downstream activation of several intracellular signalling pathways that promote proliferation, survival or even motility. When activated, EGFR dimerizes and tyrosine residues in the intracellular domain are phosphorylated. This leads to further phosphorylation and activation of proteins including Phosphatidylinositol-4,5-bisphosphate 3-kinase (PI3K), Janus Kinase (JAK), Src, Ras, and many more, all of which play a major role in cell regulation. Considering the vast number of proteins that are activated via EGFR, its involvement in cancer growth is clear. Studies on mice have shown that mutations of the *EGFRvIII* can result in GBM formation (Talasila et al., 2013). Additionally, introducing an *EGFRvIII* transgene into GBM cell lines can increase tumorigenesis through elevated proliferation and reduced apoptosis (Nishikawa et al., 1994). Mutated *EGFRvIII* has been shown to increase tumour proliferation in cells of diverse origin such as lung, breast and ovarian tissues (Ebner and Derynck, 1991). Interestingly, a study by Fan *et al.* (2013) has suggested that in GBM *EGFRvIII* is positively expressed in presence of EGFR and confer to approximately 20% of the total EGFR expression. This is interesting as it could suggest that *EGFRvIII* only occurs in GBM tumours when EGFR overexpression is present in primary GBM tumours. Because of the frequency of EGFR mutations in GBM it poses as an attractive marker for treatment. Substantial success has been observed in using tyrosine kinase inhibitors (TKIs) against EGFR mutations in

lung carcinomas but due to the complexity of GBM intra-tumour heterogeneity and challenges to drug delivery, most GBM trials have been unsuccessful (Taylor et al., 2012). Studies in heterogeneity of GBM have identified expression of cell populations with dissimilar RTKs mutations stemming from the same early genetic mutations (Snuderl et al., 2011). These findings suggest that distinct subpopulations of cells can derive from a single-cell and can also exhibit heterogeneous phenotypes contributing to GBM drug resistance. Animal models with GBM xenografts have demonstrated high differentiation in RTK signalling contributing to GBM proliferative capacities signifying high phenotypic heterogeneity as a driving hallmark of GBM (Soeda et al., 2015).

1.5.3 Platelet Derived Growth Factor Receptor

Amplifications of PDGFRs have been commonly reported in GBM tumours and are often associated with poor prognosis (Phillips et al., 2013). PDGFR is part of the tyrosine kinase receptor family and acts as a receptor for platelet derived growth factor (PDGF) and consists of five isoforms PDGF-AA, PDGF-AB and PDGF-BB. PDGF-CC and PDGF-DD. Ligand binding with PDGFR receptors induce autophosphorylation and activates a cascade of signalling pathways involved in growth and differentiation. There are two types of the PDGFR receptors, PDGFR- α and PDGFR- β both of which have varying affinities for different PDGF isoforms. PDGFR- α is more selective towards PDGF-A, -B and -C whereas PDGFR- β has higher affinity for PDGF-B and -D. Expression of the PDGFs and PDGFRs is associated with functions such as growth but their expression has also been observed at sites of epithelial-mesenchymal interactions suggesting their role in cellular differentiation and extracellular matrix communications (Fredriksson et al., 2004). Generation of paracrine and autocrine loops of PDGF and PDGFR has been found to consecutively activate signalling pathways stimulating oncogenic growth and aiding in tumour survival (Heldin, 2012b). Aberrations in PDGFR expression have been found in 13% of GBM tumours (TCGA Research Network, 2008). PDGF signalling through either of PDGFR has been found to upregulate VEGF expression leading to increased angiogenic formation (Raica and Cimpian,

2010). Inhibition of PDGFR- β *in-vitro* and *in-vivo* has been shown to successfully enhance radiosensitivity in gliomas and shows a potential as a therapeutic compound for GBM treatment (Hong et al., 2017)

1.5.4 PI3K/Akt signalling

The PI3K/Akt/mTOR pathway is integral to cellular growth and studies have demonstrated it to play a major role in cancer signalling promoting proliferation (Mao et al., 2013). PI3K/Akt/mTor is an important target as the downstream phosphorylation of substrates through this pathway potentiates anabolic processes such as mRNA translation and lipid synthesis. One of the key effectors of this pathway is Akt as its activation can induce cell growth and proliferation and its hyper activation is linked to apoptotic resistance (Testa and Tschlis, 2005). Because of its importance in cell proliferation, the PI3K/Akt/mTOR pathway is highly regulated mainly through PTEN (Phosphatase and Tensin Homologue Deleted on Chromosome Ten). PTEN negatively regulates PI3K by removing phosphate from PIP3, hence arresting the downstream activation of Akt. This suggests the importance of PTEN as a tumour suppressor. Somatic mutations of *PTEN* gene are commonly found in many cancers including GBM (Koul, 2008). This results in reduced or absent tumour suppressor function of proteins which is a likely a contributor to GBM proliferation. Additionally, PI3K has been implicated in activation of nuclear factors such as NF κ B (nuclear factor kappa-light-chain-enhancer of activated B cells) which control DNA transcription. Both, increased activation of NF κ B and inhibition of PTEN is believed to promote glioma cell proliferation (Nogueira et al., 2011). A study on topographical expression of Akt in GBM has observed a close correlation between Akt and TSC2 (Tuberous Sclerosis Complex two) showing that Akt enhances proliferation rather than inhibiting apoptosis (Riemenschneider et al., 2006).

1.5.5 Ras/Raf/MAPK

Another cascade of events originating from RTK activation is the Ras/Raf/MAPK pathway. Similarly, to PI3K/Akt/mTOR pathway, the result is increased growth and proliferation. Ras belongs to a large family of GTPases and its role in human cancers has been well established. Approximately 20% of all tumours have mutations in one of the *RAS* genes (Rajalingam et al., 2007). Because of its many effectors, Ras protein serves an important role in normal and abnormal cell physiology. The activated form of Ras can recruit other proteins such as B-Raf triggering subsequent phosphorylation of MEK protein kinase. MEK then phosphorylates MAP kinase leading to further phosphorylation of many transcription factors within the nucleus mediating cellular response and protein synthesis. Research on mice has implied that Ras alone cannot stimulate tumour growth but rather it needs active Akt expression too, to initiate GBM growth (Holland et al., 2000). With various aberrations in a numerous signalling cascades GBM tumours can evade apoptosis through consecutive activation of various kinases and their subtypes resulting in oncogenic pathway activation and increased resistance to various therapeutic agents.

One of the key regulators of Ras/Raf/MAPK pathway is a protein Neurofibromin type I (NF1) encoded by *NF1* gene. Commonly expressed in neuronal and non-neuronal tissue, NF1 protein maintains inactivation of Ras and acts as a tumour suppressor. Homozygous focal deletions of *NG1* region have been observed in mesenchymal subtypes of GBM (Verhaak et al., 2010). Deactivation and reduction of this protein has been shown to increase macrophage and microglia infiltration into GBM tumour microenvironment leading to growth factor and cytokine release facilitating tumour growth and migration (Hambardzumyan et al., 2016; Q. Wang et al., 2017a). Patients with *NF1* mutations are more predisposed to malignant tumour formation and prognosis for these patients is dismal (Campian and Gutmann, 2017)

1.5.6 P53 mutations

The involvement of tumour suppressor protein p53 encoded by *TP53* has been extensively studied in cancer. The protein product of *TP53* is a nuclear transcription factor with pro-apoptotic function and serves as a crucial step in prevention of tumour formation and initiation of apoptosis in faulty cells. Mutations or loss of P53 has been observed in over 50% of human cancers suggesting its importance as a tumour suppressor (Ozaki and Nakagawara, 2011). Distinct mutations have also been observed in glioblastoma subtypes including secondary glioblastoma with 60-70% of cases harbouring P53 mutation and primary glioblastoma with 25-30% of tumours having loss of function of P53 (England et al., 2013). P53 is activated in response to several cellular stressors such as oxidative stress, DNA damage, abhorrent cellular signalling, oncogenic activation, hypoxic states and other abnormal cellular events. Deregulation of P53 pathway plays an important role in GBM development and cancer progression. Although, *TP53* inactivation or mutations are key for pro-oncogenic development, murine studies for GBM suggest that several other common mutations are often required such as *PTEN* mutation are necessary for progenitor cell differentiation and tumorigenic potential of GBM tumours (Zheng et al., 2008). In addition to glioma development, studies in P53 suggest its mutation to be involved in malignant progression, growth and migration in primary GBM (Krex et al., 2003).

1.5.7 Prognostic Mutations of IDH & MGMT

GBM remains as one of the most aggressive brain tumours with very short survival and poor prognosis. However, research into aberrant genetic alterations has provided clinically significant biomarkers which are currently commonly used in classification and treatment of GBM. These markers include *IDH* (isocitrate dehydrogenase) type 1 and 2 and *MGMT* (O6-methylguanine-DNA methyltransferase) promoter methylation. *IDH* 1 and 2 are enzymes which catalyse decarboxylation of isocitrate to produce α -ketoglutarate and carbon dioxide. Mutation of *IDH* in GBM results in loss of function and reduced enzymatic

activity of these enzymes which result in altered epigenetic changes favouring GBM prognosis (Yang et al., 2015). The *IDH* mutations affect methylation of CpG islands. This leads to alteration of methylation landscape and reshaping of the epigenome of GBM, constituting longer survival for patients harbouring *IDH* mutation (Turcan et al., 2012). In turn, *MGMT* encodes for a DNA repair enzyme which is responsible for repair of guanine nucleotides alkylated at the O6 position (Kushwaha et al., 2014). Expression of *MGMT* responsible for the DNA repair to alkylation has been shown to reduce efficacy of TMZ treatment in patients with GBM and is one of predominant mechanisms of chemotherapeutic resistance (Zhao et al., 2018). Methylation of the promoter region of *MGMT* results in reduced *MGMT* expression and is associated with better response to TMZ treatment (Pegg, 1990).

1.6 Alternative Treatments of GBM

Progress in proteomic and genomic profiling has steadily improved diagnosis and identification of clinically relevant subtypes of GBM over the past decade, however modality of treatment hasn't prominently changed, relying on chemotherapeutic agents such as TMZ and concomitant radiotherapy. Yet, even after aggressive treatment and total resections these tumours return often with more aggressive phenotype. Additionally, the intensity of the treatment with DNA alkylating chemo-therapeutics can have detrimental health effects especially when it comes to elderly patients over 70 years of age (Saito et al., 2014). Molecular markers such as *MGMT* and *IDH* have become a useful defining marker for GBM prognosis and predictors of treatment capability. Advances in diagnosis and surgical resection methods have greatly contributed to extended survival and improved quality of life of patients. Yet, the hurdle of designing optimal treatment for managing and treating GBM remains as one of most challenging tasks in clinical oncology (Mrugala, 2013). With short survival rates and high morbidity of GBM patients, there is a substantial need for discovery of new therapeutic agents which can be used alongside current treatment options and improve current survival rates.

1.6.1 Endocannabinoid System in Glioblastoma

Cannabidiol (CBD) is a naturally occurring lipophilic molecule produced by the cannabis plant (Hartsel et al., 2016). CBD is a non-psychoactive phytocannabinoids that has demonstrated therapeutic efficacy across various pathologies and is a component of the drug formulation currently being trailed by GW pharmaceuticals for treatment of GBM (GW Pharmaceuticals, 2017). CBD has been proposed as a less toxic agent that could be used synergistically with other drugs to reduce potency and high concentration doses. It is an attractive drug as it possesses affinity for a wide range of receptors, allowing the molecule to regulate endogenous systems outside the scope of the endocannabinoid system. CBD also possess a wide therapeutic window, giving the molecule an excellent safety profile.

Studies have indicated the endocannabinoid system is altered in GBM tissue, CB2 expression is massively upregulated and the levels of expression correlate well with malignancy grade (Ellert-Miklaszewska et al., 2013). However there is little consensus on the expression levels of CB1 receptor in GBM, owing to a series of conflicting studies (De Jesús et al., 2010; Schley et al., 2009; Wu et al., 2012). Study by Wu and colleagues investigated the endogenous levels of the endocannabinoid signalling molecules 2-Arachidonoylglycerol (2-AG), anandamide (AEA), and Oleoylethanolamide (OEA) by comparing low-grade and high-grade gliomas derived from various brain regions in 32 patients, to complementary regions in healthy brain tissue. Interestingly this study revealed a significant increase in 2-AG levels, displaying a similar increase in both low- and high-grade tumours as compared to non-tumour tissue. 2-AG acts as an agonist to both CB1 and CB2 receptors and is considered as a mediator of physiological processes including immune response and neuroprotection (Sánchez and García-Merino, 2012). Interestingly, it has been suggested that in tissues with high content of 2-AG, such as in CNS, CB2 receptor can facilitate suppression of T-cells which in turn could be an important mechanism of neuroprotection (Dittel, 2008). Whether this contributes to enhanced survival of high-grade gliomas is

yet to be investigated. In contrast, AEA levels appeared to decrease, with a tendency to be lower in low grade tumours relative to high grade tumours. Research into this endocannabinoid has suggested that AEA exerts antiproliferative function in various cancers through CB1 receptor (De Petrocellis et al., 1998; Huang et al., 2011). OEA levels were not significantly changed, however there was a tendency for higher expression level in GBM tissue relative to healthy tissue. In addition, the expression and activity of metabolic and catabolic endocannabinoid enzymes were measured. Fatty acid amide hydrolase (FAAH) was decreased substantially more in high-grade gliomas (60%) than in low-grade gliomas (30%). The study also showed Monoacylglycerol lipase (MAGL), the 2-AG hydrolysing enzyme, decreased in glioma tissues relative to non-tumour tissues, whereas Diacylglycerol Lipase- α (DGL- α) showed no difference in expression levels between the groups. Because of these alterations, it can be hypothesised that drugs that target the cannabinoid system could possess therapeutic efficacy. A small number of studies have assessed the anti-cancer effects of CBD, which have generally been divided into anti-angiogenic mechanism, anti-proliferative mechanism and apoptotic mechanisms (Dumitru et al., 2018). As well as these promising anti-cancerous properties, it has been shown that CBD can kill GBM cells while at the same time leaving astrocytes intact, thereby minimizing toxic effects of the compound (Gómez del Pulgar et al., 2002). Research into endocannabinoid system shows a very promising potential for cannabinoids to be used as a therapeutic compound for cancer treatment and management, including treatment for gliomas (Rocha et al., 2014).

1.6.2 S-adenosyl Methionine Methyl Donor & Homocysteine/Methionine Cycle in Cancer & Possible Treatment Options

Aberrations in methylation patterns have been commonly reported by several GBM studies (de Souza et al., 2018; Etcheverry et al., 2010; Noushmehr et al., 2010). The variable methylation profiles greatly contribute to the highly heterogeneous nature of GBM tumours and their inherent protein expression.

Both hypermethylation of genes as well as hypomethylation leads to genetic instability and often result in stronger proto-oncogenic expression in cancer. SAM is involved in methylation of DNA and has potential to significantly alter the transcriptome and selectively inhibit pathways regulating growth, transformation and invasiveness in hepatocellular carcinoma but not in healthy cells (Wang et al., 2017). Additionally, SAM has been shown to reduce tumour size and metastasis in breast cancer xenografts proposing its role as a tumour silencing molecule (Mahmood et al., 2018). Production, recycling and regeneration of SAM is closely intertwined with homocysteine cycle and its imbalance has been connected to certain cancers (Škovierová et al., 2016).

Homocysteine is a sulphur containing amino acid, biosynthesized from methionine it is an important amino acid in the methionine-homocysteine cycle. The amino acid is continually metabolised via two main mechanism to biosynthesise either methionine via re-methylation, or cysteine through transsulfuration (Figure 1-3). Ineffective or imbalanced methionine-homocysteine metabolism can result in abnormal levels of homocysteine leading to extensive changes in tissues and far-reaching biochemical processes. High plasma levels of homocysteine has been suggested to greatly increase risk factors for cardiovascular and cerebral disease including stroke and neurodegenerative diseases such as Alzheimer's and Parkinson's disease (Dinavahi and Falkner, 2004; Garcia and Zanibbi, 2004; Setién-Suero et al., 2016; Smith and Refsum, 2016).

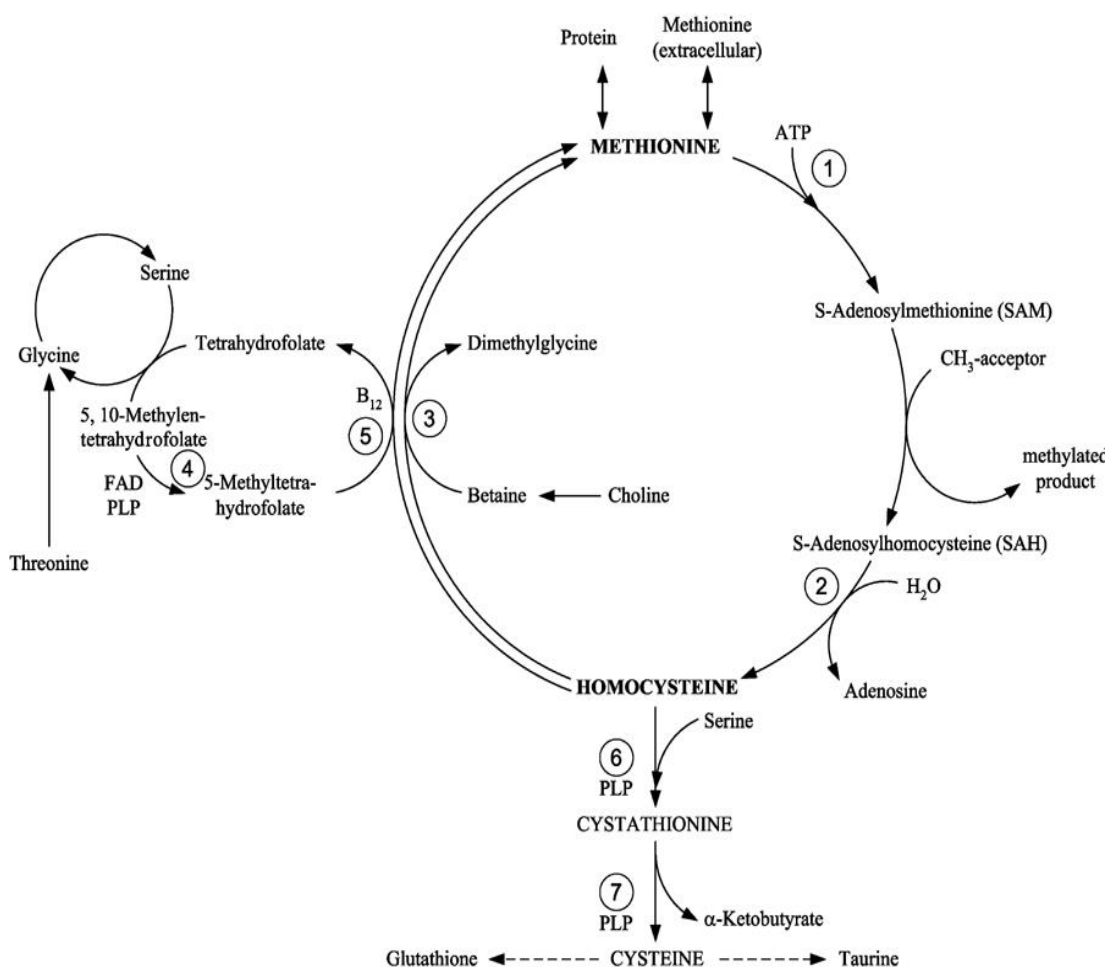


Figure 1-3/ Methionine/Homocysteine cycle showing the molecules involved and their turn-over to create various compounds. In normal metabolism the methionine and homocysteine are constantly regenerated and re-cycled. However, imbalance of one or more molecules can lead to accumulation of certain end products such as methionine or SAH. During this process methyl donor SAM is generated through addition of adenosine from ATP. SAM is then used as a methyl donor for various processes such as DNA methylation, protein methylation or it's re-used in Homocysteine cycle. Image taken from: The Molecular and Cellular Effect of Homocysteine Metabolism Imbalance on Human Health. Škovierová, H., et al. Int. J. Mol. Sci. 17.

Methionine is an amino acid crucial in make-up of proteins and important cell function molecules. During the cycle, Methionine is converted via enzyme methionine adenosyltransferase (MAT) to create a methyl donor S-adenosylmethionine (SAM). The methyl transferase SAM serves an important function in many physiological processes including DNA and protein methylation but also synthesis of molecules such as norepinephrine through Phenylethanolamine N-methyltransferase (PMT) enzyme. Enzymatic donation of the methyl group from SAM to a substrate confers its change into S-

adenosylhomocysteine (SAH) which is later catalysed into homocysteine by SAH hydrolase. Homocysteine must then be recycled into methionine by one of two ways, either through addition of methyl from methylcobalamin (a form of vitamin B12) catalysed by methionine synthase (MeSe) or addition of methyl from Betaine, catalysed by betaine-homocysteine methyltransferase (BHMT).

Concurrently, homocysteine can be converted into cysteine via enzyme cystathionine beta-synthase (CBS) which can be further processed into taurine or glutathione. Several factors can affect the balance between homocysteine and methionine. Deficiencies in folic acid (B9), vitamin B6 and B12 are a common cause for elevated homocysteine levels in blood plasma and are often concomitant with age-related cognitive decline but also confer increased a risk in cancers including colorectal and lung cancer (Hashmi, 2011; Reay et al., 2013). Concurrent low concentrations of these vitamins in serum and CSF with age, and disruptions of homocysteine metabolism are considered to be a major link to neurodegenerative disease and dementia (Stanger et al., 2009).

Ratio of SAM to SAH plays an important role in regulation of the cycle and its imbalance can have detrimental effects on cerebral function. Re-methylation of homocysteine to methionine dependent on MeSe in presence of B12 is reduced which leads to low levels of SAM by decreasing its synthesis from methionine and increasing levels of SAH. The ratio between SAM and SAH dramatically changes and animal studies have shown increased levels of SAH in brain and CSF to reflect decreased ratio of methylation(Weir et al., 1992). Reduction in SAM levels considerably reduce SAM-dependent methylation of proteins and DNA. Increased level of SAH also acts as antagonists to SAM-dependent methylation. Furthermore, this leads to preferential synthesis of homocysteine from SAH, advancing its accumulation. Significant hypomethylation of DNA CpG sites has been described in brain and blood of PD patient's but whether this is caused by SAM/SAH ratio is unclear (Chuang et al., 2017; Kaut et al., 2012; Wüllner et al., 2016).

There is substantial evidence to suggests that homocysteine cycle imbalance contributes to increased levels of ROS and consequent oxidative damage but can also regulate some antioxidant enzyme levels (Doherty, 2007;

Handy et al., 2005). Increase in homocysteine levels with concomitant decrease in glutathione and folate have been considered as a biomarker for lung cancer (Özkan et al., 2007). However, common dysregulation of the homocysteine cycle has been shown to contribute to neurodegenerative disease and seem to increase with ageing. Both factors have also been considered as a contributor to increased risk for development and formation of brain cancer including high grade gliomas. We postulate that dysregulation of this cycle might play a major role in the aggressiveness and formation of somatic mutations in GBM. Hence, we would like to assess the oxidative damage extent in various area of the tumour as well as examine regulation of various antioxidant enzymes. We would also like to assess viability of using SAM as a therapeutic compound to be used for treatment of GBM. Because of its pleiotropic functions as a methyl donor for DNA, histones and other various proteins, we suggest that it could have therapeutic and neuroprotective properties in GBM treatment.

1.7 Aims of the Study

The main objective of the study is to investigate post-translational changes across distinct GBM regions as well as expression of various proteins and signalling pathways. GBM samples from resected tumours will be analysed from protein lysates and key signalling pathways as well as vital proteins involved in a range of metabolic processes will be further investigated and validated. Study will focus on primary GBM tumours as they represent the vast majority of all GBM. People over 40 years of age are predominantly affected, both male and female. Because control samples from normal brain tissues are unattainable from live patients, control samples will be derived from previous brain studies conducted at Clinical Physiology lab at Royal Derby Hospital. Proteomic approaches including 1DE (one-dimension electrophoresis) and 2DE (two-dimension electrophoresis) will be used in combination to deliver an accurate method of identifying and quantifying proteins of interest. For discovery of novel proteins in signal transduction pathways, 1D-PAGE and 2D-PAGE can be used utilising Colloidal blue, silver or Fluorescent gel staining. Western blotting will be used to semi-quantitatively assess expression of certain proteins and their variance in different tumour regions as well as PFC (pre-frontal cortex) control tissues. Kinase targets in signal transduction pathways can be easily investigated using a Pro-Q Diamond fluorescent stain, making it ideal for phosphoproteomic studies. Used in multiplex with fluorescent probes for general protein expression, it offers direct in-gel detection of phosphorylation modifications. Additional wide array of protein assay using Milliplex technology will be used to assess phosphorylation of key regulatory pathways. As a supplementary addition to the experiment we will investigate efficacy of a few compounds in GBM U87 cell line to address possible options of GBM treatment. Two-way ANOVA analysis will be performed on the collected data to determine statistical significance of the experiment

2 Methods

2.1 Preparation of Buffers & Other Reagents

1. Tissue homogenisation buffer

Homogenisation buffer was made fresh on the day. 10 ml of homogenisation buffer was prepared containing 150 mM NaCl, 50mM Tris-HCL, 1mM EDTA, 1% (v/v) DTT, 1% (v/v) phosphatase inhibitor cocktail and 1 protease inhibitor cocktail tablet (Roche).

2. Protein precipitation wash buffer

Diethyl ether: industrial methylated spirit: ultrapure water at 10:7:2 (v/v/v)

3. NuPage MOPS running buffer

50 ml of stock NuPage MOPS buffer (20x) was diluted in 950 ml of ultrapure water to make 1000 ml of running buffer and it was used fresh on the day.

4. Transfer buffer

Stock solution of 10x transfer buffer was prepared by dissolving 288 g glycine and 60.4 g Tris base in 1500 ml of ultrapure water. Solution was topped up with ultrapure water to make 2000 ml stock. Prior to use, working buffer was made by diluting 200 ml of stock solution and 400 ml of methanol in 1400 ml of ultrapure water and chilled to 4°C.

5. Rehydration buffer

9.8 M urea, 2% CHAPS (w/v) was made as stock and stored at 1 ml aliquots at -20°C.

6. SDS-Equilibration buffer

6 M urea, 50 mM Tris-HCL at pH 6.8, 30% glycerol, 2% (w/v) SDS and few grains of bromophenol blue. Buffer was divided into 10 ml aliquots and stored at -20°C.

7. Low melting 1% Agarose

2.5 g of agarose was dissolved in 250 ml running buffer (1x) and 0.005% (w/v) of bromophenol blue was added. Solution was mixed and briefly heated in microwave to dissolve the agarose. After cooling down the solution the agarose was stored at 4°C.

8. Gel fixative solution

50% (v/v) methanol, 10% (v/v) glacial acetic acid and topped up with ultrapure water. Stored at room temperature.

9. Pro-Q de-staining solution

20% acetonitrile, 5% 1.5M sodium acetate and adjusted to pH 4 with HCL. Stored at room temperature until required.

10. PBS-Tween buffer

10x stock solution was made by dissolving 80 g NaCl, 2 g KCl, 14.4 g Na₂HPO₄, 2.4 g KH₂PO₄ in 800 ml of ultrapure water. After compounds have dissolved, pH was adjusted to 7.3 - 7.5 with HCL and topped up to 1000 ml with ultrapure water, stored at room temperature. For working solution, 100 ml of stock (10x) was dissolved in 800 ml of ultrapure water and pH was measured using pH meter and adjusted to 7.3 – 7.5 pH. Solution was topped up to 1000 ml and 0.05% (v/v) of Tween-20 was added to make PBS-T.

11. Blocking buffer

5% (w/v) of milk (Marvel – semi skimmed dried milk powder) or BSA (lyophilised powder) was dissolved in PBS-T to make 200 ml blocking buffer. All blocking buffers were prepared and used fresh.

12. Milliplex magnetic beads

20x magnetic bead solution was sonicated for 15 seconds and vortexed for 30 seconds. 150 µl of bead solution was diluted in 2850 µl of Milliplex MAP assay buffer 2 in a mixing bottle. 1x bead solution was vortexed for 15 seconds and stored in the dark at 4°C.

13. Biotin-labelled detection antibody and Streptavidin-Phycoerythrin

20x detection antibody stock and 1:25 SAPE were vortexed for 10 seconds. 150 µl of detection antibody was diluted in 2850 µl of Milliplex MAP assay buffer 2 in a mixing bottle. In a separate bottle, 120 µl of SAPE was diluted in 2880 µl of Milliplex MAP cell signalling assay buffer 2.

2.2 Samples

Proteomic characterization study of glioblastoma was performed on GBM tissues from brain tumour resections kindly provided by Dr Ruman Rahman and Dr Stuart Smith from CBTRC department at QMC, University of Nottingham. Tissues were obtained from grade IV, GBM diagnosed patients and resected using 5ALA guided surgery. The intra tumour regions and invasive margins were defined by fluorescence of tumour tissue after 5-ALA treatment and 3 intra-tumour regions were isolated. This includes tumour core, intermediate-layer and the invasive margin. Samples were stored at -80°C until required.

| <u>Tissue ID</u> | <u>Intra-tumour region</u> | <u>Tumour site</u> | <u>Gender</u> | <u>Age</u> |
|-------------------------|--|---------------------------|----------------------|-------------------|
| GBM 29.1 | Superficial enhancement (Tumour Rim) | Left frontal hemisphere | Female | 67 |
| GBM 29.2 | Fluorescent rim (Tumour Rim) | | | |
| GBM 29.3 | Non-enhancing core (Tumour Core) | | | |
| GBM 29.4 | Superior fluorescence (Tumour Rim) | | | |
| GBM 29.5 | Invasive margin | | | |
| GBM 38.1 | Superficial fluorescence (Tumour Rim) | Right frontal hemisphere | Male | 69 |
| GBM 38.2 | Central core | | | |
| GBM 38.3 | Central core 2 | | | |
| GBM 38.4 | Deep lateral fluorescence (Tumour Rim) | | | |
| GBM 38.5 | Invasive margin | | | |
| GBM 39.1 | Superficial fluorescence (Tumour Rim) | Right frontal hemisphere | Female | 58 |
| GBM 39.2 | Central core | | | |
| GBM 39.3 | Posterior core | | | |
| GBM 39.4 | Anterior enhancement (Tumour Rim) | | | |
| GBM 39.5 | Invasive margin | | | |
| GBM 40.1 | Superior enhancement (Tumour Rim) | Right frontal hemisphere | Male | 44 |
| GBM 40.2 | Central core | | | |
| GBM 40.3 | Anterior enhancement (Tumour Rim) | | | |
| GBM 40.4 | Posterior enhancement (Tumour Rim) | | | |
| GBM 40.5 | Invasive margin | | | |
| GBM 58.1 | Superficial enhancement (Tumour Rim) | Left frontal hemisphere | Male | 78 |
| GBM 58.2 | Necrotic core | | | |
| GBM 58.3 | Posterior rim (Tumour Rim) | | | |
| GBM 58.4 | Anterior rim (Tumour Rim) | | | |
| GBM 58.5 | Invasive margin | | | |

Table 1-1| GBM sample coding and demographics

GBM samples used in the study with sample ID and distinct tumour regions divided into tumour rim, tumour core and invasive margin. The distinct areas have been outlined by the surgeon with 5ALA assisted surgery and specified areas have been separated.

Brain tissue controls were matched with the GBM tissue demographics. Brain tissue controls were taken from a previous ageing brain study conducted in Clinical Sciences lab at Royal Derby Hospital and have been supplied by The Neuropsychopharmacology Research Group at the Department of Pharmacology of the Basque Country. The brain samples were obtained from subjects who died of natural causes or accidents and tissue was collected *post-mortem* with time of delay recorded. Samples from prefrontal cortex, Broadman's area 9 were dissected and stored at -80°C until required.

2.3 Sample Homogenisation

Brain tissues were stored in -80°C freezer in 1 ml vials. Prior to dissection, samples were placed on dry ice in a fume hood in sterile conditions. Brain samples, while still frozen, were cut into smaller fragments using a surgical scalpel, weighed and placed in another 1ml tube. Approximately 50 to 60 mg of tissue was dissected and kept frozen at -80°C. Tissue samples were placed in a glass Dounce homogeniser kept on ice and 2 ml of homogenisation buffer was added. Twenty even and slow strokes were applied with the plunger until homogenate appeared consistent in form and colour. Total homogenate was aspirated to a labelled tube and frozen at -80°C until further use.

2.4 Cellular Fractionation

Cell fractionation relies on separation of complex protein mixtures from tissue into their subcellular components. Separation of subcellular components serves as an important step in studying and assessing specific intracellular components of the cell proteome. Various methods can be used to isolate and purify specific components based on their weight, size, solubility or charge. In this study, differential centrifugation was used to obtain plasma membrane, cytosolic and nuclear crude fractionates for analysis.

To acquire fractionated sample, 1.5 ml of total protein homogenate was placed in an Eppendorf and centrifuged for 10 minutes at 500 x g in 4°C centrifuge. Supernatant was retained into a new Eppendorf and the pellet was re-suspended in 500µl of homogenisation buffer to retain crude nuclear fraction. Supernatant was further spun at 21,300 x g for 40 minutes at 4°C. The upper part of the sample was retained as a crude cytosolic fraction and pellet was re-suspended in 300µl of homogenisation buffer to make a membrane fraction. All samples were snap frozen in liquid nitrogen and kept in -80°C freezer until further use.

2.5 Protein Quantification

To determine total protein content of cytosolic, membrane and nuclear fractionates from brain and GBM tissue homogenates, a modified Lowry assay (Lowry *et al.*, 1951) was performed using Bio-Rad DC kit. The colorimetric assay is an easy and widely used method for determination of total protein content of samples with no or small quantities of detergents and reducing agents. Proteins in the sample react with cupric sulphate and tartrate in alkaline solution to produce tetradentate copper-protein complexes. Addition of Folin-Ciocalteu Reagent to this solution reduces chelated copper complexes producing blue coloured, water-soluble agent which can be measured at 740nm. The unknown concentration of each sample was compared to a set of protein standards made from Bovine Serum Albumin 2 mg/ml. A range of standards from 20 µg to 1.25 µg were made by diluting 2mg/ml BSA with 10mM Tris/HCL at pH 8. GBM and control samples were thawed on ice and diluted in 10mM Tris-HCL to make up two dilutions of 1:10 and 1:20 in 100µl solution. For the assay, 40 µl of buffer blank, protein standard and diluted protein samples were pipetted in duplicate into a 96-well plate. Following, 20 µl of Reagent **A** and 160 µl of Reagent **B** was added consecutively. Plate was incubated at room temperature for 20 to 30 minutes before reading it using a Multiskan Spectrum Microplate Reader at 740 nm excitation. Using Excel software, absorbance (nm)/amount of standard protein (µg) was plotted with linearity of the equation of R^2 falling in range

between 96 - 99%. Total protein concentration of each sample was calculated from the intercept of the line from standard curve.

2.6 Protein Precipitation with Acetone

Acetone precipitation was used for purification of proteins and removal of contaminants for downstream applications such as 2D-PAGE and Mass Spectrometry. This method is commonly used for precipitation of most soluble proteins.

Precipitation was performed with 100% acetone cooled to -20°C. Desirable amount of proteins was placed in an acetone compatible plastic 2 ml tubes. Four times volume of acetone was added to the sample and the contents were vortexed for 20 seconds. Sample was then incubated on ice for 60 minutes. After the incubation, samples have been centrifuged at 14,000 x g for 10 minutes at 4°C. The supernatant was aspirated carefully not to dislodge the pellet. The precipitate was washed 3 times in acetone wash buffer and centrifuged again at 14,000 x g. After the third wash, the pellet was air dried for approximately 15 min and resuspended in solubilisation solution.

2.7 SDS-PAGE

2.7.1 Sample Preparation for 1D SDS-PAGE

Approximately 100 µl of sample was prepared for SDS-PAGE. Protein fraction extracts were prepared to 1 µg/µl concentration in 10mM Tris-HCL buffer pH 7.5 with 10x reducing agent and 4x LDS buffer. Samples were vortexed and heated to 70°C for 10 minutes on block heater to denature the proteins and afterwards cooled on ice. Samples in the buffer were then pulsed on a centrifuge

for 5 seconds at 5000 x g to collect precipitated material and were either run on SDS gels immediately or stored at -20°C.

2.7.2 Preparation of Pre-cast Gels

Precast NuPAGE Novex gels (10% Bis-Tris, 1.0 mm x 12/10-well) were purchased from Invitrogen and stored at 4°C. Invitrogen NuPage gels offer greatest separation of medium and small proteins and prevent protein modifications by maintaining a neutral pH. NuPAGE ZOOM protein gels (4-12% Bis-Tris, 1.0 mm x IPG-well) were used for running small 2D-PAGE gels. Some gels were also hand cast, including large 16 x 20 cm 2D-PAGE gels and some 10 x 8 cm 1D-PAGE gels. Prior to electrophoresis, gels were brought to room temperature for 10 to 15 minutes. Pre-cast gels were removed from their packaging and cover strip was taken off. Combs were carefully removed from pre-cast and hand-cast gels and rinsed in ultra-pure distilled water. Gels were then ready to use.

2.7.3 Hand-casting Polyacrylamide Gels for 1D- & 2D-PAGE

Hand-cast gels were prepared with Bio-Rad Mini-PROTEAN system for 1D-PAGE gels (10.0x8.0cm) and PROTEAN II system for 2D-PAGE large gels (20.0x18.3cm). SDS-PAGE was performed either on large 12% or small 10% polyacrylamide gels overlaid with 4% and 5% resolving gel respectively. Gel plates were thoroughly washed and cleaned in 70% ethanol and ultrapure distilled water. Small gels were prepared with 1.0 mm spacers and 10 well combs for 1D-PAGE and 17cm IPG-well comb for 2D-PAGE gels. The plates were assembled and clamped secure in their casting system. Stacking and resolving gel solutions were prepared separately with volumes shown below. Additional 10ml of stacking solution was prepared to create a small gel strip at the bottom of the casting forms to prevent leakages.

Composition of resolving 1D-PAGE gels (10%) and 2D-PAGE gels (12%)

| <u>Reagents</u> | <u>1D-PAGE</u> | <u>2D-PAGE</u> |
|----------------------------|----------------|----------------|
| Distilled H ₂ O | 4.1ml | 33.5ml |
| 30% acrylamide solution | 3.3ml | 40ml |
| 0.5 Tris-HCL, pH 8.8 | 2.5ml | 25ml |
| 10% (w/v) SDS | 100µl | 1ml |
| 10% (w/v) APS | 100µl | 500µl |
| TEMED | 5 µl | 50µl |

Composition of stacking 1D-PAGE gels (4%) and 2D-PAGE gels (5%)

| <u>Reagents</u> | <u>1D-PAGE</u> | <u>2D-PAGE</u> |
|----------------------------|----------------|----------------|
| Distilled H ₂ O | 3.4ml | 13.58ml |
| 30% acrylamide solution | 850µl | 3.4ml |
| 1.5M Tris-HCL, pH 6.8 | 625µl | 2.6ml |
| 10% (w/v) SDS | 50µl | 200µl |
| 10% (w/v) APS | 50µl | 200µl |
| TEMED | 5µl | 20µl |

After addition of 10% (w/v) ammonium persulphate (APS) and TEMED, stacking and resolving gel solution polymerises within half an hour and mixture needs to be distributed into plates quickly. Resolving solution was first poured into glass plates with enough space left to fit the combs and spare space for the stacking gel. A layer of water-saturated butan-2-ol (1:1, v/v) was added to keep resolving gel levelled and prevent gel drying. After polymerisation of the resolving gel, butan-2-ol was decanted and stacking gel was poured into the top of the plate. Combs were inserted immediately to create wells for samples. Gels were covered in paper towels wetted with distilled water and wrapped in cling film. Hand-cast gels were ready to be run on the same day or stored in the cold at 4°C.

2.7.4 Running 1D-PAGE

Clean gels were placed in an electrophoresis tank (X-Cell SureLock Mini Cell or Mini-PROTEAN Tetra) and secured with tank locks. The inner chambers were filled half full with MOPS running buffer and 0.5ml of antioxidant was added before topping up the chambers. Antioxidant in inner chamber migrates along with the proteins and prevents the oxidation of amino acids during electrophoresis. The outer chamber was filled halfway with MOPS running buffer. Gel wells were then loaded with 5 μ l of protein standard, 20-25 μ l (approx. 1 μ g/ μ l concentration) of protein sample and remaining empty wells were loaded with 1x loading buffer. Electrophoresis was set to 125V constant voltage with PowerPac™ Basic Power Supply and ran for approximately 95 minutes or until the tracking dye reached the bottom of the gel cassette. After the run, the casing of cassettes was removed, and gels were washed in ultrapure distilled water and placed in a plastic container containing either fixative solution for gel staining or cold transfer buffer for protein transfer onto membranes.

2.8 2D-PAGE

2.8.1 Protein Solubilisation & Isoelectric Focusing

2D-PAGE begins with IEF by separation of the proteins in first-dimension according to their pI. The range of pH used in IEF is critical as proteins will migrate across the pH gradient to the point where they carry no net charge. For this study, broad pH (pH 3 – 10) was used first to view majority of the proteins on one gel and then narrower range was used (pH 4.7 – 5.9) for better resolution of these proteins.

For small gels, 100 to 300 μ g of proteins were used and for large 2D-PAGE gels protein content was scaled up to 1000 μ g. To remove contaminants and salts that could interfere with isoelectric focusing, acetone precipitation was

performed. 9.8M urea and 2% CHAPS rehydration buffer stock was thawed to room temperature. Prior to sample re-solubilisation, 0.5% (v/v) of IPG carrier ampholytes matching strip pH (3 – 10 or 4.7 – 5.9), 1% (v/v) of 200mM TBP reducing agent and 12 µl of de-streak reagent was added to rehydration buffer stock solution to make 1 ml working solution. Sample was vortexed for 30 seconds or longer to break-up the pellet. Samples were then incubated for 1 hour at room temperature. Meanwhile, IPG strips were removed from -20°C freezer and brought to room temperature. Either 17 cm or 7 cm strips, pH 3 – 10 or 4.7 – 5.9 were used. After 1-hour incubation period, solubilized proteins were placed in a rehydration tray and overlaid with IPG strips gel side down. Strips were overlaid with 1 ml of mineral oil to prevent evaporation and proteins were first passively rehydrated for 1 hour at room temperature and then actively rehydrated. Active rehydration was performed at low voltage (50 V) for 16 hours using Protean IEF cell internal protocol.

Following active rehydration, wetted paper wicks were placed in the focusing tray underneath the gel strips in place of the cathode and anode wires. Wicks collect salts and other contaminants which can increase conductivity at the electrodes and cause hot spots, burns or general discontinuities in the gel. After the placement of the wicks, strips were focused using standard internal pre-set protocols for 17 cm and 7 cm IPG strips with current limit of 50µA/strip, rapid ramping and hold setting on. Focusing time lasted for 16 – 20 hours after which strips were either run on 2D gels or stored at -20°C until required.

2.8.2 Running 2D-PAGE Gels

Focused strips were run on 2D gels to separate proteins by their molecular weight. Strips were equilibrated to solubilise focused proteins and allow SDS binding in preparation for the second dimension. DTT and iodoacetamide were used to reduce and then alkylate sulphhydryl groups respectively. Strips were first washed for 15 minutes in equilibration buffer containing 2% (w/v) DTT and then washed in the equilibration buffer containing 2.5% (w/v) iodoacetamide also for

15 minutes. After equilibration, strips were washed in MOPS running buffer for 5 minutes and were placed in the well of either Novex Zoom Bis-Tris gel or pre-prepared 2D hand-cast gel. 10 µl of protein standard was pipetted in the first well and the IPG strip was overlaid with warm molten but not hot, 1% agarose to fix it in place. 7 cm strips were resolved using Bio-Rad's Mini Protean tetra-cell at constant 125V for 2 hours. 17 cm strips were resolved using Bio-Rad's Protean II xi cell system with cold water cooling and 4°C temperature for 20 hours with constant current of 22 mA. After the run gels were fixed overnight and stained with either colloidal blue or silver stain.

2.9 Gel Staining

After 1D-PAGE and 2D-PAGE, separated proteins were visualised using specific stains to visualise total and phosphorylated proteins. In this study, 3 different protein stains were used for protein staining on polyacrylamide gels. Pro-Q diamond stain was used for total phosphorylation visualisation, colloidal blue and silver stains were used for total protein visualisation.

2.9.1 Pro-Q Diamond Staining

To visualise total phosphorylation of proteins, 1D-PAGE gels were stained with phosphospecific Pro-Q Diamond stain. After electrophoresis, gels were placed in a clean plastic container with approximately 20 ml of gel fixative solution and were incubated overnight (~16h) in a cold room at 4°C. On the next day gels were washed with ultrapure distilled water 3 times to remove any residual fixative solution. Gels were then incubated in 10 ml of Pro-Q Diamond stain for 90 minutes in the dark at room temperature. Stain was poured off and 10 ml of Pro-Q de-stain solution was added. Gels were incubated in the de-staining solution for 30 minutes in the dark at room temperature. This step was repeated 3 times to reduce the background stain. Following de-staining, gels

were washed in ultrapure water for 20 minutes and imaged using ChemiDoc MP default settings for Pro-Q Diamond stain.

2.9.2 Colloidal Blue Staining

Total protein content on 1D and 2D gels was visualised using colloidal blue staining kit. The colloidal blue stain can detect as low as 10 ng of proteins in a gel. After 1D or 2D-PAGE separation, gels were fixed overnight at 4°C in a fixative solution on a rotary shaker. Fixative solution was discarded, and gels were washed 3 times in ultrapure water. Gels were then fixed in Colloidal blue fixing solution containing 20% (v/v) methanol, 20% (v/v) strainer A for 10 minutes on a rotary shaker at room temperature. Then 5% (v/v) of strainer B was added and gels were stained overnight. Next day, gels were de-stained several times with ultrapure water and imaged with ChemiDoc MP using white sample tray for colloidal blue stains.

2.9.3 Silver Staining

The silver staining technique is a very sensitive total protein staining technique that can detect less than one nanogram of proteins separated on a polyacrylamide gel. SilverQuest™ silver staining kit from Life technologies was used in this study. Silver stain was used to detect low protein quantities separated on 2D-PAGE gels and technique was performed according to manufacturer's protocol.

200 ml of sensitizing solution (30% (v/v) ethanol, 10% (v/v) sensitizer, topped up with ultrapure water), staining solution (1% (v/v) strainer, topped up with ultrapure water) and developing solution (10% (v/v) developer, 2 drops of developer enhancer, topped up with ultrapure water) were prepared fresh before staining. After electrophoresis, gels were washed in ultrapure water and then fixed in a fixative solution overnight. Fixative was decanted, and gels were

washed in 30% ethanol solution for 10 minutes. Ethanol was discarded, and sensitizing solution was added. Gels were incubated in a sensitizing solution for 10 minutes on a rotary shaker. Gels were then washed in 30% ethanol and then in ultrapure water consecutively for 10 minutes. Silver stain solution was added, and gels were incubated for 15 minutes. Gels were then washed briefly in ultrapure water and then developing solution was added. After proteins reached desired intensity (5 to 10 minutes after adding the developing solution) stopper solution was added. Gels were washed in ultrapure water and imaged using ChemiDoc MP.

2.10 Mass Spectrometric Analysis

Proteins separated by gel electrophoresis were sent for MS/MS analysis for identification of unknown polypeptide sequences. Separated bands or spot were first chosen from selected gels. Separated proteins were then accordingly excised using a scalpel and were placed in 1.5ml Eppendorf's with approx. 1ml of ultrapure water to prevent dehydration and drying out of gel cuts. Samples were stored at 4°C until further analysis. Selected samples were then sent to Life Sciences Department at University of Nottingham for MS/MS identification. Data of identified amino acids and matching proteins was then was received and matched to bands on the gel.

2.11 Western Blotting

After the separation of proteins by 1D SDS-PAGE, proteins were transferred onto a polyvinylidene difluoride (PVDF) membrane and were probed for specific antibodies. Firstly, gels were run according to SDS-PAGE conditions detailed in **2.8.3**. After running SDS-PAGE, gels were placed in 20 ml of transfer buffer (25mM Tris-base, 192mM Glycine, 20% (v/v) Methanol). Meanwhile, PVDF membranes were activated by soaking in 100% methanol and subsequent equilibration in transfer buffer until fully soaked in transfer buffer. PVDF

membranes are highly hydrophobic therefore methanol is used to allow aqueous solutions such as transfer buffer to penetrate the membrane and improve binding capacities of proteins. After membranes were activated, gels were then placed in transfer cassette on the cathode side with PVDF membrane on the anode side both supported by three sets of filter paper and supporting sponge on each side as shown in Figure 1. Transfer tank was placed in a box with ice to maintain running conditions cold and preventing overheating. The transfer sandwiches were placed in a transfer tank with an ice pack and run at 80V constant voltage for 120 minutes with a BioRad power pack. Transfer was paused after one hour to change the ice pack to keep transfer cool. After the run, the PVDF membranes were removed and stained with Safe Stain according to manufacturer protocol for visualisation of total protein transfer. Membranes were then air dried for further protein fixation on the PVDF membrane.

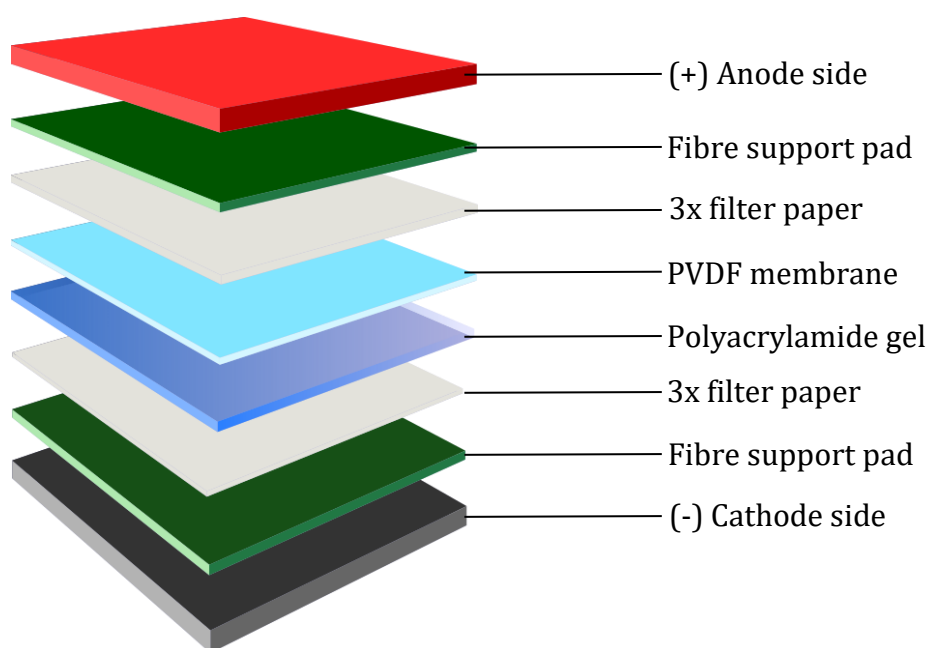


Figure 2-1| Order of Western Blotting 'transfer sandwich' set up for electrophoretic protein transfer from polyacrylamide gel to PVDF membrane. 'Transfer sandwich' was assembled on the cathode (negative plate) and all the materials were soaked in cold transfer buffer and placed on top of the cathode in order shown. Image author's own.

2.12 Staining PVDF membranes

To confirm efficiency of the transfer and for normalization of proteins the membranes were stained with MemCode™ Reversible Protein Stain kit. The stain is very sensitive but doesn't permanently bind to proteins and has minimal nonspecific interaction with PVDF. It is also compatible with Western Blot and does not interfere with HRP chemiluminescent detection. It serves as a good method of total protein visualisation without any downstream interference. Staining process was followed as per supplier instruction and membranes were imaged for quantification.

After the transfer, PVDF membranes were rinsed in a plastic container with ultrapure water three times. Approximately 10 ml of MemCode™ sensitizer was added and membranes were agitated on a rocker for 2 minutes. Sensitizer solution was removed, and 10 ml of MemCode™ Reversible Stain was added. The membranes were shaken on a rocker for approximately 1 minute after which stain was decanted and MemCode™ De-stain solution was added. Container was shaken manually, and solution decanted. This was repeated 3 times. Following, a De-stain:Methanol (1:1) solution was added and container was agitated for 5 minutes at a moderate speed. Solution was removed and membranes rinsed 3 times with ultrapure water. Membranes were imaged using ChemiDoc MP using Coomassie Blue protocol. The stain was then removed by immersing the PVDF in MemCode™ Eraser/Methanol (1:1) solution for 20 minutes. Solution was decanted, and membranes were rinsed again with ultrapure water 3 times. PVDF membranes were then left to air dry to increase permanent binding of proteins. The membranes were then ready for immunoblotting.

2.13 Immuno-Detection of Proteins

The PVDF membranes were activated with 100% methanol and equilibrated in PBS-T for 30 minutes. Afterwards, membranes were blocked for 1 hour with 5% non-fat milk (Marvel) or BSA blocking buffer. This step was

performed prevent unspecific binding of proteins. For PY20 tyrosine antibody, membranes were specifically blocked in 5% (w/v) BSA. BSA blocking was performed as casein protein contained in milk can interfere with some phospho-specific antibodies leading to weaker signal. Primary antibodies were diluted in a blocking buffer at 1:500 or 1:1000 concentration unless otherwise stated and membranes were blotted overnight (approx. 16h) in a cold room at 4°C. The following day the PVDF membranes were washed three times in PBS-T for 5 minutes and incubated with anti-species secondary antibody at 1:1000 dilution for 1 hour at room temperature. Membranes were then washed 3 times in PBS-T for 10 minutes each time. Then, the PVDF membranes were incubated in Chemiluminescent substrate A and B solution (1:1) for 5 minutes at room temperature. After incubation, protein expressions on PVDF membranes were visualised using ChemiDoc MP and quantified using ImageLab 6.0.

2.14 Detection of Oxidative Stress with OxyBlot™ Kit

Proteins are a common target of oxygen free radicals and other reactive oxygen species. The subsequent attachment of reactive electrophiles such as carbonyl compounds can irreversibly alter protein structure and function. Modification of proteins in such fashion can occur in physiological and pathological processes. Formation of carbonyl groups on protein side chains can therefore be used as biochemical marker of general oxidative stress. OxyBlot™ kit allows for immunoblot detection and quantification of carbonyl groups introduced into proteins by oxidative modification.

For the OxyBlot™ method, desired concentration of proteins was calculated using modified Lowry protocol and 20 µg of protein was used for each sample. Samples were first denatured by addition of SDS to a final concentration of 6%. Samples were then derivatized by addition of 1x DNPH solution and incubation at room temperature for 15 to 20 minutes. For the negative controls, 1x derivatization-control solution was added instead. After derivatization, appropriate amount of neutralising solution was added to all tubes. Reducing

agent 2-mercaptoethanol was also added to the sample to achieve 0.74M final concentration. Samples were then either run on 1D-PAGE gels or stored at -20°C.

Prepared samples were run on a 10% Polyacrylamide gel as described in chapter 2.7.4. and transferred onto a PVDF membrane as described in chapter 2.10. Membranes with blotted OxyBlot™ samples were blocked for 1 hour at room temperature in 5% milk (Marvel) made in PBS-T buffer (w/v). PVDF membranes were then sealed in plastic pouches and blocked with OxyBlot™ 1^o Antibody and blocking buffer at 1:150 (v/v) dilution for 16 hours at 4°C. Next day, membranes were washed in PBS-T 3 times for 5 minutes each. Then, membranes were incubated in 2^o OxyBlot™ antibody in blocking buffer at 1:300 dilution (v/v) for 1 hour at room temperature. After the incubation, membranes were washed again with PBS-T 3 times for 5 minutes. Membranes were covered in chemiluminescent reagent for 5 minutes and then imaged using ChemiDoc MP.

2.15 Quantification of Proteins on Gels & PVDF membranes

Relative protein expression was measured using Bio-Rad's Image Lab (ver. 6.0.1) software. Adjusted volume of protein bands and total lane protein expression was quantified with mean background subtracted automatically. Data was exported to GraphPad-Prism and changes in expression of various proteins were analysed.

2.16 Normalisation of Protein Expression

Differences and variations in sample loading between lanes are often unavoidable even after sample quantification and uniform sample loading. Normalisation is a robust method that serves as an internal loading control and correction for technical errors and small discrepancies between samples (Taylor and Posch, 2014). Housekeeping proteins (HKP) that are universally and abundantly expressed across cells such as actins, tubulins or GAPDH, are the

most common choice of normalisation control. However, studies suggest that some of the most common HKP have differential expression in pathological conditions therefore use of single HKP as normalisation control might be limited (Lee, 2018). In this study, total protein was used as an alternative to HKP normalisation. Total protein is a simple and effective way to determine whether equivalent loading has been achieved (Eaton et al., 2013). Results obtained from protein bands have been corrected according to the matching expression of total protein on stained PVDF membranes. These values were then used for statistical analysis of protein expression.

2.17 Milliplex MAP Assays

Milliplex MAP is a multiplex quantitative immunoassay able to identify total and phosphorylated protein levels from cell lysates and tissue homogenates. It uses fluorescent-coded magnetic beads for detection of major proteins in many various cellular pathways. Beads are covered in a specific capture antibody which bind to the analyte. Biotinylated detection is introduced to the bead bound analyte and Streptavidin-Phycoerythrin conjugate is added to complete the assay. Samples are run through MAGPIX system and phycoerythrin is excited by laser illumination to produce fluorescent signal that can be quantified and relative protein expression in a sample can be quantified. In this study, we investigated various pathways and the phosphorylation states of various proteins. In this study, 3 different kits have been used. Details of the target proteins are shown in Table 2-2.

| Milliplex MAP Kit | Target Proteins |
|--------------------------|---|
| Phosphor/Total mTOR | Total mTOR, phospho-mTOR (Ser2448) |
| Phosphor/Total JNK | Total JNK, phospho-JNK (Thr183/Tyr185) |
| 9-Plex Multi-Pathway | ERK/MAP kinase (Thr185/Tyr187), Akt (Ser473), STAT3 (Ser727), JNK (Thr183/Tyr185), p70 S6 kinase (Thr412), NF-κB (Ser536), STAT5A/B (Tyr694/699) CREB (Ser133), p38 (Thr180/Tyr182) |

Table 2-2 Kits used in Milliplex MAP assay with their corresponding target proteins and phosphorylation site. JNK and mTOR kits were specific for total and phosphorylated protein expression. 9-Plex targeted a wide range of only phosphorylated proteins. Specific site of phosphorylation is described in the table.

Protein homogenates were diluted in Milliplex assay buffer at least 1:1 dilution. 25 µg of protein was prepared per well for each sample (concentration of 1 µg/µl). Black, clear bottom 96-well plate was pre-wetted with 50 µl of assay buffer on a rotary shaker for 10 minutes at room temperature. Assay buffer was decanted and 25 µl of sample was added to each well. 1x bead suspension (prepared in advance) was vortexed for 10 seconds and 12.5 µl was added to each well loaded with the sample. Plate was incubated overnight (16 – 20 hours) at 4°C, protected from light on a rotary shaker with moderate speed. Next day, handheld magnet was attached to the plate and beads settled for 120 seconds. With magnet still attached solution was decanted by gently tapping the plate onto a paper towel. Magnet was then removed, and plate was washed with 100 µl of assay buffer per well. Magnet was attached again, and beads settled for 120 seconds. Assay buffer was then decanted. This process was repeated twice. After washing the plate, 12.5 µl of detection antibody was added and plate was incubated for 1 hour on a rotary shaker at room temperature. After incubation, handheld magnet was attached to the plate and after 120 seconds, detection antibody was decanted. 12.5 µl of SAPE was added and left to incubate on rotary shaker for 15 minutes. Without removing SAPE, 12.5 µl of amplification buffer was added and plate was further incubated for 15 minutes on a rotary shaker. Then handheld magnet was attached, and SAPE/amplification buffer was decanted. 100 µl of assay buffer was added to each well and plate was analysed using Luminex MAGPIX system's pre-programmed protocols.

2.18 Cell Culture

2.18.1 Media Preparation & Cell Maintenance

U87 MG cells were maintained in high glucose (4.5g/L) DMEM media containing L-glutamine and sodium bicarbonate with addition of 10% FBS and 1% P/S. All media was prepared under sterile condition. To make the growth media solution, 55ml of stock media was first removed from 500 ml bottle and 50 ml of FBS and 5 ml of P/S was added.

Cells were maintained in T75 flasks with 15 ml of growth media and cultured in an incubator set to 37°C and 5% CO₂. Flasks were checked daily and media was changed every other day. Cells were split and passaged when confluence reached 70% or more. U87 doubling time takes approximately 24 hours and cells were usually passaged twice a week depending on initial seeding concentration.

2.18.2 Seeding Cells from Frozen

Before seeding the cells, T75 flask with appropriate amount of growth media was placed in an incubator set to 37°C to pre-warm the media. Meanwhile, cryovials with frozen cells were removed from liquid nitrogen storage tanks and immediately transferred to a warm water bath set to 37°C. Cells were then transferred to the pre-warmed flask using a 2 ml Pasteur pipette and placed in an incubator with 5%CO₂ at 37°C. After the first 24h, media was replaced, and cells were monitored daily.

2.18.3 Passaging Cells

Cells were passaged when confluence in the flask reached 70% or more. To passage cells, media in the flask was first removed and cells were briefly washed with HBSS to remove any residual serum. After the wash, 3 ml of Trypsin-EDTA was added per T75 flask and cells were incubated at 37°C, 5% CO₂ for 2 to 5 minutes. After cells were detached, 3 ml of pre-warmed media was added to terminate trypsin reaction. Cells were aspirated from the plate into a 15 ml falcon tube and spun down at 800 rpm for 5 minutes. Supernatant was carefully discarded, and cell pellet was resuspended in 2 ml of growth medium. Cells were then seeded at desired volume into a new T75 flask containing 14 ml of pre-warmed media or onto a 96-well plate with 100 µl of media per well.

2.18.4 Counting Cells

Number of viable cells was determined before seeding onto T75 flasks and 96-well plates. Cell passaging was performed as described in chapter 2.18.3. After resuspension of cellular pellet in growth medium, equal amounts of cell suspension and trypan blue were mixed in an Eppendorf to make 20 µl and 10 µl of this solution was placed onto a cell counting slide. Cells were counted using TC10 automated cell counter. Viability of the cells was measured by the uptake of trypan blue. Live cell count was used to calculate seeding density for T75 flask and 96-well plates.

2.18.5 Treating Cells

U87 cells have been treated with a variety of agents to measure efficacy and toxicity to the cancer cell line. Three different agents have been used either alone or in combination to elicit effect on the cell culture after 24 hours and 48 hours of treatment. Viability and proliferation of the cells was assessed using an

MTT assay after given timepoint. All drug treatments were carried out on 96-well plates under normal culture conditions. During passaging, cells have been seeded onto 96-well plates at 5×10^3 cells per well and treatment was commenced after 4 to 6 hours post seeding to allow cell attachment to the plate.

2.18.5.1 Etoposide

50 mM Etoposide stock was stored at -20°C. Following concentrations were prepared for cell treatment in growth media: 0.005mM; 0.001mM; 0.005mM; 0.01mM; 0.05mM; 0.1mM; 0.5mM; 1mM; 2mM.

2.18.5.2 SAM

50mM of SAM stock was prepared by dissolving 23 mg of powder in 906 µl of media under sterile conditions. Following concentrations were then prepared in growth media: 0.001mM; 0.005mM; 0.01mM; 0.05mM; 0.1mM; 0.5mM; 1mM; 5mM; 10mM; 20mM.

2.18.5.3 CBD

CBD was prepared by firstly dissolving powder in ethanol and diluting it down to 100 µM concentration in media. Following concentrations were then made: 2.5 µM; 5 µM; 7.5 µM; 10 µM; 12.5 µM; 15 µM; 20 µM; 25 µM; 30 µM; 35 µM; 40 µM; 45 µM; 50 µM.

2.18.5.4 Antagonist + CBD

Many studies have shown CBD's actions are mediated independent of receptor activation, however as the pharmacology of CBD has begun to unravel, new receptor targets have come to light presenting the possibility by which CBD could mediate its effects through. Therefore, for this study a wide range of antagonists was used to probe the mechanism of action of CBD. These are listed in the table below:

| Antagonist name | Target Receptor |
|-----------------|---|
| Way100 | 5-HT(1A) (serotonin receptor) |
| CID16200 | GPR55 (G protein-coupled receptor) |
| AM630 | CB2 (cannabinoid receptor) |
| GW662 | PPAR- γ (Peroxisome proliferator-activated receptor gamma) |

Table 2-2/ Table showing antagonist product name and their designed receptor target

2.18.6 Cell Proliferation Assay with MTT

To assess cell proliferation and viability MTT assay was used. Active cells can convert MTT tetrazolium salts into formazan dye by cell enzymes such as dehydrogenases and reductases. Quantity of formazan which is proportional to viable cells can then be measured at 570 nm absorbance (Riss et al., 2004). Stock solutions of MTT were stored at -20°C protected from light. After thawing MTT, 1 ml of stock solution was diluted in 9 ml of pre-warmed growth media. Cells seeded on a 96-well plate was removed from an incubator and media was gently aspirated from the wells. 100 μ l of media/MTT solution was added to all the wells and plates were wrapped in aluminium foil and placed back in an incubator. Cells were incubated for 2 hours after which media was aspirated off again and 100 μ l of DMSO and 2-propanolol (1:1 (v/v)) was added to each well to solubilise formazan. Cells were incubated at room temperature for 10 minutes and absorbance at 570 nm was read using Multiskan Spectrum Microplate Reader.

2.19 Statistical analysis

To carry out statistical analysis of obtained data, GraphPad-Prism (ver. 7.03) software was used. ANOVA and Student's t-test, statistical significance was accepted at $P < 0.05$ threshold. For data not fitting Gaussian distribution (non-parametric), Mann-Whitney test was used instead of Student's t-test. Error bars plotted on graphs are presented as SEM unless otherwise stated.

3 Results

3.1 1D-SDS PAGE

To better understand the changes in GBM proteome, samples have been fractionated using a centrifugal differentiation method to separate cytosolic, membrane and nuclear compartments of cells. Proteins from crude cytosolic, membrane and nuclear fractions were separated by their denatured molecular weight using one-dimensional polyacrylamide gel electrophoresis. Tumour samples have been resolved along controls to allow for comparison of protein expression between GBM tissue and healthy brain. Colloidal blue staining allowed for visualisation of total protein whereas Pro-Q Diamond is specific for visualisation of total phosphorylation. Total protein expression was initially investigated to determine whether there are major proteomic differences in GBM tumours total protein as compared to normal brain. Electrophoretic separation of proteins serves as simple but very powerful method to observe minor to great proteomic changes in tissues and can be used as a first step in high throughput separation of complex protein mixtures. In our experiments colloidal blue stain was used as it is a cost effective and reliable method of total protein staining that can detect proteins of as low as 10ng in a polyacrylamide gel.

3.1.1 1D-PAGE Analysis of Proteins with Colloidal Blue Total Protein Staining

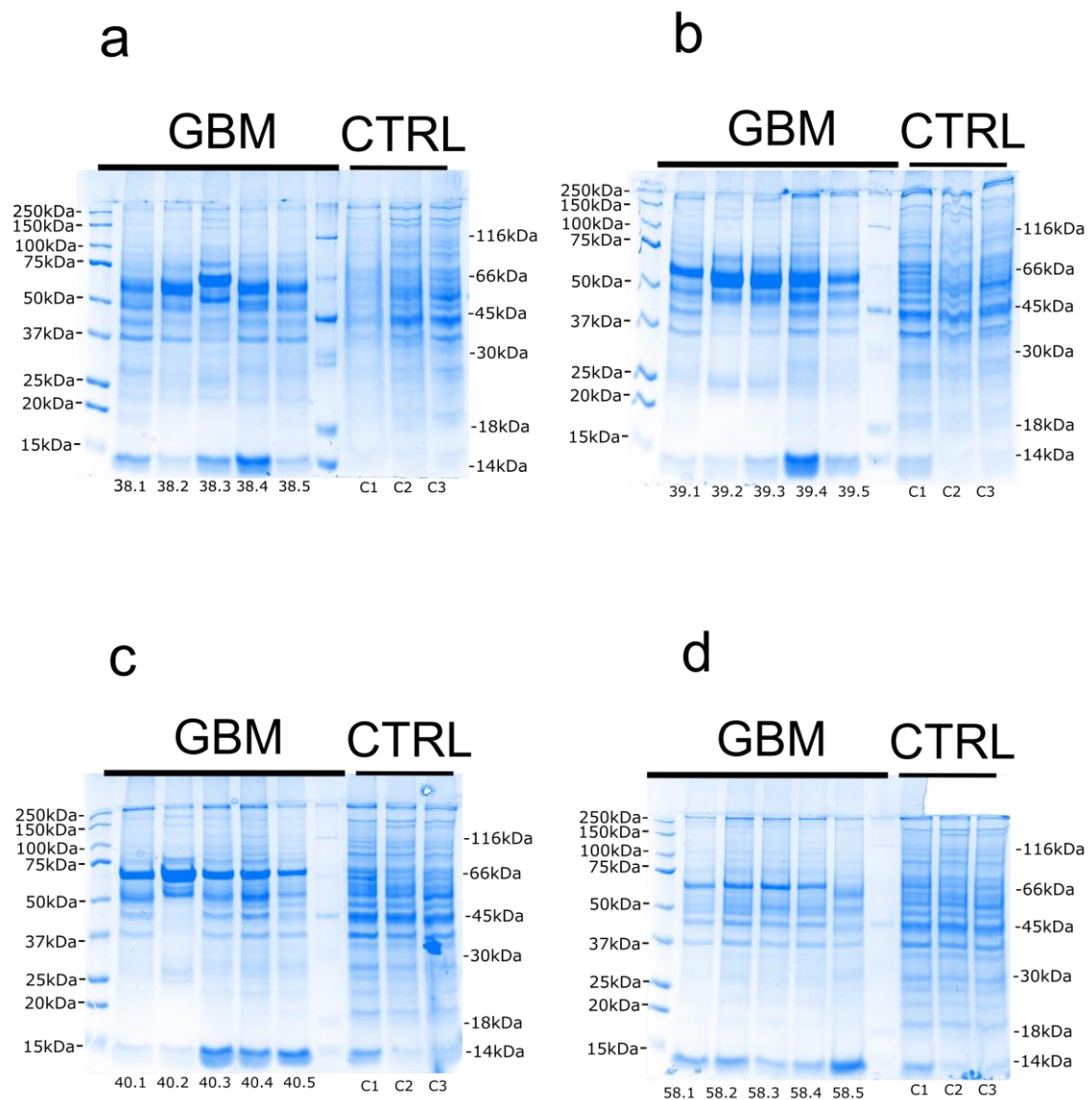


Figure 3-1/ Gels of cytosolic proteins separated by 1D-PAGE and stained with colloidal blue for total protein visualisation. 25 μ g of cytosolic proteins has been resolved for each sample from five different regions of GBM tumour tissue from four patients along with three control samples from healthy brain tissue (a-d). First lane of each gel has been loaded with Prestained Protein Standard and seventh well was loaded with Peppermint Stick Standard for phosphorylation specific dyes.

Separation of cytosolic proteins has revealed the discrete proteome of GBM tissue in four patients and five distinct tumour regions. Figure 3-1 shows cytosolic total protein of all samples resolved by 1D-SDS page. Total protein separation has exhibited some reduction of certain proteins between 15kDa to 20kDa, such as that on sample 38.2, 38.3 (Figure 3-1, a), 39.1 to 39.3 (Figure 3-1, b), 40.1, 40.2 (c) and 58.1 to 58.5 (d). Additionally, there was visible increase in protein content at approximately 66kDa for GBM samples 38 (a), 39 (b) and 40 (c), especially for lanes 38.3 (a) and 40.2 (c). Sample 58 (d) has also exhibited increase in protein content at approx. 66kDa, but it was not as prominent as other GBM tumours. Several small proteins below 15kDa also had differential expression between various tumour sites and healthy tissue. Nevertheless, resolution of cytosolic proteins displayed very similar proteomic pattern to control healthy brain tissue. Controls remained relatively constant in total protein content across all gels suggesting that changes in proteomic content could be due distinct differences in samples rather than loading and running methods. The 1D-PAGE separation was successful at resolving cytosolic GBM and brain tissue proteins and suggests that there might be some specific changes in protein expression between GBM samples and healthy tissues. On the other hand, it also shows that several proteins display similar pattern to healthy brain tissue. Further proteomic characterisation was carried out to define differences between GBM and healthy brain in cytosolic proteins.

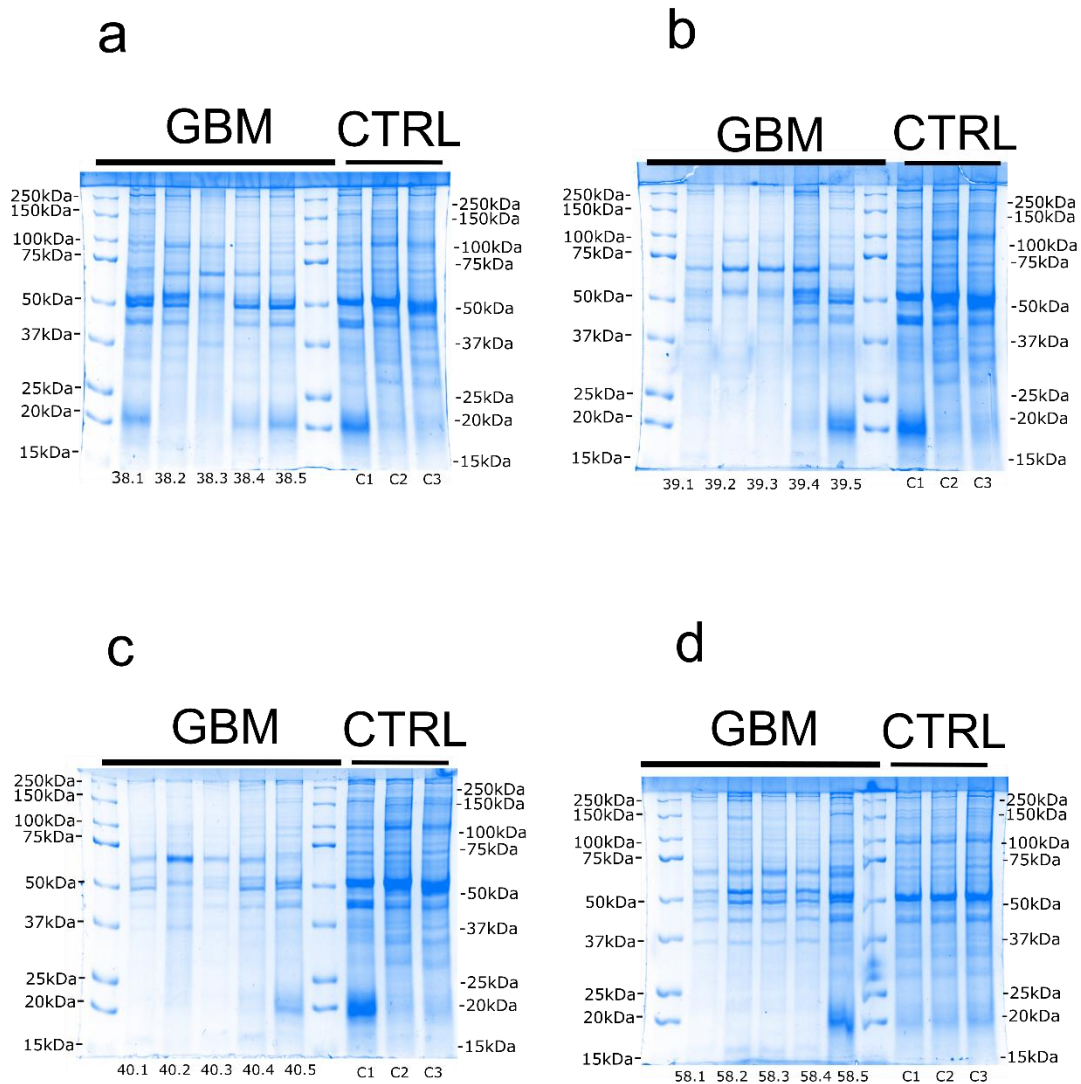


Figure 3-2| Gels of nuclear proteins separated by 1D-PAGE and stained with colloidal blue for total protein visualisation. 25 μ g of nuclear proteins has been resolved for each sample from five different regions of GBM tumour tissue from four patients along with three control samples from healthy brain tissue (a-d). First and seventh lane of each gel has been loaded with Prestained Protein Standard for determination of molecular weight.

Following cytosolic separations of proteins, we have separated nuclear fractionate of GBM and healthy brain tissue shown in Figure 3-2. The differences between GBM and healthy tissue were less projecting, though some differences were visible. There was reduction of some protein content especially in sample 39 (b), lanes 39.1, 39.2 and 39.3, sample 40 (c), lanes 40.1, 40.2 and 40.3 and sample 58 (d), lane 58.1, particularly below molecular weight below 37kDa. Also, an additional band at approx. 50kDa was visible including sample 38 (a), lane; 38.1, 38.2, 38.4 and 38.5, sample 39 (b), lane; 39.1, 39.4 and 39.5, sample 40 (c), lane; 40.1, 40.4, 40.5, sample 58 (d) in all lanes. Apart of those and few other

minor differences, the nuclear fraction displayed similar total protein expression to healthy brain tissue. Nuclear sample was successfully resolved on 1D-PAGE gels though further investigations are necessary to define specific proteomic differences between healthy and brain tumour tissue.

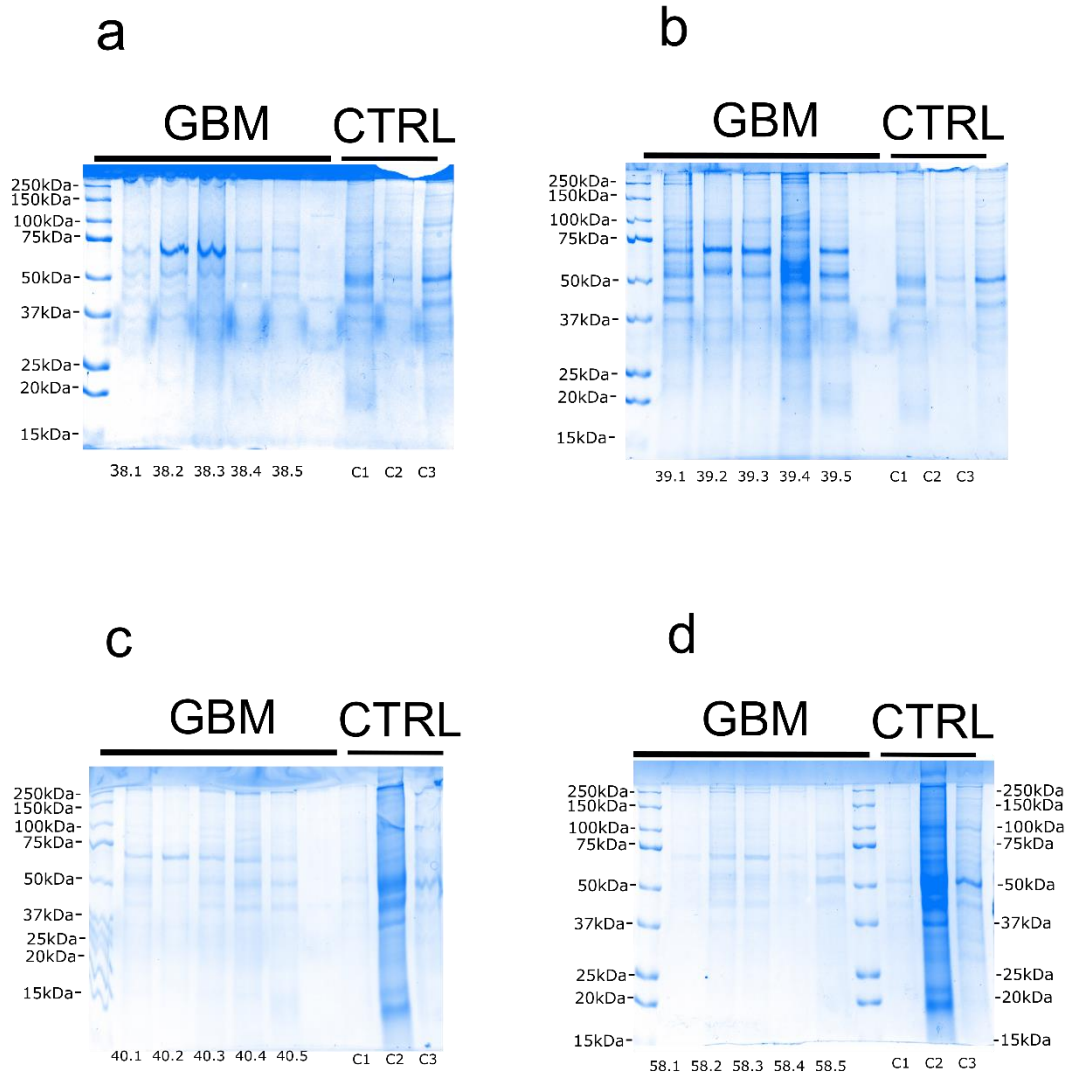


Figure 3-3| Gels of membrane proteins separated by 1D-PAGE and stained with colloidal blue for total protein visualisation. 25 μ g of membrane proteins has been resolved for each sample from five different regions of GBM tumour tissue from four patients along with three control samples from healthy brain tissue (a-d). First and seventh lane of each gel has been loaded with Prestained Protein Standard and seventh well was loaded with Peppermint Stick Standard for phosphorylation specific dyes (apart of gel 'd' where seventh well was loaded with Prestained Protein Standard) for determination of molecular weight. However, protein standard in the seventh lane has not worked in gels 'a to c'.

Membrane bound proteins were resolved by 1D-PAGE in a same way as cytosolic and nuclear proteins, shown in Figure 3-3. The results show a lot of variability between gels as well as samples which could be related to sample preparation or SDS-PAGE running condition. Some proteins in sample 38 (a) have displayed wavy pattern which could be due to running conditions or uneven gel composition. This can also be seen in the gel for sample 40 (c) where protein standard is extremely wavy below 50kDa mark. Controls have also been poorly resolved and a lot of streaking can be seen in gels 'c' and 'd' especially in second control, 'C2'. For most of GBM samples, resolution of proteins below 37kDa has been lost, as well as for several control samples. This suggests that the preparation of samples as well as conditions of running the gel should be further optimised to reduce variability in samples and gels. Whether this is due to large size of most of membrane bound proteins or actual loss of proteins needs to be further defined. Low abundance of proteins in samples 40 (c) and 58 (d) is also problematic as the bands are barely visible. To avoid this, gradient concentration gels (i.e. 4-12% acrylamide gels) could be used to determine optimal gel conditions of variously sized membrane proteins. Alternatively, membrane bound proteins could be run on gels with low percentage acrylamide concentration such as 4% to 8% to accommodate large protein size. Clean up of all samples should be considered in the future as residues of phospholipid bilayer residue could be interfering with protein quantification and resolution of proteins causing smearing and low abundance of protein in gels. Precipitation methods which could result in better resolution and cleaner separation should be considered if carrying out further delineation of membrane bound proteins. Additionally, buffers should be considered in sample preparation as harsher conditions for protein lysates could enhance solubilisation of hard to solubilise proteins. Nevertheless, some differences were observed in membrane proteins especially for gels 'a' and 'b' just below 75kDa marker. However, due to poor reproducibility and resolution of gels with lack of appropriate control the conditions for separation should be further optimised for any future investigations of membrane bound proteins in GBM and healthy brain tissue.

3.1.2 1D-PAGE Analysis of Proteins with Pro-Q Diamond Total Phosphorylation Staining

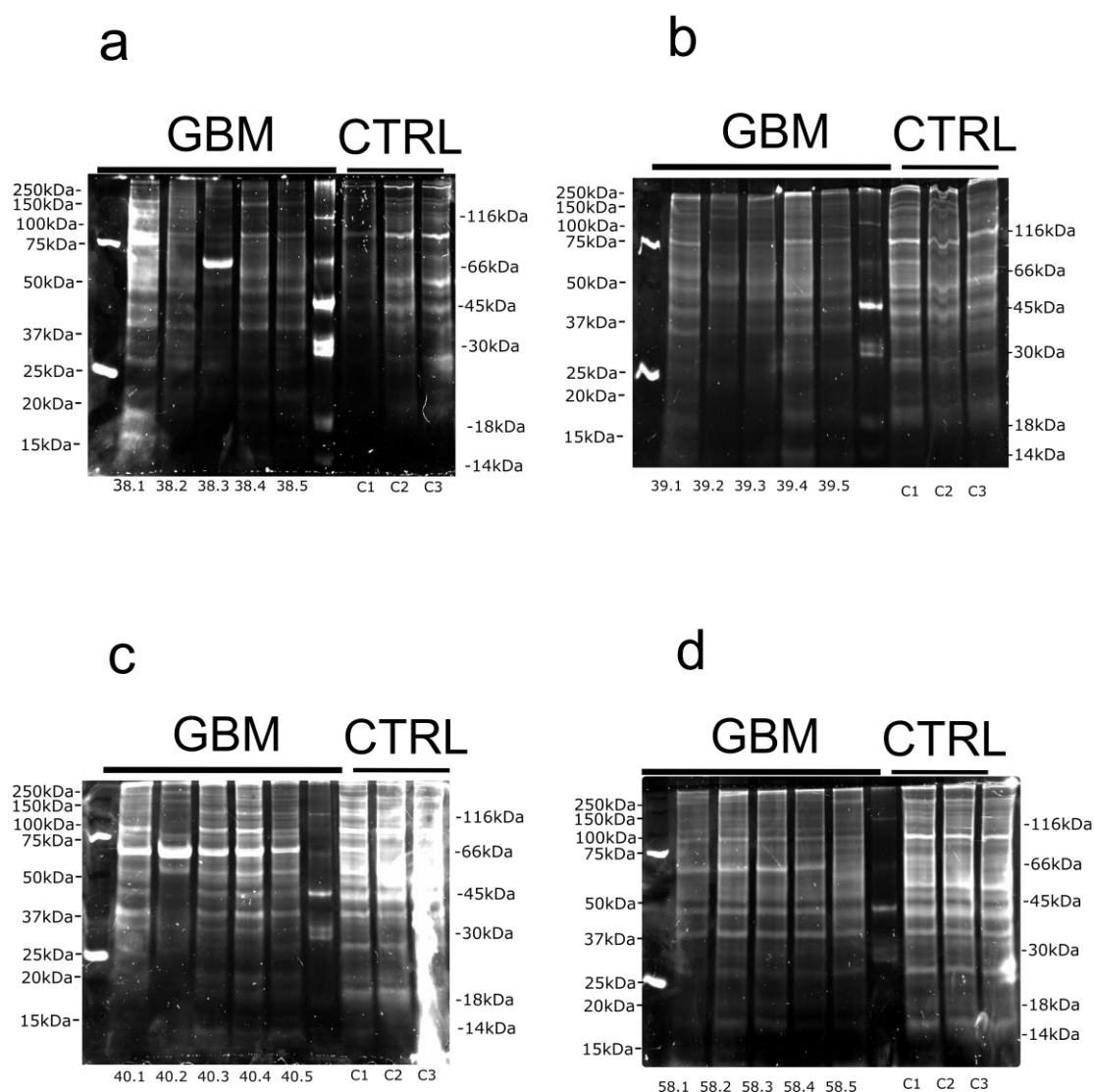


Figure 3-4| Gels of cytosolic proteins separated by 1D-PAGE and stained with Pro-Q Diamond for total protein phosphorylation visualisation. 25 μ g of cytosolic proteins has been resolved for each sample from five different regions of GBM tumour tissue from four patients along with three control samples from healthy brain tissue (a-d). First and seventh lane of each gel has been loaded with Prestained Protein Standard and seventh well was loaded with Peppermint Stick Standard for phosphorylation specific dyes.

In addition to colloidal blue staining, cytosolic proteins have been stained with phospho-specific dye to reveal changes in total protein phosphorylation, seen in Figure 3-4. Staining for total phosphorylation of proteins revealed few changes in total protein phosphorylation across different tumour regions in. Because phosphorylation is one of the most common PTMs in cells, phosphorylation cell-wide phosphorylation of many proteins of all samples was expected. Similarly, to colloidal blue total protein stain there was increased phosphorylation at highly expressed sites particularly at a region of approx. 66kDa molecular weight. This can be seen in gel 'a' lane 38.3 and gel 'c' all lanes. This could be caused by already increased cytosolic content of these bands as seen in Figure 3-1. Of interest is one highly prominent band at lane 38.3 at 66kDa (c) which stands out from other bands and lanes. This corresponds to samples at the tumour core and similar expression can be seen in gel 'c', lane 40.2 which also corresponds to the tumour core. Whether this is the same protein showing similar properties and amount of phosphorylation should be further investigated.

Pro-Q diamond has been successful at staining of phosphorylated proteins in cytosolic fractionate for all GBM samples and healthy brain tissue. This is further confirmed by presence of Peppermint Stick protein standard. Peppermint Stick standard contains two proteins ovalbumin and β -casein which are phosphorylated. During Pro-Q diamond staining, only these proteins had a detectable signal as compared to other proteins in the standard which can be seen in Figure 3-1 on lane seven of each gel. This shows that mainly phosphorylated proteins have been detected. However, to optimise the detection and visualisation of phosphorylated proteins the background of the obtained image would need to be adjusted and normalised to positive control of the Peppermint Stick phosphorylated proteins. In addition, two proteins from Pre-stained protein marker, at molecular weight of 25kDa and 75kDa, have also produced a signal from the Pro-Q diamond stain. Although the manufacturer does not disclose the content of the Pre-stained molecular protein marker, these could also contain phosphorylated proteins which produce a strong signal. Because of technical difficulties and lack of necessary reagents, Pre-stained Protein Marker

has been used in further 1D-PAGE experiments and Pro-Q diamond staining instead of Peppermint Stick protein marker.

Furthermore, ChemiDoc MP imaging system used in the experiments does not reach the optimal wavelength for the detection of phosphorylated proteins by Pro-Q diamond stain. As per manufacturer instructions, the optimal excitation/emission is approx. 530-560nm wavelength, though it can also be detected by transilluminator at 300nm wavelength with reduced sensitivity (Invitrogen, 2010). ChemiDoc MP transilluminator has therefore been set for the default Pro-Q Diamond detection at 300nm wavelength though this can lead to three- to ten-fold lower sensitivity. The detectable range of the wavelength should be considered when using Pro-Q diamond stain and appropriate equipment should be used for the optimal detection of the signal in future experiments.

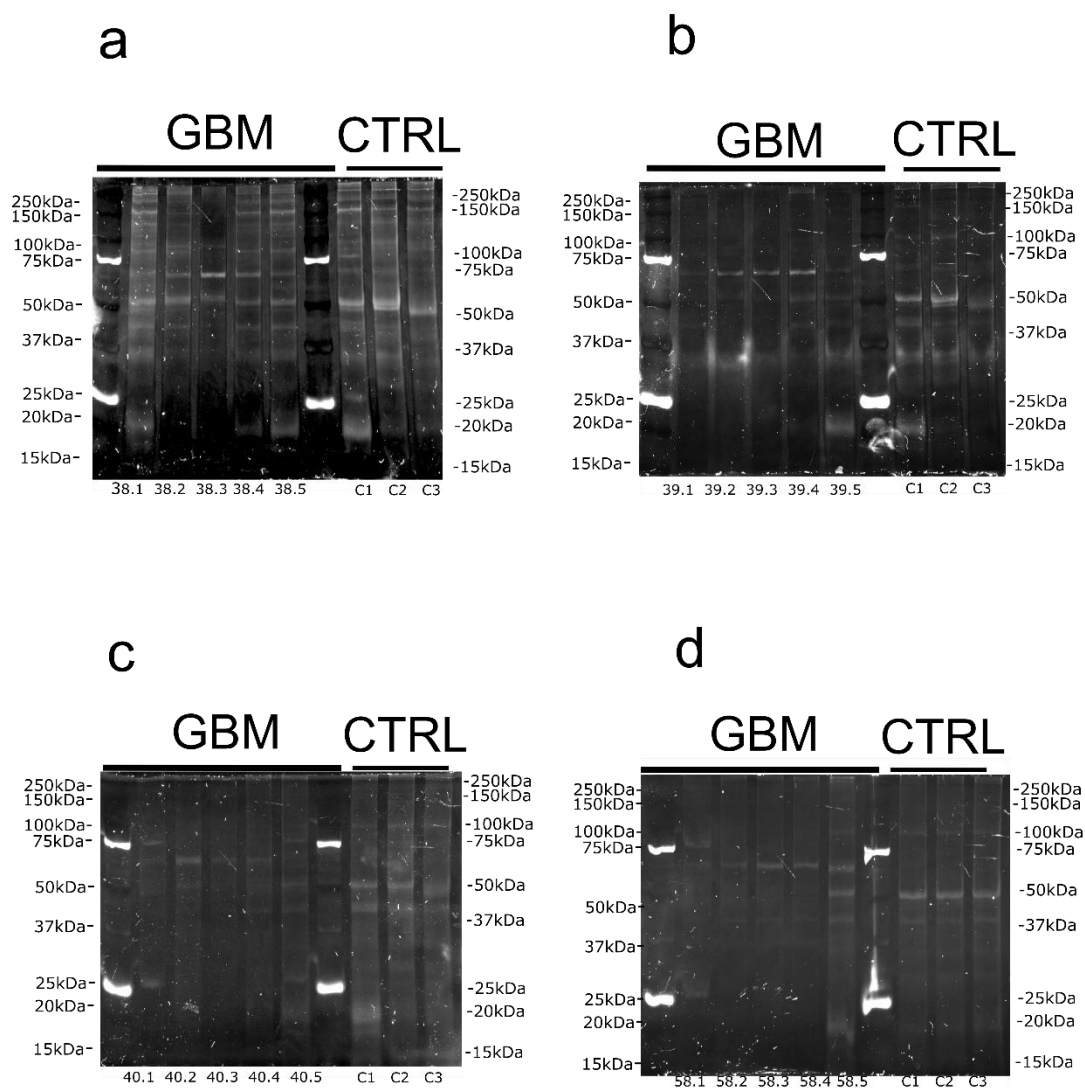


Figure 3-5| Gels of nuclear proteins separated by 1D-PAGE and stained with Pro-Q diamond for total protein phosphorylation visualisation. 25µg of nuclear proteins has been resolved for each sample from five different regions of GBM tumour tissue from four patients along with three control samples from healthy brain tissue (a-d). First and seventh lane of each gel has been loaded with Prestained Protein Standard for determination of molecular weight.

Pro-Q diamond staining of the nuclear fractionate has produced a detectable signal as shown in Figure 3-5. The bands in gel 'a' are most prominent and bands in gels 'b', 'c' and 'd' are very faint. This suggests that staining for phosphorylation in the nuclear protein fraction might not have been optimal and could be further optimised. Although separation and staining of these proteins has been successful it is difficult to distinguish any minor or major differences in

phosphorylation of various proteins. Some bands are more prominent such as those on gel 'b' below 75kDa mark of sample 39, GBM tissue. There was some unique phosphorylation across few samples. For example, there is a repeating pattern across all GBM samples of proteins just below 75kDa marker which is consistent with total protein gels. It is difficult to determine whether this is particularly different from the controls, however. Optimisation of this technique is necessary to reach any conclusion on total phosphorylation changes in nuclear fractionate between GBM and healthy brain tissue. Seeing as the total protein staining with colloidal blue has yielded good results for protein separation it should also be considered that perhaps less phosphorylation could be occurring in the nucleus. The more probable cause of the poor signal is likely due to methodology not being optimised for the specific proteins. Contents such as DNA, lipids and various salts could potentially interfere with signal. Methods for desalting and delipidating the protein lysate prior to SDS-PAGE electrophoresis could avoid high background and poor specificity. It is therefore highly recommended that such methods be used for future research into phosphoproteins.

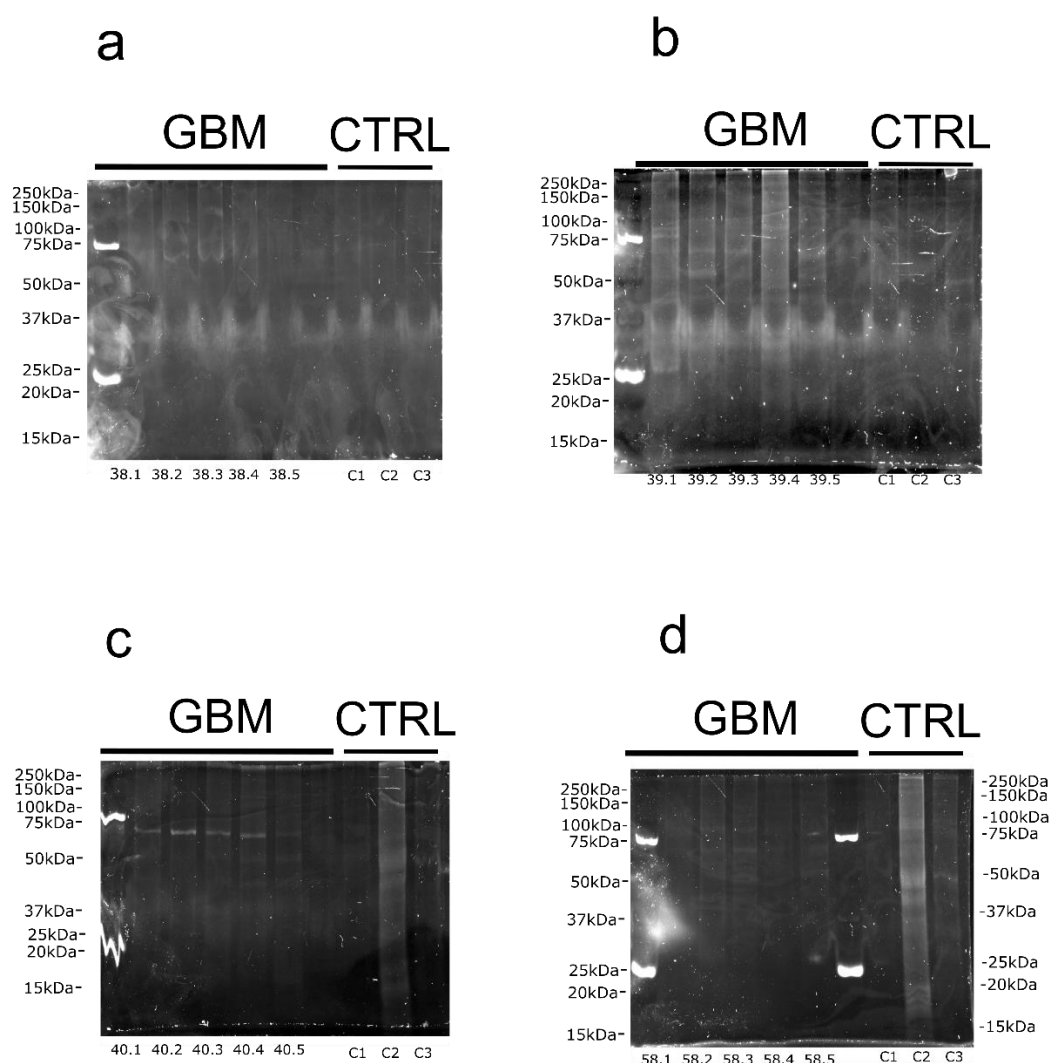


Figure 3-6| Gels of membrane proteins separated by 1D-PAGE and stained with Pro-Q diamond for total protein phosphorylation visualisation. 25µg of membrane proteins has been resolved for each sample from five different regions of GBM tumour tissue from four patients along with three control samples from healthy brain tissue (a-d). First and seventh lane of each gel has been loaded with Pre-stained Protein Standard and seventh well was loaded with Peppermint Stick Standard for phosphorylation specific dyes (apart of gel 'd' where seventh well was loaded with Pre-stained Protein Standard) for determination of molecular weight. However, protein standard in the seventh lane has not worked in gels 'a to c'.

Following in the same steps as with the previous phospho-specific stain of nuclear fraction, the staining of membrane bound proteins with Pro-Q diamond stain was least successful and yielded poor signal from most samples. This is represented by Figure 3-6 of total phosphorylation staining of membrane fractionate. Amassing results from staining with colloidal blue of total protein, it should again be stressed that membrane bound proteins need to be specifically

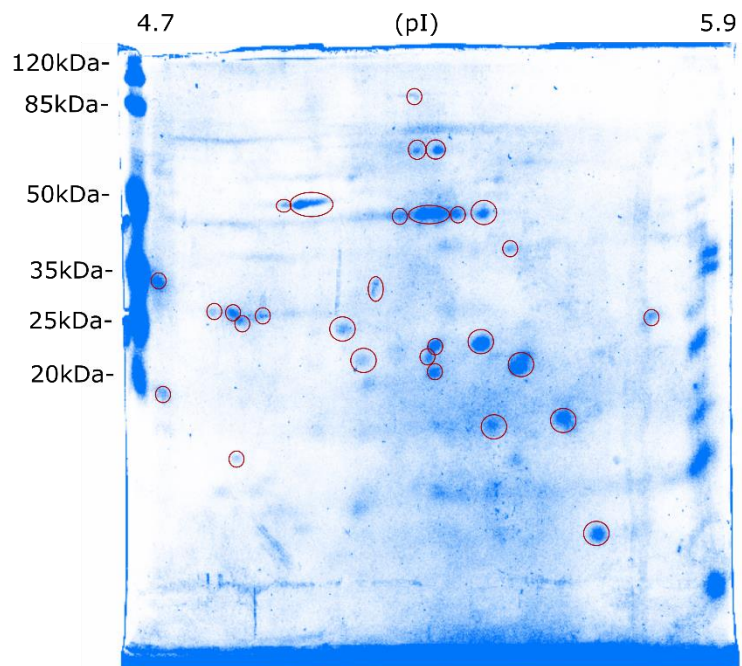
optimised before electrophoretic separation. The images from Figure 3-6 are very difficult to interpret and further tweaking of the staining process as well as sample preparation is necessary.

3.2 2D-PAGE

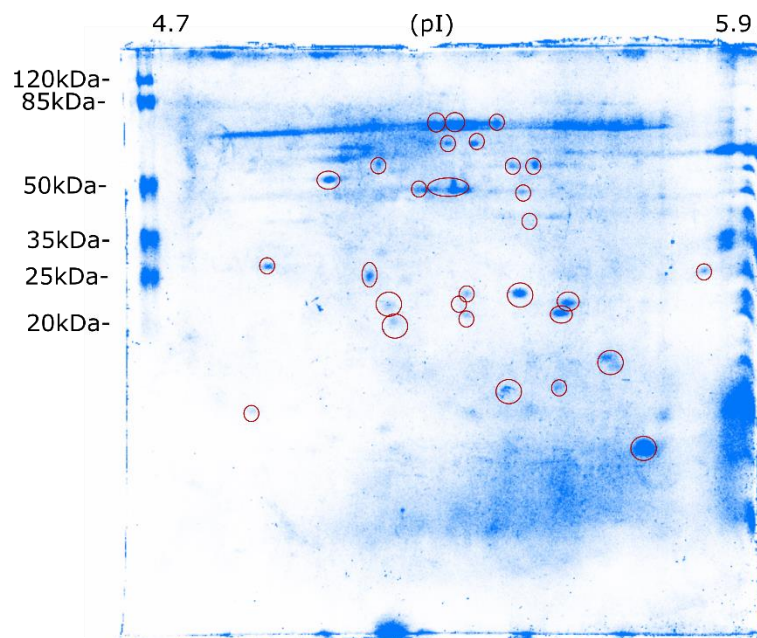
To further our methodology of proteomic investigations, 2D-PAGE was used to resolve proteins according to their molecular weight and net charge. Addition of second dimension to molecular weight separation of proteins offers a robust method for investigation of proteomic changes and PTM's of complex samples. The modification of proteins often confers difference in charge resulting in change of protein's isoelectric point. Therefore, methods such as 2D-PAGE are ideal for identifications of these modifications including phosphorylation, ubiquitination, acetylation and other. Additionally, 2D-PAGE is commonly used for profiling of expression and presence or absence of spots is informative of the varying promote. The separation of a complex protein mixture into its individual components through 2D-PAGE remains as a powerful proteomic tool and often precedes sequencing methods for high throughput analysis.

In this study, GBM tumour proteome expression was compared to a healthy brain PFC but also, expression of proteins was investigated within three different GBM regions. Resolved proteins gave been stained for total protein and imaged for spot detection.

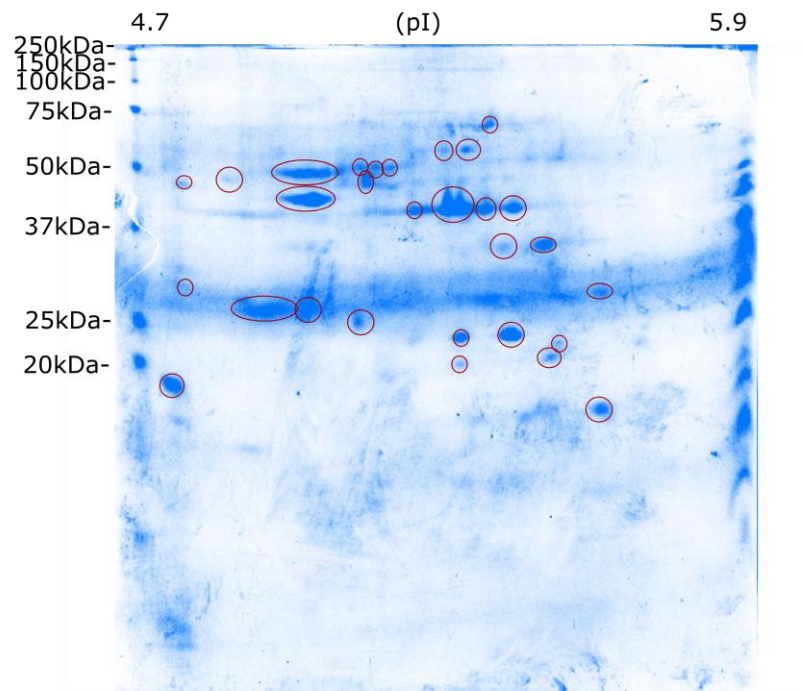
a Sample 38.1 Tumour Rim



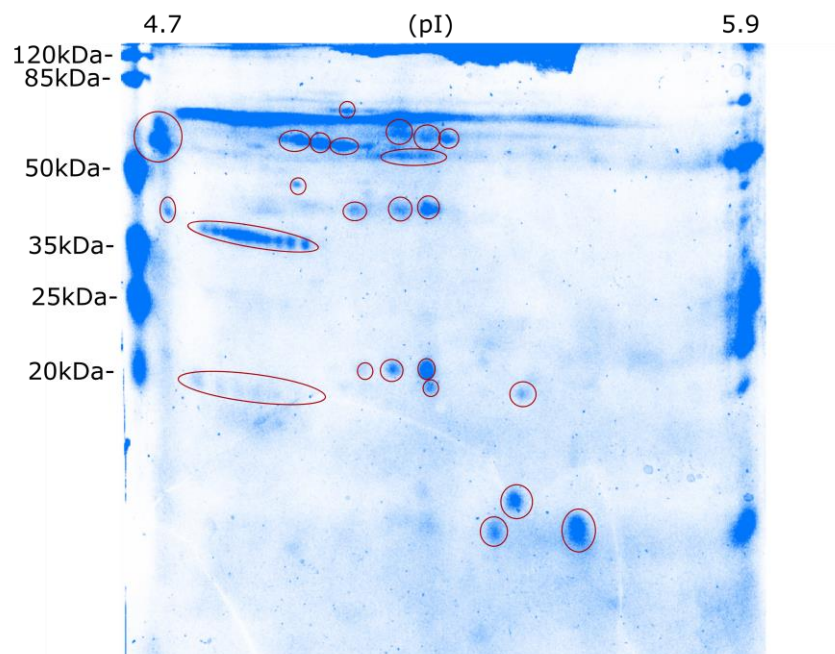
b Sample 38.2 Tumour Core



c Sample 38.4 Tumour Rim



d Sample 38.5 Invasive Margin



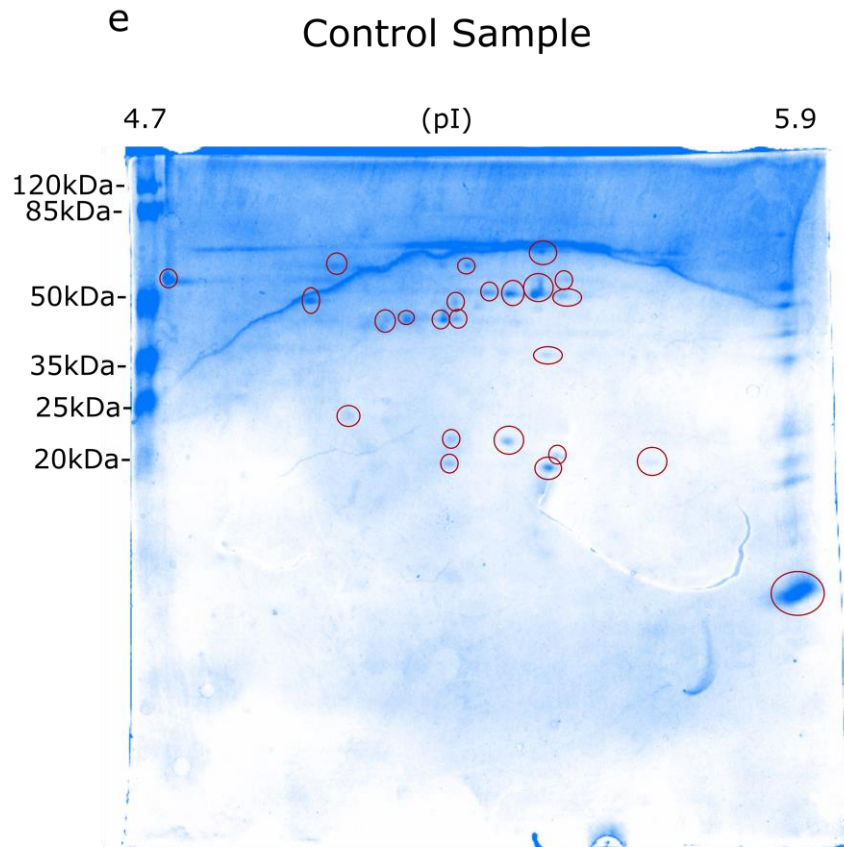


Figure 3-7| Images of 2D-PAGE separated four GBM samples and one healthy brain tissue control sample. Samples have been separated according to their MW (vertical) and their isoelectric point (horizontal, pI 4.7 to 5.9 left to right). IEF was performed on 17cm IPG strips of pH range between 4.7 to 5.9. IPG strips were then resolved on large 20cmx18cm polyacrylamide gels for approx. 20h and stained with colloidal blue overnight. Samples on gels 'a' to 'd' represent GBM tissue from all areas stated above each corresponding gel. Gel 'e' represents control sample from healthy tissue. Each separate protein resolved by the gel electrophoresis has been marked with the red circle.

2D-PAGE separation was successful at resolving complex cytosolic protein lysates by the pI and molecular weight shown on Figure 3-7. Four distinct regions have been chosen from one patient and resolved on a large polyacrylamide gel. To visualise the separation of proteins in each sample, colloidal blue total protein stain has been used. The optimisation has been done using various buffers and strips. At the end, good separation of proteins has been achieved though further optimisation could be beneficial and eradicate certain artefacts that are visible such as horizontal streaking and spot repetition. There were some patterns observed across gels including GBM and control. Many

unique protein spots have been noted to be expressed differentially in most gels. There were also repeated spots at 20kDa MW between ~5.0-5.5 pH which are visible in the invasive margin (Figure 3-7, 'd') but not in any other gel, even in PFC control.

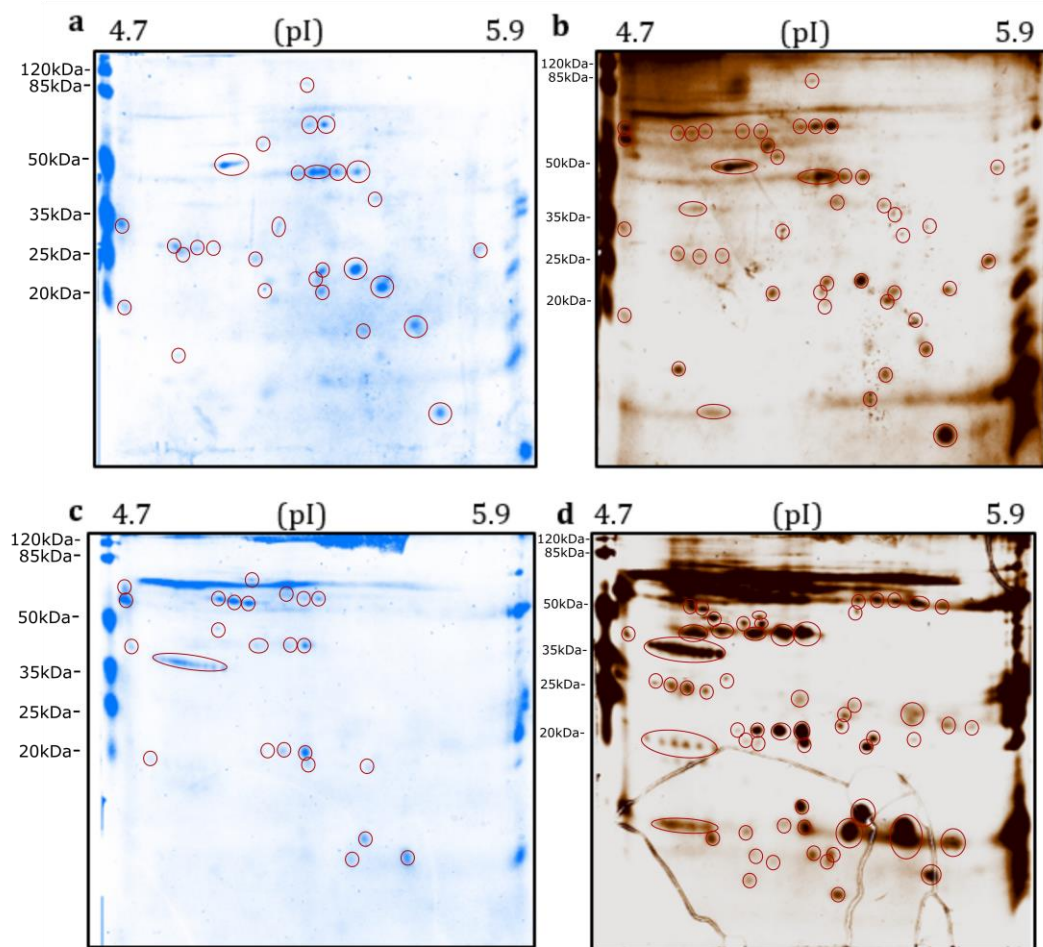


Figure 3-8| Comparison of two 2D-PAGE gels stained with colloidal blue followed by silver stain. GBM samples 38.1 and 38.5 have been resolved by 2D-PAGE to investigate proteomic changes and possible PTM. Gels have been stained with colloidal blue stain to visualise total protein, de-stained with ultra-pure and re-stained with the silver stain. Protein pI is represented horizontally from low pI (4.7) to high pI (5.9). Protein separation and detected proteins and possible PTM have been marked with red circles on all images. Image 'a' and 'b' represent tumour rim, image 'c' and 'd' represent invasive margin. Gel 38.1 'a', 29 proteins were resolved and visible with colloidal blue stain. Corresponding gel 'b' stained with the silver stain shows 45 distinct spots

Two samples have been compared and stained with two total protein stains of varying sensitivity, represented by Figure 3-8. Large 2D gels have been used for the best resolution of the protein sample. Colloidal blue can detect as

low as 10ng of proteins whereas silver stain can detect as low as 0.25ng of protein.

Less sensitive staining with colloidal blue has been performed first and two gels have been imaged for spot analysis. In the gel 38.1 (a), 29 proteins were visually detected, and 24 proteins were detected in gel 38.5 (c). After de-staining with ultrapure water, a more sensitive Silver staining was performed. With Silver stain, detection of the resolved proteins was greatly improved where 44 distinct spots were observed in gel 38.1 (b) and 60 spots were counted on gel 38.5 (d). There were also visible changes in protein expression across two different tumour sites with varying patterns of expression. Several changes in protein expression which could be associated with protein modifications were observed. PTMs are often observed as neighbouring spots with different MW or pI. This sort of shift is seen on all gels though whether this is due to change in electric charge or size due to active modifications needs to be further investigated with proteomic methods such as western blotting, immunoprecipitation or mass spectrometry. Also, this shouldn't be mistaken with 2DE artefacts caused by running methods. Horizontal streaking as seen in top of gel 'c' and 'd', between 50- to 85kDa are possibly caused by contaminants in the sample such as salts or lipids. De-salting and removal of contaminants could reveal more spots and result in better separation of some proteins. Additionally, some spots show repeated patterns across varying pI. Although these appear as separate spots, they most likely represent the same protein being repeated several times and are marked as such with horizontally elongated red circles on Figure 3-8. This is most likely a cause of IEF of the IPG strip and optimisation of voltage and time applied to the strip can be further optimised. Overall, 2D-PAGE has been successful at resolving distinct proteomic changes between tumour sites though further studies are necessary in identifying of these differences and matching these to specific proteins and their possible alterations and expressions. In addition, silver stain is a far more sensitive staining method and should be a preferred method of detection of resolved proteins on large polyacrylamide gels. However, it is a generally more expensive and colloidal blue stain could be used as a

preliminary investigation for successful separation of complex protein mixtures by 2D-PAGE. Though we have probably detected some PTMs with both stains, Silver stain was far superior in detecting resolved protein.

3.3 Mass Spectrometry analysis

Tandem Mass Spectrometry (MS/MS) serves as a next step in identification of unknown proteins in a complex sample. It is often used as a follow up to electrophoretic separation which enables identification of unknown polypeptide sequences in specific bands or spots. Identified amino acid sequences can then be matched with available protein databases such as Swiss-Prot, UniProt ("UniProtKB/Swiss-Prot," 2019). In this study, specific bands which conferred most change from control samples in 1D-PAGE as well as spots identified by 2D-PAGE with potential of being modified were sent for Mass Spectrometry identification. Proteins were first excised and prepared for MS/MS analysis.

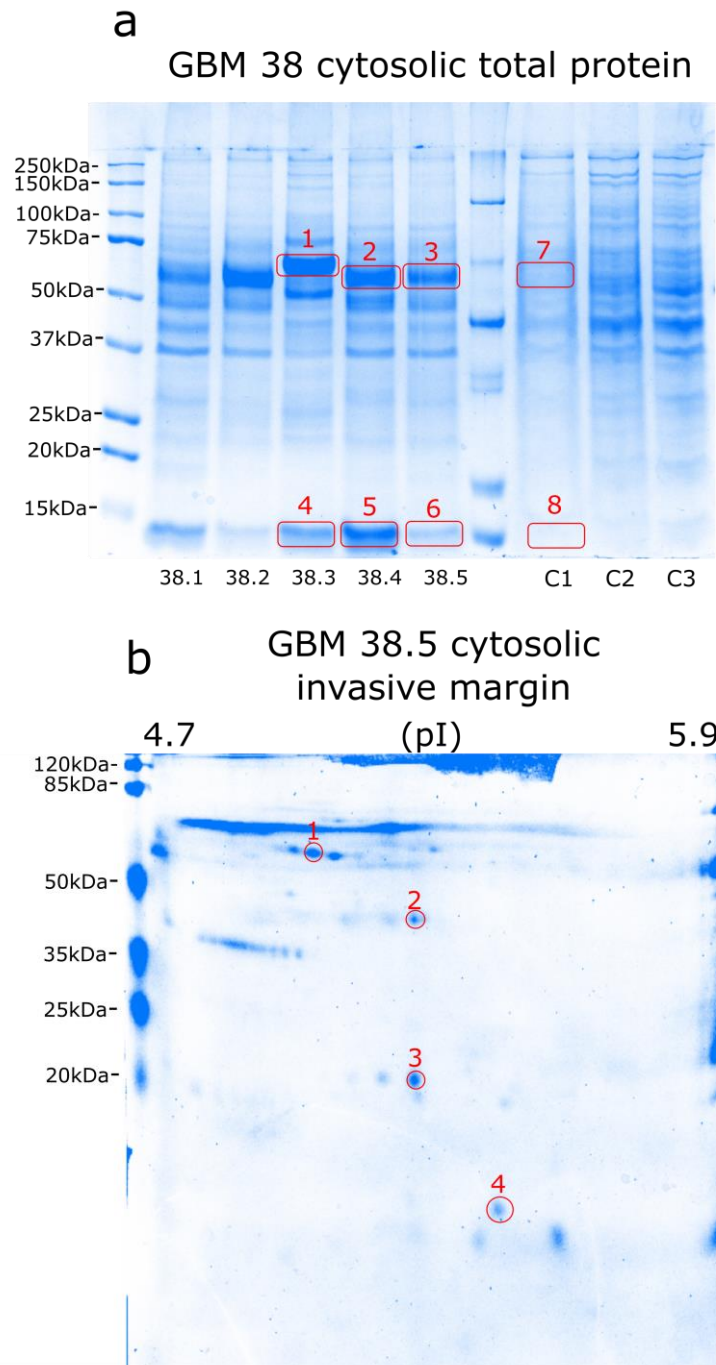


Figure 3-9/Images of excised proteins sent for MS/MS analysis. Eight bands from 1D-PAGE separated gels have been excised (marked with red rectangles) and sent for mass spectrometric analysis 'a'. Four spots from 2D-PAGE separated gels have also been excised and sent for analysis (marked with red circles) 'b'.

1D-
PAGE
(a)

| Band no. | Score | Mass | Protein Match (SwissProt) |
|-----------------|--------------|-------------|----------------------------------|
| 1 | 3160 | 71317 | Serum albumin OS |
| 2 | 1928 | 71317 | Serum albumin OS |
| 3 | 1462 | 71317 | Serum albumin OS |
| 4 | 605 | 16102 | Haemoglobin subunit beta OS |
| 5 | 777 | 16102 | Haemoglobin subunit beta OS |
| 6 | 533 | 16102 | Haemoglobin subunit beta OS |
| 7 | 935 | 71317 | Serum albumin OS |
| 8 | 552 | 16102 | Haemoglobin subunit beta OS |

2D-
PAGE
(b)

| Spot no. | Score | Mass | Protein Match (SwissProt) |
|-----------------|--------------|-------------|----------------------------------|
| 1 | 467 | 46878 | Alpha-1-antitrypsin OS |
| 2 | 108 | 42052 | Actin, cytoplasmic 1 OS |
| 3 | 269 | 30759 | Apolipoprotein A-I OS |
| 4 | 106 | 15991 | Transthyretin OS |

Table 3-1/*Table of MS/MS identified proteins showing protein score, molecular mass of protein in Daltons (Da), and proteins matched on SwissProt database.*

Several bands and spots were excised and sent for MS/MS analysis shown in Figure 3-9. Selected bands with strong expression were chosen and matching bands of a control sample were also selected. Similarly, four bands from a 2D-PAGE gel were chosen and sent for MS/MS identification. Results from MS/MS analysis are represented in Table 3-1. Several protein sequences have been found per band though only the top scoring polypeptide sequences were selected for each band as this indicates a more confident match of a protein. The 1D-PAGE analysis of the bands identified the upper row of bands (1, 2, 3 and 7, Figure 3-9 'a') to match Serum albumin. The lower row of bands (4, 5, 6 and 8, Figure 3-9, 'b') was identified as haemoglobin. 2D-PAGE gel spots were also successfully identified as cytoplasmic proteins Alpha-trypsin, Actin, Apolipoprotein A1 and Transthyretin.

3.4 Western Blotting

Expression of various proteins has been investigated by western blotting to identify disparity in protein expression of various tumour regions to a healthy brain. Proteins associated with a range of cellular functions and post-translational modifications were assessed. Some of these functions include structural integrity, cellular signalling, ROS regulation and protein repair mechanisms. By assessing a variety of metabolic and structural processes, the aim was to narrow down the processes which are significantly altered in GBM brain tumours and may be preferentially up or down regulated to favour cancer progression and growth. Through assessment of common proteins associated with these major metabolic pathways we hoped to clarify the functional and physiological changes that occur in various regions of the tumour and whether they are a generally occurring or heterogeneous events of GBM tumours.

Below, data is presented through a set of western blotting images of all screened samples and their quantified expression in matching graphs. Relative expression of proteins in tumour regions has been calculated as percentage change from mean expression of control samples.

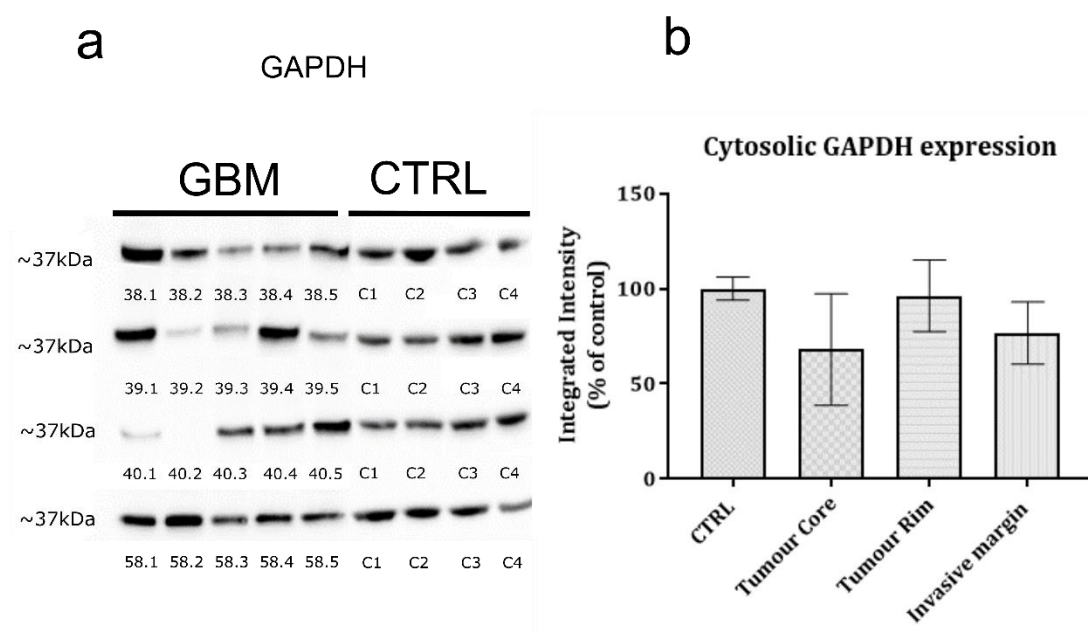


Figure 3-10/ Cytosolic expression of GAPDH in GBM and control PFC samples
Western blot of cytosolic GAPDH expression from 4 patients (GBM38, GBM39, GBM40, GBM58) and 5 tumour samples corresponding to tumour core, tumour rim and invasive margin and 4 PFC controls (a). Graph shows integrated intensity of GAPDH expression (b) from Western Blotting data. Bar charts represent tumour area mean expression as a percentage of the control group mean. Data was analysed by non-parametric One-way ANOVA (Kruskal-Wallis test) and statistical significance set at $P < 0.05$. Mean \pm SEM plotted; no significance was found.

GAPDH is an important enzyme involved in glycolysis and it is steadily expressed in majority of tissues making it ideal as a housekeeping protein. However, the expression of GAPDH can be altered in many diseases including cancer. Screening for GAPDH has revealed a generally varied expression in GBM between regions but also across various samples. Expression of GAPDH in 'healthy' brain control samples was consistent in all four samples and across four blots. For GBM samples the expression was varied and, in a few samples, the content of GAPDH was visibly low or absent (Figure 3-10 sample 39.2, 39.3, 40.1, 40.2). Tumour core displayed the lowest amount of GAPDH but also greatest deviation of the mean most likely due to high expression of GAPDH in sample 58.2. Tumour rim expression of GAPDH was most similar to controls with small decrease in GAPDH content and slightly higher variability between samples. Invasive margin was again lower than control but not significantly. There was no significant variation between expressions of GAPDH in control samples compared to tumour regions, but it can be inferred that expression of this enzyme

shows slight to moderate changes in cytosolic GAPDH content predominantly in tumour core.

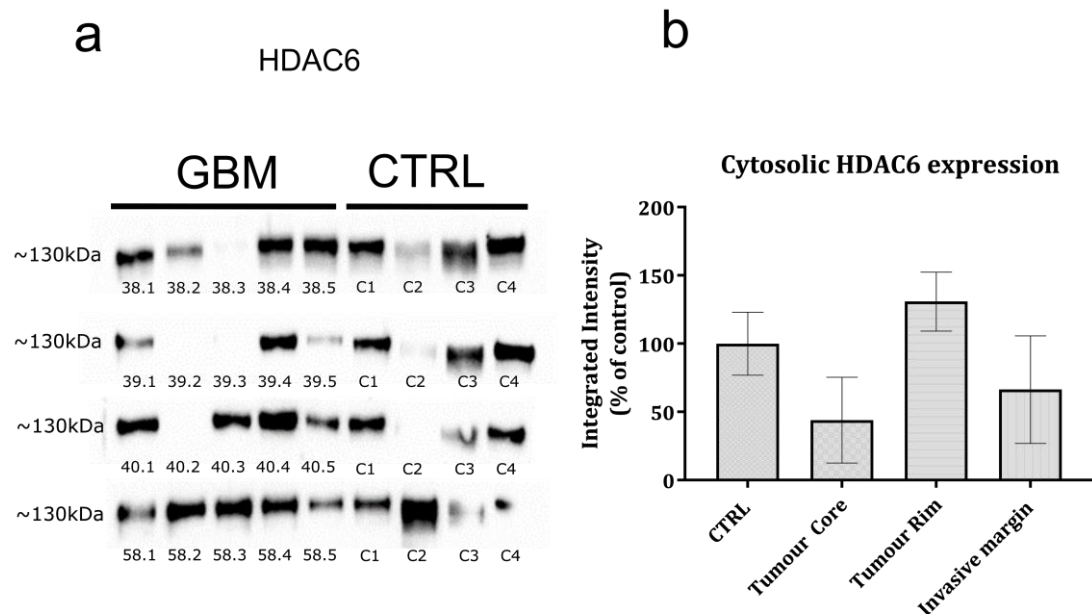


Figure 3-11| Cytosolic expression of HDAC6 in GBM and control PFC samples
Western blot of cytosolic HDAC6 expression from 4 patients (GBM38, GBM39, GBM40, GBM58) and 5 tumour samples corresponding to tumour core, tumour rim and invasive margin and 4 PFC brain controls (a). Graph shows integrated intensity of HDAC6 expression (b) from Western Blotting data. Bar charts represent tumour area mean as a percentage of the control group mean. Data was analysed by non-parametric One-way ANOVA (Kruskal-Wallis test) and statistical significance set at $P < 0.05$. Mean \pm SEM plotted, no significance was found.

HDAC6 belongs to a class II of a family of histone deacetylase enzymes and participates in histone acetylation and de-acetylation. Moreover, it also targets other substrates including α -tubulin, cortactin and heat shock protein 90 (HSP90). Its upregulation has been associated with increased proliferation and invasion in cancer (Li et al., 2018).

Our study of expression of this enzyme shown in Figure 3-11, presented variability in protein content of cytosolic HDAC6 in control samples and all three GBM tumour regions though no significance was found between any of the regions and control. Tumour core expression was most noticeably decreased by over 50% followed by invasive margin reduction of approximately 45%. However, the SEM was very hefty in both regions. There was decreased expression or absence of bands in several samples (Figure 3-11, a, lane 38.3, 39.2,

39.3, 40.2 and C2) most of which correspond to tumour core but also one control sample. In contrast, expression of HDAC6 in tumour rim had a 30% increase as compared with control. Variability of control was also existent, so it needs to be considered whether the expression of HDAC6 has a moderate variability in brain tissue but also in GBM tumours. Only GBM 58 tumour showed strong expression of HDAC6 in all samples though it was also varied.

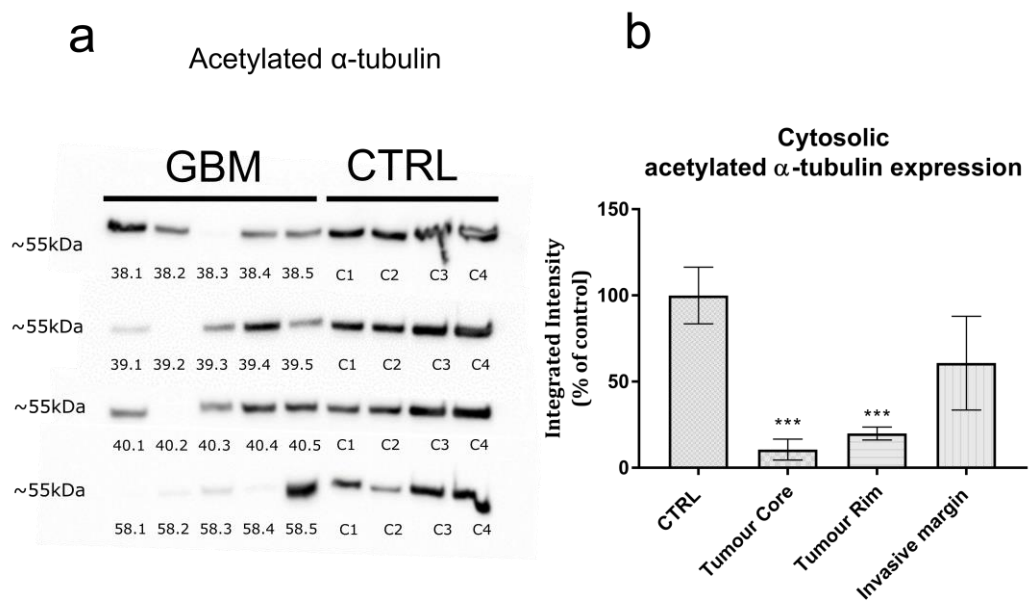


Figure 3-12| Cytosolic expression of Acetylated α -tubulin in GBM and control PFC samples
Western blot of cytosolic acetylated α -tubulin expression from 4 patients (GBM38, GBM39, GBM40, GBM58) and 5 tumour samples corresponding to tumour core, tumour rim and invasive margin and 4 PFC brain controls (a). Graph shows integrated intensity of acetylated α -tubulin expression (b) from Western Blotting data. Bar charts represent tumour area mean expression as a percentage of the control group mean. Data was analysed by non-parametric One-way ANOVA (Kruskal-Wallis test) and statistical significance set at * $P < 0.05$; ** $P < 0.01$; *** $P < 0.001$. Mean \pm SEM plotted. Multiple comparisons revealed significance for following regions: CTRL vs. Tumour Core, $P = 0.0002$ (***), CTRL vs. Tumour Rim, $P = 0.0003$ (***)

Microtubule α -tubulin is an important protein responsible for many functions including structural integrity and polarity a cell. Microtubules undergo several post translational modifications including acetylation. Acetylation of α -tubulin is considered to act as a stabiliser of this microtubule and confers longevity of the protein (Janke and Montagnac, 2017). Acetylated α -tubulin is also a substrate for HDAC6 which in turn deacetylates the microtubule. Changes

in PTM of microtubules can facilitate change in structural integrity of a cell or even affect their polarity. Here we assayed acetylation of α -tubulin in four GBM patients in three distinct regions of a tumour and compared its expression to four PFC controls. We have also attempted to measure non acetylated α -tubulin expression though results were unsuccessful. Repetition of the experiment for α -tubulin needs to be performed to investigate whether unsuccessful blotting was due to the method or antibodies used. This would be very beneficial for determination of total α -tubulin to its acetylated form to determine whether there is specific decrease of acetylated α -tubulin or α -tubulin reduction in general.

Figure 3-12 shows differential expression acetylated of α -tubulin in GBM samples and distinct tumour regions. Results suggest decreased acetylation of α -tubulin in all GBM regions as compared to control with two regions significantly reduced. Tumour core and tumour rim have significantly lower expression of acetylated α -tubulin ($p=0.0002$ and $p=0.0003$ respectively). Tumour rim was decreased by approximately 50% though the results found no significance. There was absence or hardly detectable signal of acetylated α -tubulin in few samples including sample 38.3, 39.2, 40.2 and 58.1, most of which coincide with tumour core area. Additionally, sample GBM58 had consistently lowest expression of acetylated α -tubulin in most lanes apart from 58.5 which represents GBM invasive margin. Expression of acetylated α -tubulin in control samples was generally constant though some artefacts from western blotting run are present such as dropping or wavy bands.

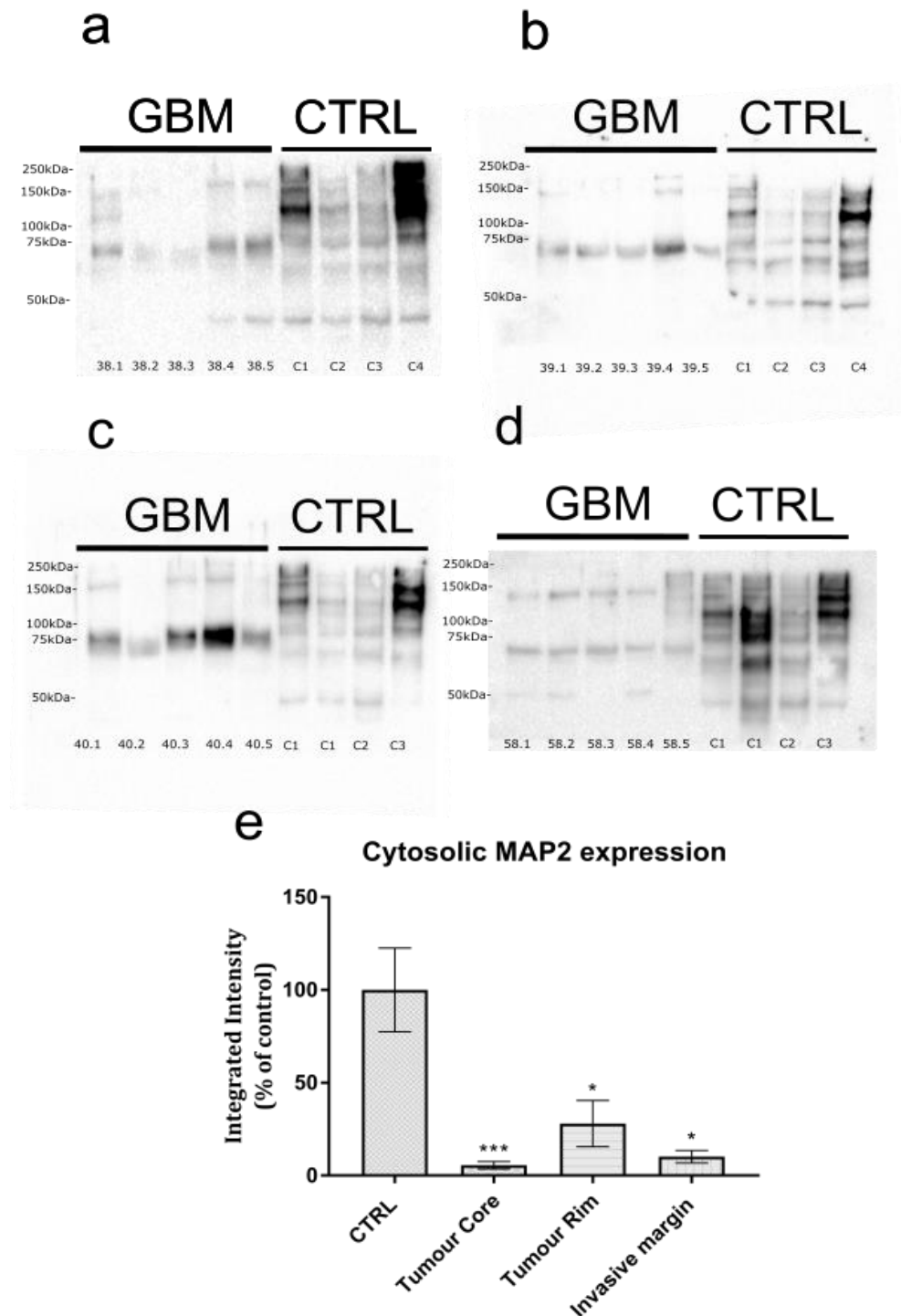


Figure 3-13| Cytosolic expression of MAP2 in GBM and control PFC samples
 Western blot of cytosolic MAP2 expression from 4 patients (GBM38, GBM39, GBM40, GBM58) and 5 tumour samples corresponding to tumour core, tumour rim and invasive margin and 4 healthy brain controls (a,b,c,d). Graph shows integrated intensity of MAP2 expression (e) from Western Blotting data. Bar charts represent tumour area mean expression as a percentage of the control group mean. Data was analysed by non-parametric One-way ANOVA (Kruskal-Wallis test) and statistical significance set at * $P < 0.05$; ** $P < 0.01$; *** $P < 0.001$. Mean \pm SEM plotted. Multiple comparisons revealed significance for following regions: CTRL vs. Tumour Core, $P = 0.0009$ (***), CTRL vs. Tumour Rim, $P = 0.0193$ (*), CTRL vs. Invasive Margin, $P = 0.0391$ (*).

Microtubule-associated protein 2 (MAP2) are responsible for many microtubule related functions including assembly, organisation, stabilisation, polarisation and crosslinking. MAP2 plays an important role in neuronal cytoskeleton organisation because of their involvement in phosphorylation and modifications of cytoskeletal proteins (Sánchez et al., 2000). Multiple isoform variants of MAP2 exist in human brain derived from various splice variants. The protein undergoes extensive phosphorylation and other PTMs and appears as several bands on a western blot.

We have measured total MAP2 expression in both GBM brain tumours and four PFC controls. There was a significant reduction of MAP2 in all three tumour sites. Tumour core had lowest expression with 95% significant reduction ($p=0.0009$). Both tumour rim and invasive margin were also significantly reduced ($P=0.0193$ and $=0.0391$ respectively). Tumour rim had 75% reduced expression whereas invasive margin had 90% decrease as compared to control. The expression between tumour regions was also moderately varied with tumour rim having highest expression out of three regions and tumour core and invasive margin being considerably lower in content. There was some variability in controls mostly at isoforms larger than 100kDa though most samples displayed consistent expression.

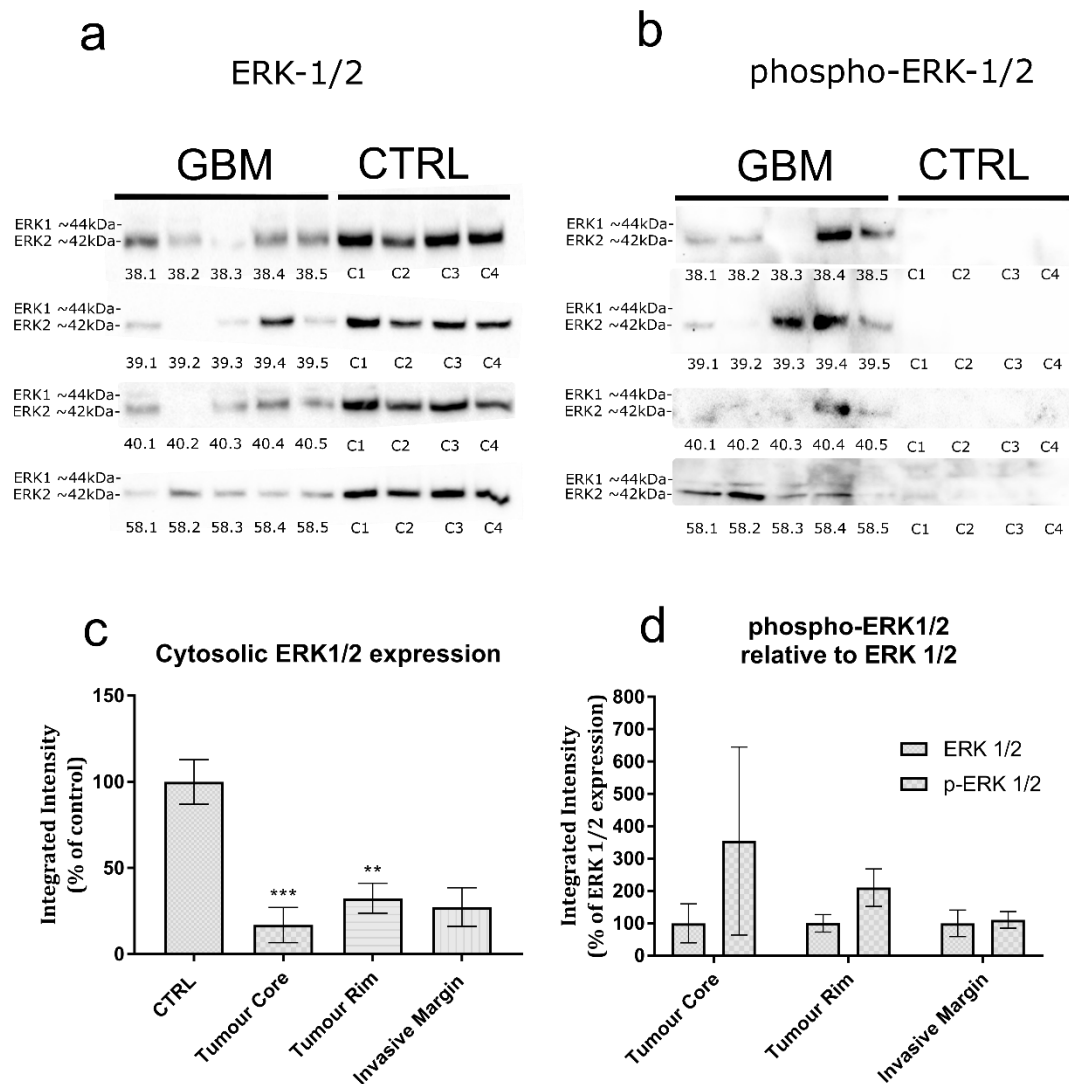


Figure 3-14| Cytosolic expression of ERK1/2 and phosphorylated ERK1/2 in GBM and control PFC samples. Western blot of cytosolic ERK1/2 and phosphorylated ERK1/2 expression ('a' and 'b' respectively) from 4 patients (GBM38, GBM39, GBM40, GBM58) and 5 tumour samples corresponding to tumour core, tumour rim and invasive margin and 4 PFC brain controls. Graph 'c' shows integrated intensity of ERK1/2 expression from Western Blotting data. Graph 'd' shows integrated intensity of phosphorylated ERK1/2 as a percentage change from non-phosphorylated ERK1/2 expression. Bar charts represent tumour area mean expression as a percentage of the control group mean. Data was analysed by non-parametric One-way ANOVA (Kruskal-Wallis test) and statistical significance set at * $P < 0.05$; ** $P < 0.01$; *** $P < 0.001$. Mean \pm SEM plotted. Multiple comparisons for ERK1/2 (c) revealed significance for following regions: CTRL vs. Tumour Core, $P = 0.0009$ (***), CTRL vs. Tumour Rim, $P = 0.0093$ (**), CTRL vs. Invasive Margin, $P = 0.057$. No significance was found between ERK1/2 and phosphorylated ERK1/2.

ERK1/2 (Extracellular Signal-regulated Kinases (1/2)) are protein kinases responsible for a range of cellular functions and are involved in a multitude of intracellular signalling pathways. Phosphorylation of ERKs leads to their activation and consequent phosphorylation of their target substrate. They are responsible for activation of cytosolic and nuclear pathways involved in transcription, survival, cell cycle progression and many more. The list of ERK substrates is very extensive hence they have key role in regulation of cell metabolism in healthy and pathogenic cells. In this study, we have assessed cytosolic total ERK1/2 expression as well as their phosphorylated form in four GBM tumours and four PFC controls.

Total cytosolic ERK1/2 represented in Figure 3-14, 'a', revealed decreased expression in all three areas of the tumour. 80% decrease from control in the tumour core reached a strong significance ($p=0.0009$) and 75% reduction in tumour rim was also significant ($p=0.0093$). There was also reduction in the invasive margin with a value closely approaching significance ($p=0.057$). The expression of total ERK1/2 was consistent in all PFC samples. Variability between band expressions showed similar to previously assessed protein lack of expression in tumour core region. In contrast, the phosphorylated ERK1/2 was found to be expressed in all GBM samples to some degree whereas we were not able to detect any in PFC control samples. Henceforth we compared expression of total ERK1/2 with phosphorylated-ERK1/2 as a ratio of integrated expression. Although there was no significant difference between the total and phosphorylated ERK1/2 there was clear approx. three-fold increase in tumour core though with large deviation of SEM and approx. two-fold increase tumour rim. The invasive margin had same expression total and phosphorylated ERK1/2. Also, the lack of PFC phosphorylated ERK1/2 is quite surprising especially considering its normal expression of total ERK1/2. Whether this is due to the samples, method or antibodies used needs to be further questioned whether with use of positive control or through other means.

3.5 Redox Regulation & Oxidative damage

Oxidative damage caused by ROS is a common feature of cancer and has been reported to be dysregulated in brain tumours including GBM (Rinaldi et al., 2016). In this study, we first investigated oxidative stress by measuring total protein carbonylation using an OxyBlot™ kit. Carbonylation of proteins occurs from addition of carbon monoxide into substrates and is considered as a marker of oxidative stress.

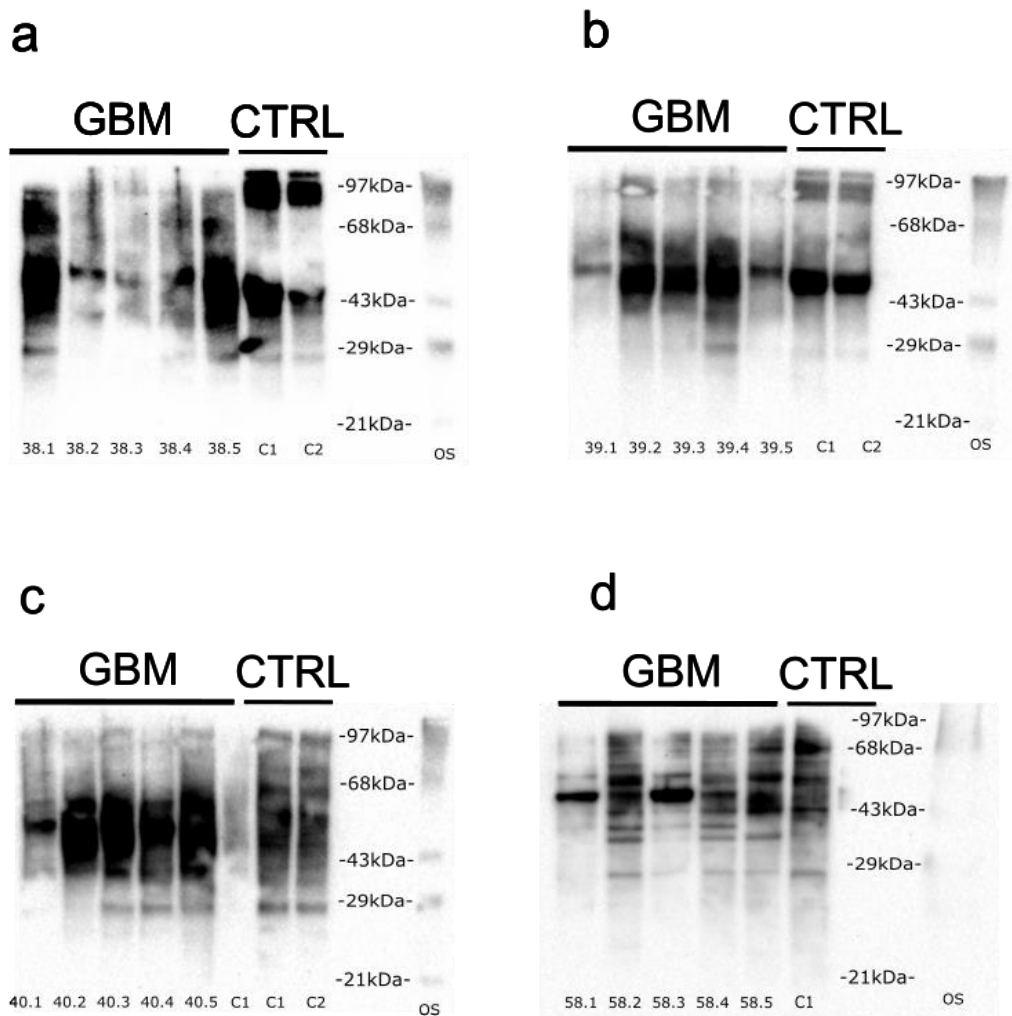


Figure 3-15| Cytosolic expression of carbonylated proteins in GBM and control PFC tissue detected by OxyBlot™ kit. Western blot of cytosolic Carbonylation of proteins ('a','b','c','d') from 4 patients (GBM38, GBM39, GBM40, GBM58) and 5 tumour samples corresponding to tumour core, tumour rim and invasive margin and 2 PFC brain controls (second control in 'd' has not worked). OxyBlot™ protein standard with carbonylated is marked as OS and has been used for the determination of molecular weight.

Analysis of western blotting images for oxidatively damaged proteins through addition of carbonyl groups to amino acid residues is presented in Figure 3-15. The separation of proteins was poor in three out of four experiments. Images for blots 'a-c' were transferred from hand cast gels whereas image of blot 'd' was performed with a ready-made gel. This drop in quality is very obvious and makes it difficult to determine specific bands on any of the blots from hand-made gels. Total oxidation has therefore been calculated and presented in Figure 3-16. Because of the variability of the signal detected it is difficult to distinguish specific changes though some specific oxidation can be seen in most blots at approximately 50kDa MW. Best resolution of carbonylated cytosolic proteins has been achieved in GBM58 blot and oxidation of specific protein regions can be observed (d). There is clear alteration of specific proteins such as in lane 58.1, 58.2, 58.3 and 58.4 at MW of ~50kDa. Also, there are specific bands appearing just below 43kDa MW marker which are not present in the PFC control. In the future, separation of carbonylated proteins should be performed using ready-made gels for assessment of oxidation at specific protein regions.

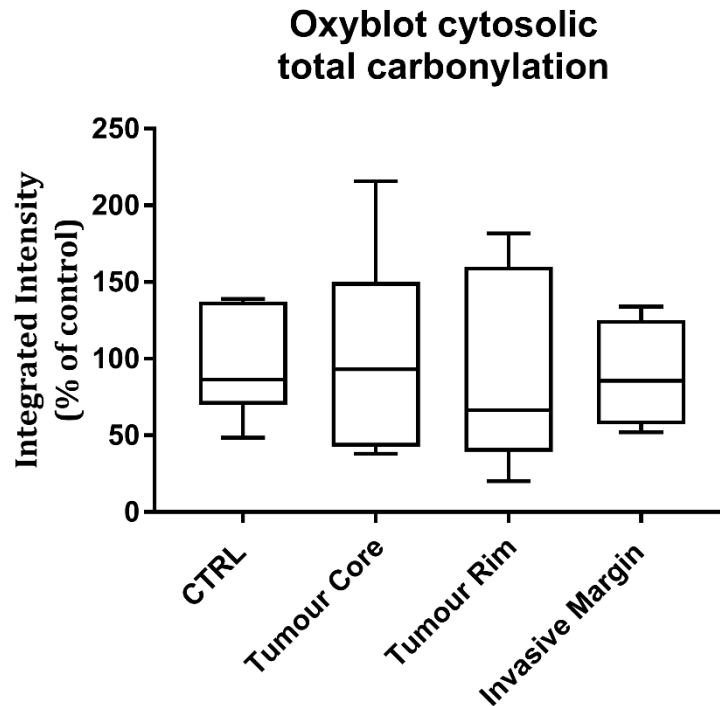


Figure 3-16| Graph of total Carbonylation quantified from Oxyblot western blotting data. Distribution of the data is represented by a box chart. Box charts represent tumour area distributed expression as a percentage of the control group mean. Data was analysed by non-parametric One-way ANOVA (Kruskal-Wallis test) and statistical significance set at * $P < 0.05$; ** $P < 0.01$; *** $P < 0.001$. No statistical significance was found.

Western blot immuno-detection of cytosolic carbonylation suggests global oxidative damage in both GBM and PFC (Figure 3-15). Total oxidation of cytosolic proteins between PFC and tumour has not reached significance and the mean of total oxidation remained consistent across all regions as well as the PFC. It is worth to add that oxidation in tumour core had the largest disparity of data with the highest point reaching over two-fold increase. Tumour rim had varied expression of oxidatively damaged proteins and invasive margin had expression closely resembling the healthy tissue.

After assessment of oxidation we were prompted to see whether the levels of certain antioxidant and repair enzymes reflected the amount of oxidation.

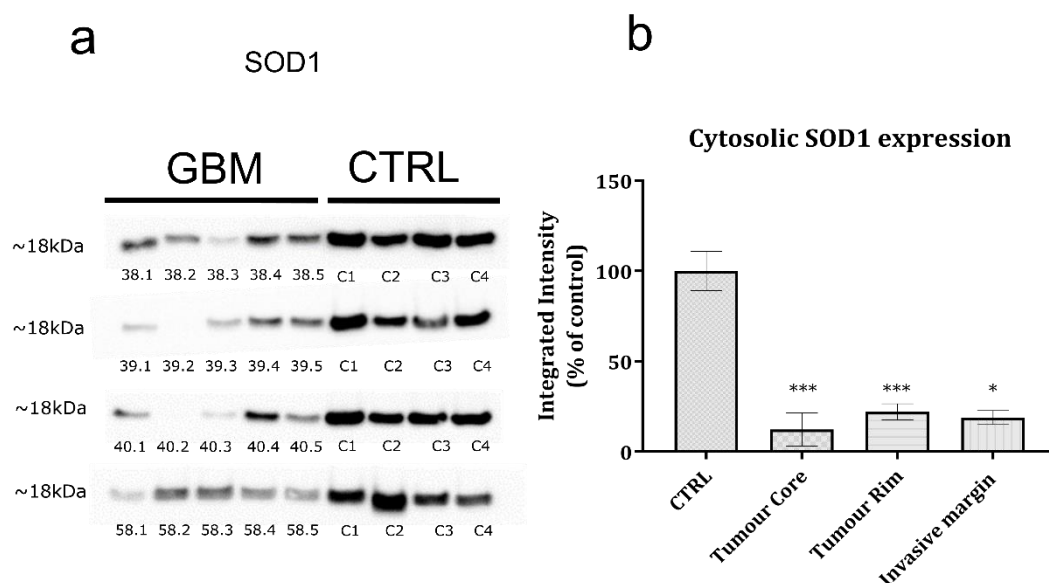


Figure 3-17| Cytosolic expression of SOD1 in GBM and control PFC samples
Western blot of cytosolic SOD1 expression from 4 patients (GBM38, GBM39, GBM40, GBM58) and 5 tumour samples corresponding to tumour core, tumour rim and invasive margin and 4 PFC controls (a). Bar chart represents integrated intensity of SOD1 expression (b) from Western Blotting data. Bar charts represent tumour area mean as a percentage of the control group mean. Data was analysed by non-parametric One-way ANOVA (Kruskal-Wallis test) and statistical significance set at * $P < 0.05$; ** $P < 0.01$; *** $P < 0.001$. Mean \pm SEM plotted; Multiple comparisons revealed significance for following regions: CTRL vs. Tumour Core, $P = 0.0001$ (***), CTRL vs. Tumour Rim, $P = 0.0009$ (*), CTRL vs. Invasive Margin, $P = 0.0225$ (*).

SOD's are a family of antioxidant enzymes responsible for reduction of superoxides ($O_2^{\cdot-}$) through catalytic conversion into hydrogen peroxide (H_2O_2). The regulation of SOD is often dependent on the ROS cellular concentration in the cell and amount of oxidative stress. Working along with other antioxidant enzymes SOD maintains redox metabolism and prevents excessive PTM and toxicity caused by ROS. Three isoforms of SOD exist in cells localised to cytoplasm, nucleus or mitochondria. SOD1 relates to the cytoplasmic isoform of the enzyme. Alterations of SOD expression via either up-regulation or down-regulation have been documented in cancer (Papa et al., 2014). We have assessed SOD1 expression in the GBM tissue and compared it with the PFC brain tissue.

Western blotting disclosed strong 80-90% reduction of cytosolic SOD1 across all GBM samples and stable SOD1 expression in the PFC (Figure 3-17). We noted strong significant decrease between control and tumour core ($p = 0.0001$)

as well as tumour rim ($p=0.0009$) and weaker statistical significance in invasive margin ($p=0.0225$). Cytosolic SOD1 was universally reduced across all GBM sites and almost completely absent in two samples which correspond to tumour core (Figure 3-17, a, lane 39.2 and 40.2).

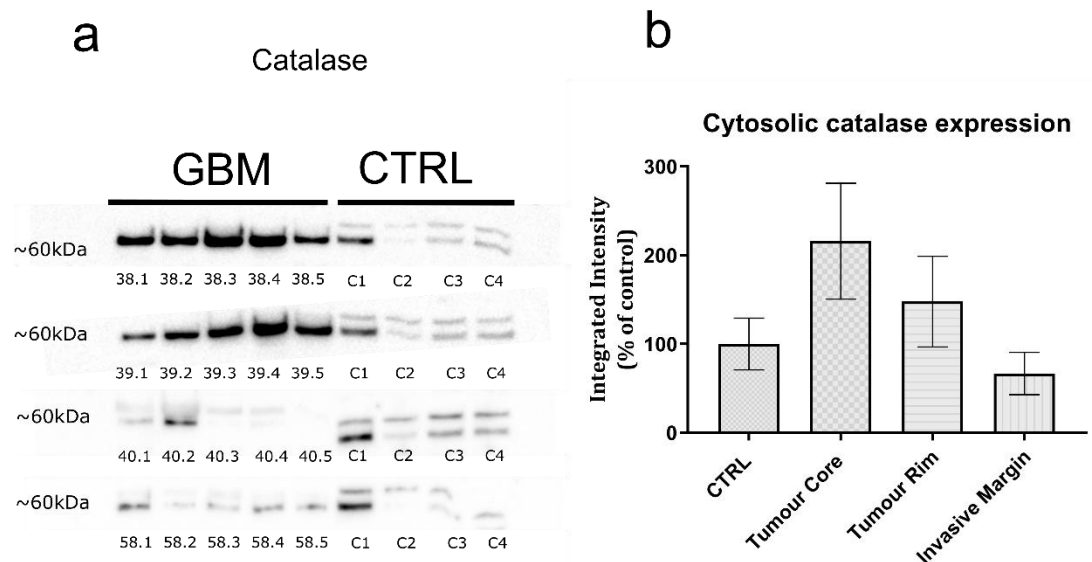


Figure 3-18| Cytosolic expression of CAT in GBM and control PFC samples
Western blot of cytosolic CAT expression from 4 patients (GBM38, GBM39, GBM40, GBM58) and 5 tumour samples corresponding to tumour core, tumour rim and invasive margin and 4 PFC controls(a). Graph shows integrated intensity of CAT expression (b) from Western Blotting data. Bar charts represent tumour area mean as a percentage of the control group mean. Data was analysed by non-parametric One-way ANOVA (Kruskal-Wallis test) and statistical significance set at $P<0.05$. Mean \pm SEM plotted; no significance was found.

Catalase is an oxidant enzyme, responsible for catalytic reduction of hydrogen peroxide into water (H_2O) and oxygen (O_2). Along with SOD, Catalase maintains redox balance through removal of ROS. There is evidence to support that catalase expression is altered in cancer where its overexpression confers chemo-therapeutic and ionising radiation resistance whereas its downregulation can lead to high concentration of hydrogen peroxide and increased onco-genesis through activation of proliferation signalling.(Glorieux et al., 2015).

The expression of cytosolic catalase has displayed general variability between different patients (Figure 3-18). Catalase was highly expressed in two tumours (GBM38 and 39, a) but interchangeably expressed in the remaining

two samples (GBM40 and 58, a). There was no significant difference found between the PFC and GBM samples though integrated expression of tumour core and tumour rim were highly increased, with 100% increase in the tumour core and 50% increase in tumour rim. Invasive margin expression was weakly decreased. This could possibly indicate heterogeneous expression of the antioxidant enzyme between different patients as two tumours present increase of catalase while the other two show decrease of the protein. Blotting image shows that there might be less variability between tumour regions and most of the change is due to variable expression of catalase between the patients.

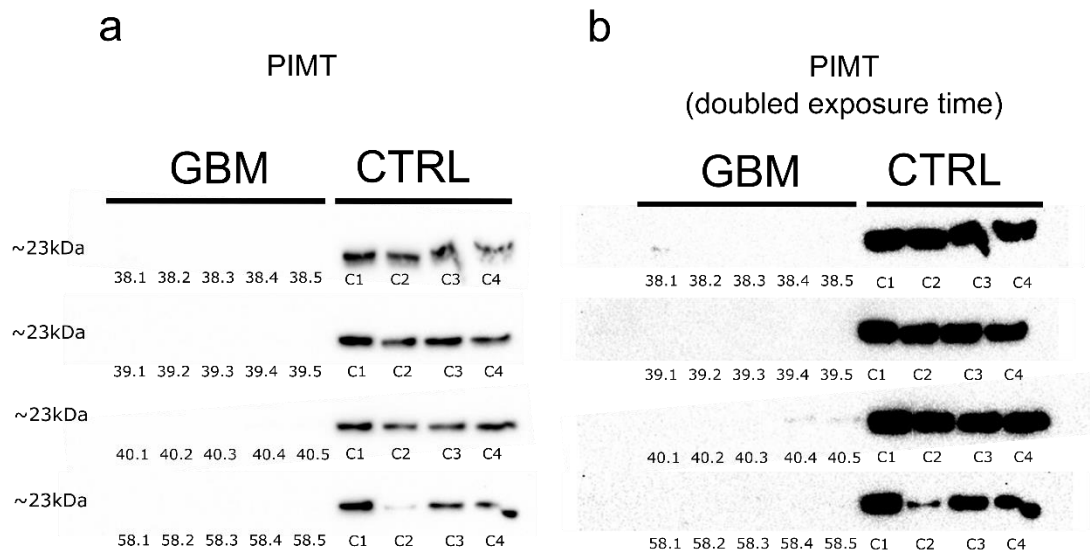


Figure 3-19| Cytosolic expression of PIMT in GBM and control PFC
 Western blot of cytosolic PIMT expression from 4 patients (GBM38, GBM39, GBM40, GBM58) and 5 tumour samples corresponding to tumour core, tumour rim and invasive margin and 4 PFC controls (a). The blot 'a' was exposed for 5 seconds whereas blot 'b' has been exposed for 10 seconds.

Proteins constantly undergo enzymatic and non-enzymatic modifications. Spontaneous deamidation of asparagine and dehydration of aspartate leads to formation of aspartyl residues and accumulation of damaged proteins (Desrosiers and Fanélus, 2011). Isoaspartyl modified proteins are recognised by protein L-isoaspartyl methyltransferase (PIMT) which catalyses addition of a methyl group from SAM to the affected isoaspartyl residues in order to repair

them. Studies on PIMT KO mice show that accumulation of Isoaspartyl has detrimental effects in the brain suggesting the neuroprotective function of PIMT in the brain (Dimitrijevic et al., 2014). We probed for cytosolic PIMT expression in GBM and PFC brain tissue to assess whether there are any changes in the expression of the repair enzyme.

Western blotting of cytosolic PIMT showed no expression in GBM tissue although there was steady expression in PFC (Figure 3-19, 'a'). The blot has been initially exposed for 5 seconds where no signal was detected. The same blots were then exposed for 10 seconds and there was possible weak signal in lane 40.4 and 40.5 shown in Figure 3-19, 'b'. The blot could possibly be exposed for longer though it was not carried out due to oversaturation of PFC control samples. The signal might have been so low that it was not detectable by short exposure. Longer exposure could be beneficial in detection of the low abundance of the protein.

3.6 Milliplex Phosphorylation Assay

Milliplex offers a multiplex technology which allows for a wide range of analysis on multiple protein targets in a single assay. The mechanism is ideal for studying of signalling pathways which involve a multitude of kinases and other protein substrates. This also enables for mapping of certain signalling cascades such as transcription signalling pathway or kinase activation. In this study three different kits have been used to investigate various proteins and their consecutive phosphorylation. 9Plex kit was used to investigate a wide range of phosphorylated proteins detailed in Table 2-2. mTOR and JNK kits were used to investigate total expression as well as phosphorylation of these proteins only. These targets are all major kinases linked to key signalling pathways involved in cell migration, cell cycle control, transcription, cell survival and proliferation. Four different GBM tumours and three distinct regions from tumour core, tumour rim and invasive margin were investigated along four PFC control samples.

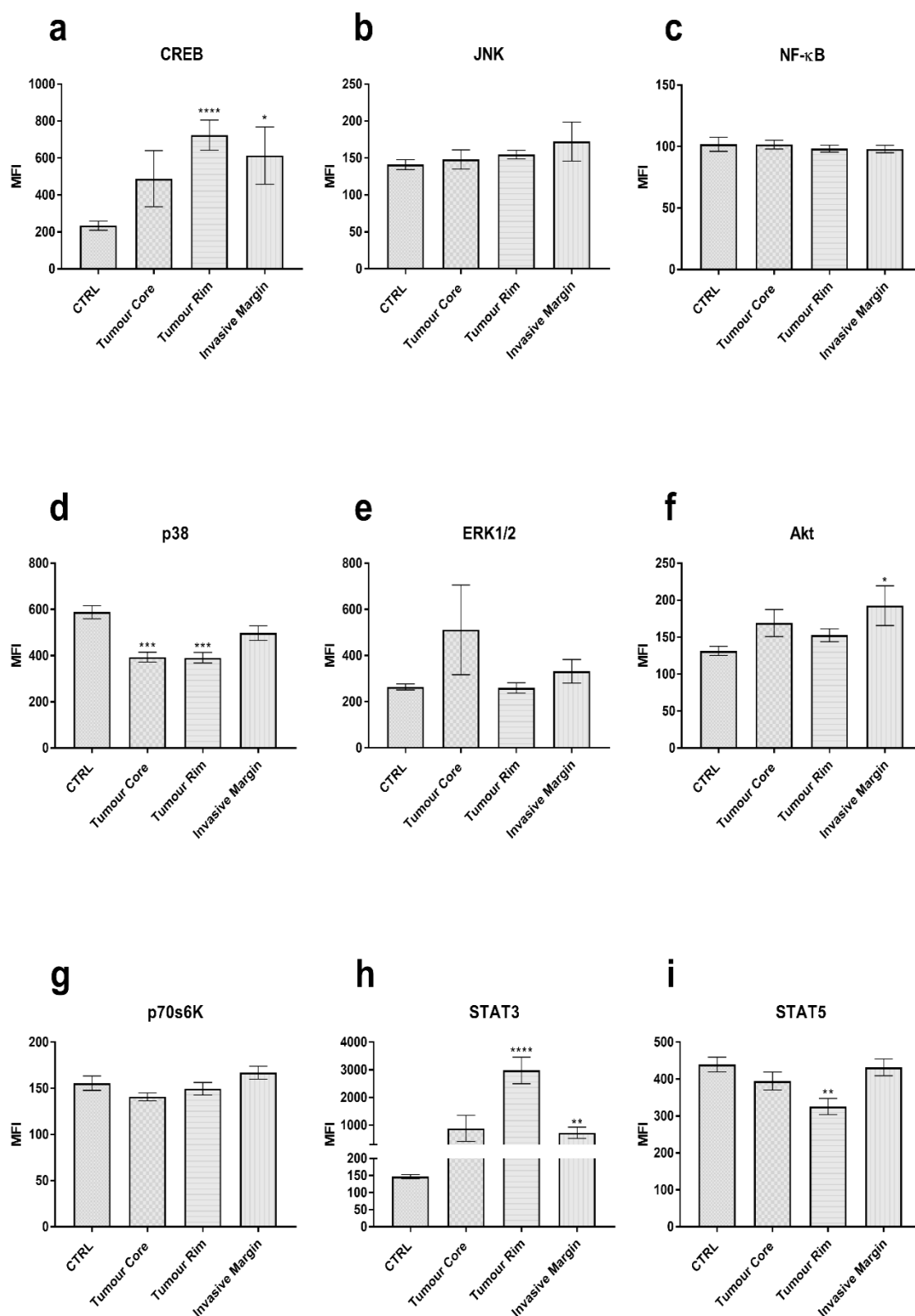


Figure 3-20| Expression of cytosolic phosphoproteins assessed through Milliplex MAP technology. Expression is plotted as the Median Fluorescent Intensity (MFI). Data was analysed by non-parametric One-way ANOVA (Kruskal-Wallis test) and statistical significance set at * $P < 0.05$; ** $P < 0.01$; *** $P < 0.001$. Mean \pm SEM plotted.

| | | | |
|---------------|--------------------------|------|---------|
| CREB | CTRL vs. Tumour Core | ns | 0.5872 |
| | CTRL vs. Tumour Rim | **** | <0.0001 |
| | CTRL vs. Invasive Margin | * | 0.0331 |
| JNK | CTRL vs. Tumour Core | ns | >0.9999 |
| | CTRL vs. Tumour Rim | ns | 0.6849 |
| | CTRL vs. Invasive Margin | ns | >0.9999 |
| Nf-κ-B | CTRL vs. Tumour Core | ns | >0.9999 |
| | CTRL vs. Tumour Rim | ns | >0.9999 |
| | CTRL vs. Invasive Margin | ns | >0.9999 |
| p38 | CTRL vs. Tumour Core | *** | 0.0008 |
| | CTRL vs. Tumour Rim | *** | 0.0001 |
| | CTRL vs. Invasive Margin | ns | 0.5151 |
| ERK1/2 | CTRL vs. Tumour Core | ns | 0.4996 |
| | CTRL vs. Tumour Rim | ns | 0.373 |
| | CTRL vs. Invasive Margin | ns | >0.9999 |
| Akt | CTRL vs. Tumour Core | ns | 0.3064 |
| | CTRL vs. Tumour Rim | ns | 0.3697 |
| | CTRL vs. Invasive Margin | * | 0.0366 |
| p70s6K | CTRL vs. Tumour Core | ns | 0.3807 |
| | CTRL vs. Tumour Rim | ns | >0.9999 |
| | CTRL vs. Invasive Margin | ns | 0.5826 |
| STAT3 | CTRL vs. Tumour Core | ns | 0.1201 |
| | CTRL vs. Tumour Rim | **** | <0.0001 |
| | CTRL vs. Invasive Margin | ** | 0.0056 |
| STAT5 | CTRL vs. Tumour Core | ns | 0.8033 |
| | CTRL vs. Tumour Rim | ** | 0.0022 |
| | CTRL vs. Invasive Margin | ns | >0.9999 |

Table 3-2/ Multiple comparisons of MFI from Milliplex Map 9Plex analysis between 3 tumour regions and PFC brain control. Data was analysed by non-parametric One-way ANOVA (Kruskal-Wallis test) and statistical significance set at * $P<0.05$; ** $P<0.01$; *** $P<0.001$; **** $P<0.0001$.

Milliplex analysis of phosphoproteins is represented in Figure 3-20. The wide array of protein phosphorylation has been assessed revealing variable phosphorylation of certain signalling kinases and transcription factors. Data has been divided into three regions in the same manner as previous experiments. Significance has been plotted on the graphs with asterisks though for better visualisation the significance from One-way ANOVA, multiple comparisons have been presented in the Table 3-2. Firstly, few proteins showed small or no change in phosphorylation between tumour and control samples, these include JNK (b), NF- κ B (c) and p70s60K (g). Expression of CREB (a) has been increased in all GBM tumour tissues with strong significance between PFC control and tumour rim ($p < 0.0001$) and significant increase of expression in invasive margin ($p = 0.0331$). Invasive margin expression was lower than that of the tumour rim. Next, expression of kinase p38 was significantly reduced by approximately 20% in tumour core and tumour rim ($p = 0.0008$ and $p = 0.0001$ respectively). Invasive margin expression of p38 (d) was also decreased as compared to control though it did not reach significance. Expression of phosphorylated ERK1/2 (e) also had moderate variability and we observed increase of the protein in tumour core which reflects our results of western blotting for ERK1/2 (Figure 3-14, 'b'), though tumour rim and invasive margin do not resemble this. Also, signal for PFC controls was also detected which we were not able to achieve with western blotting (Figure 3-14, 'b'). It is possible that the antibody was not specific for the same phosphorylation site as the Milliplex 9Plex (Thr185/Tyr187) and manufacturer does not list the specificity of the antibodies for phosphorylation of ERK1/2. The phosphorylation of ERK1/2 in tumour rim was the same as PFC control and invasive margin was slightly increased. We have also observed significant increase of Akt (f) in the invasive margin of the tumour ($p = 0.0366$) and not in other areas. Lastly, there was interesting increase of STAT3 (h) which had an overwhelming overexpression of this transcription factor in all tumour regions as compared to control. The tumour rim had the greatest expression with almost thirty-fold increase and reached strong significance ($p < 0.0001$). Tumour core had not reached significance, probably due to large variability of data though it had around ten-fold increase along with invasive margin which in contrast was significant ($p = 0.0056$). STAT5 (i) phosphorylation was generally normal in

invasive margin and tumour core and was significantly decreased in tumour rim (p=0.0022).

We have also used analysed total protein expression with phosphorylated modification in mTOR and JNK using Milliplex.

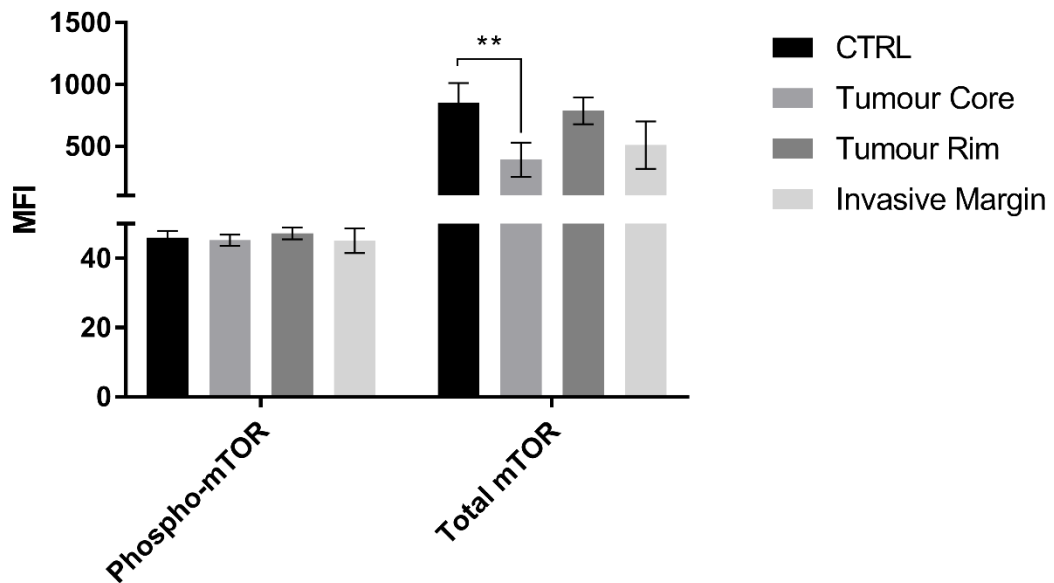


Figure 3-21/ Multiple comparisons of MFI from Milliplex phospho-mTOR and total mTOR analysis between 3 tumour regions and PFC brain control. Data was analysed by non-parametric. One-way ANOVA (Kruskal-Wallis test) and statistical significance set at * $P < 0.05$; ** $P < 0.01$. Mean \pm SEM plotted. Multiple comparisons revealed significance for following regions: for total mTOR CTRL vs. Tumour Core: $p = 0.0081$

Results of phosphorylated mTOR were very consistent in all samples. Expression of total mTOR was much higher as compared to its phosphorylated variant. Additionally, tumour core was significantly reduced when compared to control (p=0.0081). There was some drop in expression of invasive margin too though not significant.

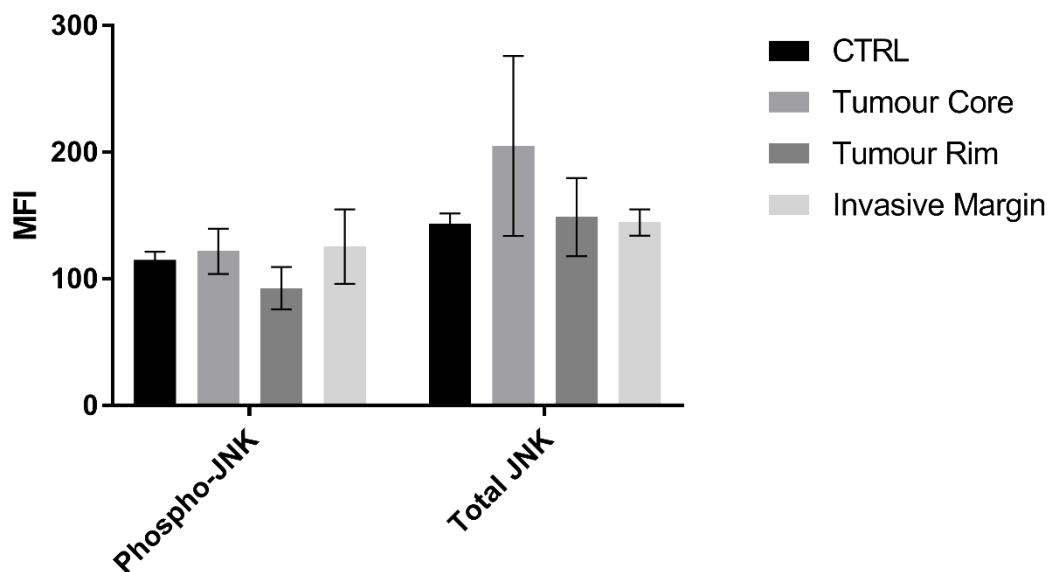


Figure 3-21/ Multiple comparisons of MFI from Milliplex phospho-JNK and total JNK analysis between 3 tumour regions and PFC brain control. Data was analysed by non-parametric One-way ANOVA (Kruskal-Wallis test) and statistical significance set at * $P < 0.05$. No significance was found.

Investigation of JNK showed relatively similar amount of phosphorylation between all samples and increase of total JNK in tumour core compared to PFC controls. However, the expression was highly variable and did not reach significance.

3.7 U87 Cell Line Study

In addition to assessment of brain tissue, we carried out work on U87 glioblastoma cell line. We aimed to assess efficacy of various compounds and their effect on proliferation of U87 glioblastoma cell line. These compounds included common chemotherapeutic drug Etoposide, methyl donor SAM and commercially available CBD extract. We aimed to determine the dose response of the glioma cell line and establish whether they pose a useful treatment option for patient diagnosed with GBM. This was a preliminary assessment to determine the value of these therapeutic compounds. However due to time constraints we were only able to partially establish dose response curve from these experiments. Although the data presented here is not complete, it still serves as a valuable indicator of possible effectiveness of these agents and validity of methods used for cell study with U87 cell line.

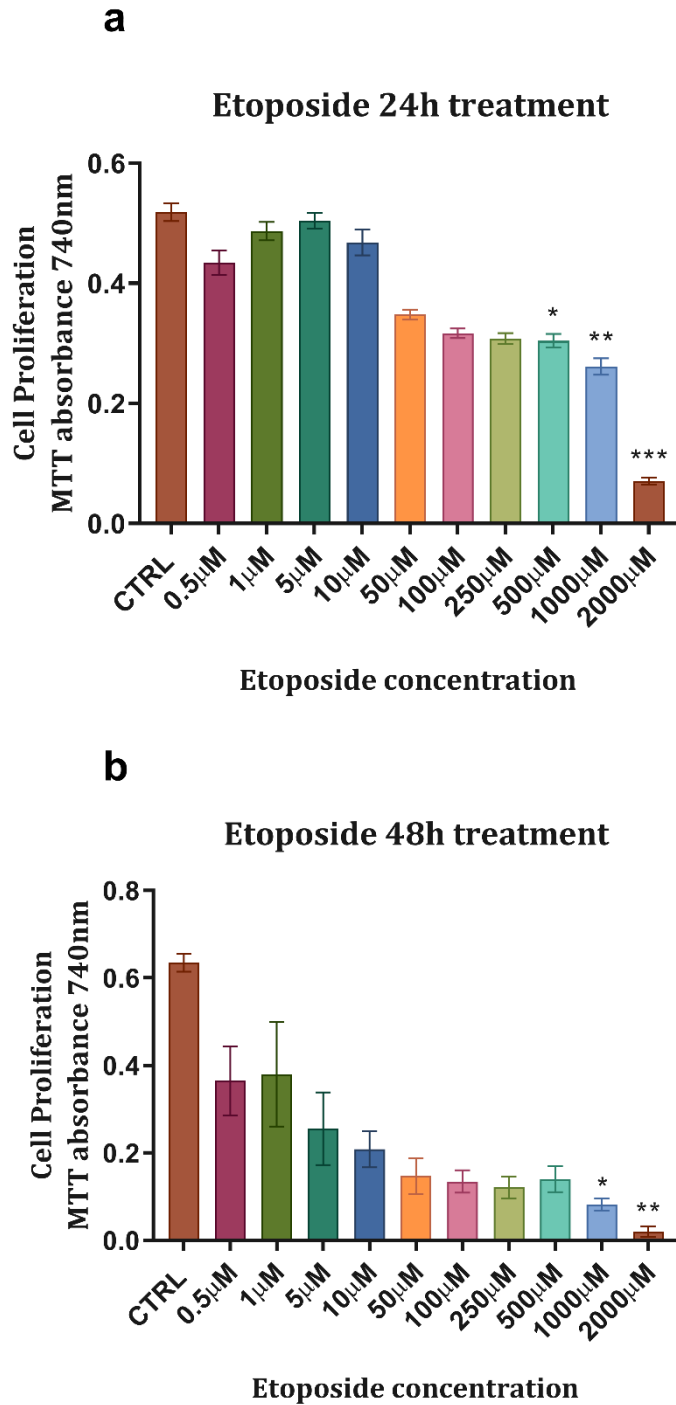


Figure 3-22| Proliferation assay of U87 glioblastoma cell line using MTT assay showing response to treatment with chemotherapeutic Etoposide after 24 hours (a) and 48hours (b). MTT absorbance was read at 740nm wavelength. Higher absorbance signifies higher proliferation and cell content. Range of concentrations was used to determine dose response. Data was analysed by non-parametric One-way ANOVA (Kruskal-Wallis test) and statistical significance set at * $P < 0.05$; ** $P < 0.01$. Mean \pm SEM plotted; Multiple comparisons revealed significance between the control and doses for following concentrations: for 24h: 500 μ M, $p = 0.0458$; 1000 μ M, $p = 0.0043$; 2000 μ M, $p = 0.0005$; for 48h: 1000 μ M, $p = 0.0475$; 2000 μ M, $p = 0.0038$.

The treatment of U87 cells with Etoposide has decreased cell proliferation in both 24 hours and 48 hours (Figure 3-22, 'a' and 'b' respectively). After 24 hours a dose of 50 μ M was necessary to elicit noticeable effect on U87 proliferation and 2000 μ M was required to greatly reduce the proliferation. Treatment after 48 hours was much more effective. Only 0.5 μ M has had visible effect with over 30% reduction of proliferation and over 50% reduction with 5 μ M concentration. 500 μ M was necessary to reach significant reduction of proliferation after 24 hours. 1000 μ M was needed in 48-hour treatment to reach significant reduction even though decrease of proliferation was more prominent. This is most likely due to variability of absorbance readings and more experiments are necessary to accurately measure the inhibition of proliferation. With 2000 μ M dose of Etoposide there was very small amount of detectable metabolic activity as detected by MTT assay. A wider range of concentrations would be beneficial for determination of IC₅₀ for both, 24-hour treatment and 48-hour treatment. However, Etoposide was successful at reducing proliferation of U87 GBM cell line.

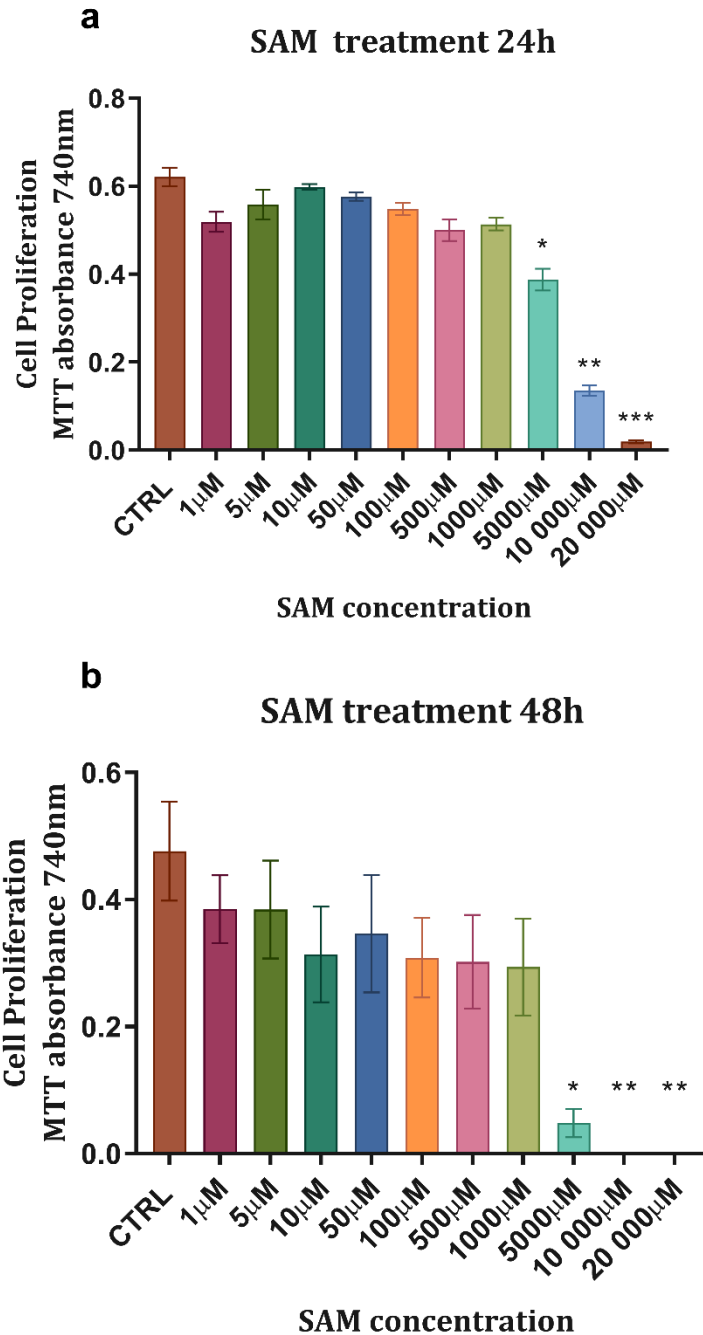


Figure 3-23| Proliferation assay of U87 glioblastoma cell line using MTT assay showing response to treatment with methyl donor SAM after 24 hours (a) and 48hours (b). MTT absorbance was read at 740nm wavelength. Higher absorbance signifies higher proliferation and cell content. Range of concentrations was used to determine dose response. Data was analysed by non-parametric One-way ANOVA (Kruskal-Wallis test) and statistical significance set at * $P < 0.05$; ** $P < 0.01$; *** $P < 0.001$. Mean \pm SEM plotted; Multiple comparisons revealed significance between control and doses for following concentrations for 24h: 5000 μM , $p = 0.0155$; 10000 μM , $p = 0.0031$; 20000 μM , $p = 0.0005$. for 48h: 5000 μM , $p = 0.0487$; 10000 μM , $p = 0.005$; 20000

The treatment of U87 with SAM has showed much higher resistance of cells to the methyl donor compound, both after 24 hours and 48 hours (Figure 3-23, 'a' and 'b' respectively). 5000 μM was needed to significantly reduce proliferation by 30% and with 10,000 μM and 20,000 μM concentration proliferation was also significantly reduced. After 48 hours there was much more variability in reduction of proliferation and there was considerable significant reduction after 5000 μM dose and no proliferation at 10000 μM and 20000 μM . Results show that high dose is necessary for reduction of proliferation of GBM cell line but perhaps, SAM could be used in conjuncture with other therapeutics to reduce the strength of a dose and possible toxicity effects. Further experiments are necessary to accurately estimate the IC₅₀ of SAM in inhibition of cellular proliferation of cancer cells. It would also be beneficial to determine SAM's effect on non-cancerous astrocytic and neuronal cells. This would be very useful in determining the viability of SAM as a therapeutic compound to be used for GBM patients.

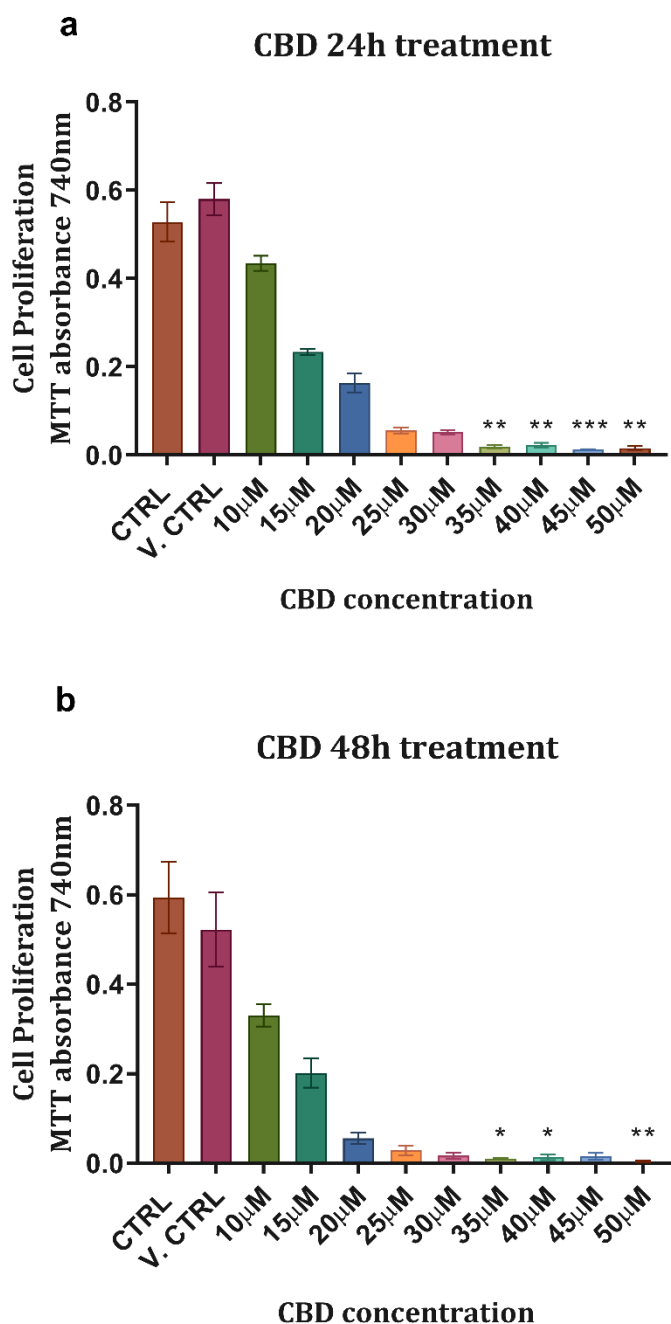


Figure 3-24| Proliferation assay of U87 glioblastoma cell line using MTT assay showing response to treatment with CBD after 24 hours (a) and 48hours (b). MTT absorbance was read at 740nm wavelength. Higher absorbance signifies higher proliferation and cell content. Range of concentrations was used to determine dose response. Data was analysed by non-parametric One-way ANOVA (Kruskal-Wallis test) and statistical significance set at * $P < 0.05$; ** $P < 0.01$; *** $P < 0.001$. Mean \pm SEM plotted; Multiple comparisons revealed significance between vehicle control (v.control) and doses for following concentrations for 24h: 35 μM , $p = 0.0043$; 40 μM , $p = 0.0096$; 45 μM , $p = 0.0007$; 50 μM , $p = 0.002$; for 48h: 35 μM , $p = 0.0323$; 40 μM , $p = 0.027$; 50 μM , $p = 0.0015$.

We have found commercially available CBD to have a very positive effect in reducing proliferation of U87 GBM cell line after treatment for 24 hours and 48 hours (Figure 3-24, 'a' and 'b' respectively) 10 μM of CBD dose was enough to reduce proliferation by 30% and 15 μM was able to reduce the proliferation by 60% just after 24 hours. Significant reduction was reached at 35 μM onwards for both timepoints, excluding 45 μM at 48 hours with over 90% reduction of proliferation. With 48 hours treatment, proliferation was reduced by about 50% with only 10 μM concentration. After 20 μM proliferation was reduced by 90%. However, it needs to be noted that there was some reduction associated with vehicle control (ethanol) which could have contributed to enhanced reduction of CBD after 24 hours. Whether this is indeed the case needs to be investigated and more dose response experiments carried out to establish CBD's reliability and reducing proliferation. From the dose response we have determined the IC₅₀ of CBD after 24 hours and 48 hours, seen below in Figure 3-25.

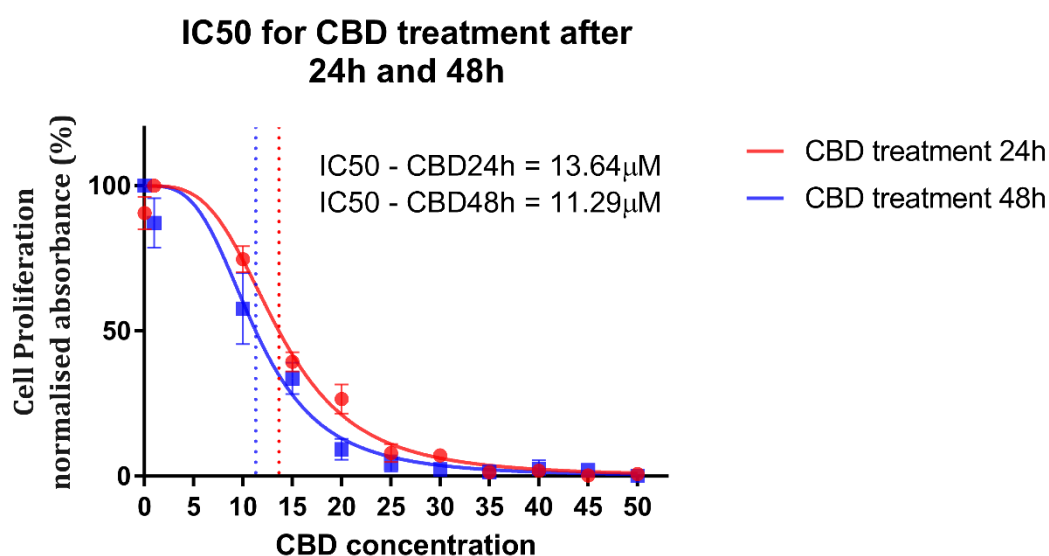


Figure 3-25| IC₅₀ of CBD on proliferation of U87 glioblastoma cell line using MTT assay showing response to treatment with CBD after 24 hours (red) and 48hours (blue). MTT absorbance was read at 740nm wavelength. Higher absorbance signifies higher proliferation and cellular metabolism. Range of concentrations was used to determine IC₅₀. IC₅₀ - 24h=13.64 ($R^2=0.9855$); IC₅₀ - 48h=11.29 ($R^2=0.9687$)

IC₅₀ of CBD after 24 hours was calculated at 13.64 μ M and after 48 hours it was estimated to be 11.29 μ M. Coefficient of determination showed good linear fit and low variance for treatment after 24 hours ($R^2=0.9855$) and a little higher variance for 48-hour treatment ($R^2=0.9687$). These results suggest that low doses of CBD are successful in reducing proliferation of U87 GBM cell line though further investigation is necessary to determine its efficacy as GBM treatment option.

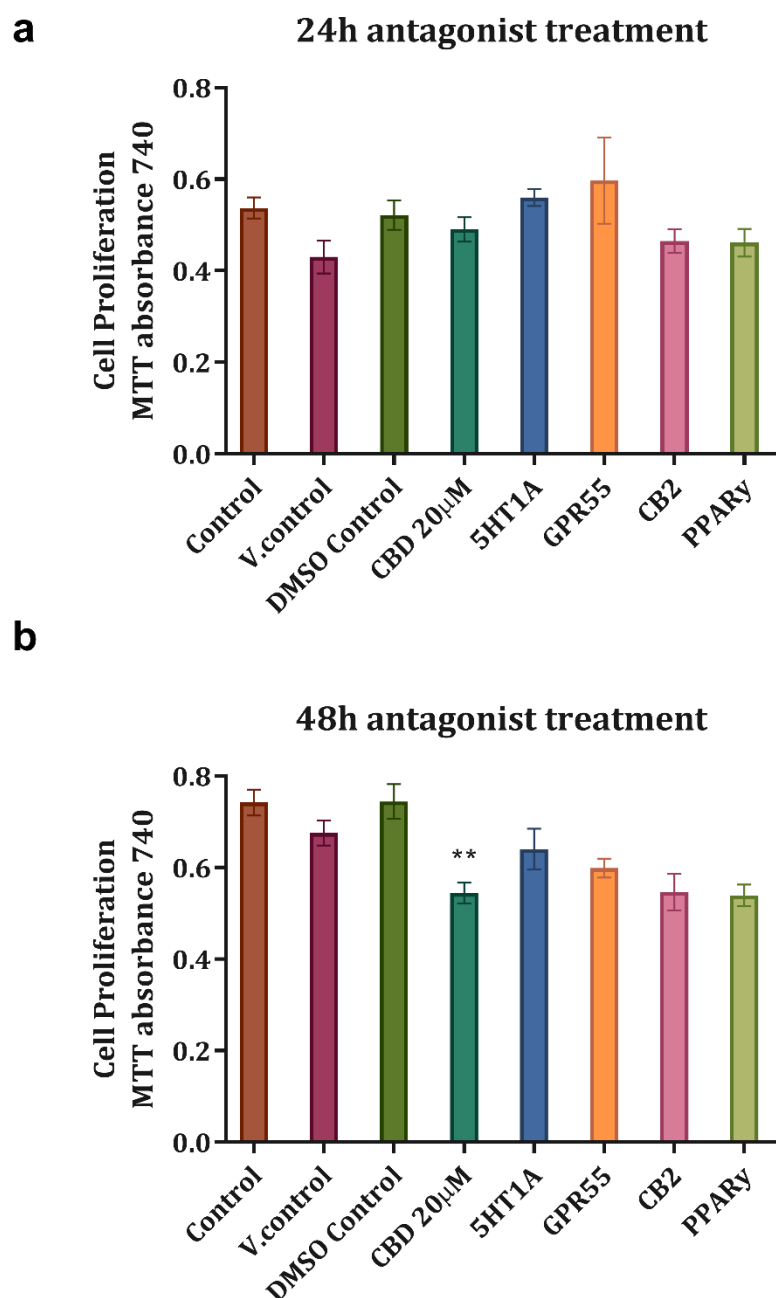


Figure 3-26|Investigation of mode of action of CBD by using specific antagonists. Proliferation assay of U87 glioblastoma cell line using MTT assay showing response to treatment with CBD and specific set of antagonists after 24 hours (a) and 48hours (b). MTT absorbance was read at 740nm wavelength. Higher absorbance signifies higher proliferation and cell metabolism. One concentration of CBD was used to determine response of cells treated with various receptor antagonists. Multiple comparisons revealed significance between vehicle control (v.control) only for CBD 48h treatment with $p=0.0017$.

Because of low doses of CBD required for reduction of proliferation, we wanted to investigate the mode of action of this compound to study inhibition of

GBM more closely. We used 20 μ M of CBD to reduce the proliferation of U87 cells by over 50%. However, we were not able to reproduce our previous findings and inhibition of proliferation with CBD was not successful at 24 hours though there was about 15% significant reduction of proliferation after 48 hours with just CBD treated cells. This could possibly be explained by CBD not being dissolved properly or losing its potency due to degradation in solution. Vehicle control alone has decreased proliferation of cells more than with CBD. After 48 hours the reduction of proliferation with CBD was more noticeable. We found two possible candidates responsible for CBD's way of inducing inhibitory effects on cancer cells. Proliferation of cells treated with 5HT1A and GPR55 had higher observed proliferation rate even after treatment with CBD for both treatment timepoints. Proliferation after 24 hours had similar rate to the control and reduced inhibition of proliferation after 48-hour treatment with CBD. This poses a possible mode of action for CBD to be partially responsible through these receptors though because of variability of the data and failure to replicate dose response from previous experiment proposes that the results may not be fully reliable and more investigations should be carried out to confirm current hypothesis that CBD works through one of these receptors.

4 Discussion

The investigation of various proteins and their succeeding PTM has revealed proteome-wide dysregulation in GBM. Results obtained mostly agree with current literature and indicate that aberration in protein expression and modifications are a common feature of GBM. Various protein changes and modifications can be observed both in separate tumours and across different tumour regions from the same tissue providing further evidence for GBM's inter- and intra-tumour heterogeneity. With use of various proteomic methods, we were able to assess, to a degree, these aberrations as well as compare efficacy of well-established proteomic tools in investigations of protein modifications and aberrant protein expression.

4.1 Assessment & Evaluation of Proteomic Methods Used

In this study, a range of proteomic techniques were used to investigate aberrant proteomic patterns of GBM and various regions of the tumour. Using very well-established techniques such as gel electrophoresis to more recent Multiplex MAP technologies, we have begun to paint a picture of various alterations that occur in GBM. With every following methodology we were able to describe various changes that occur in various tumour regions as well as evaluate successes and failures of methods and techniques used. Through trial and error, we were able to optimise certain techniques and carry out experiments with more confidence and accuracy.

Separation of proteins with 1D-PAGE and total protein staining let us assess major or minor differences in expression of cytosolic, nuclear and membrane proteins. Cytosolic and nuclear separation revealed variability in total protein expression between control samples but also between different tumour regions (Figure 3-2, 3-3). Results showed general absence of proteins in some areas,

especially of the lower molecular weight proteins of cytosolic and nuclear fractions. Perhaps transcription and expression of several proteins has been altered reducing the total protein expression and leading to preferential overexpression of oncogenic proteins and signalling cascades. We have also observed strong expression of some specific protein regions. Because of general alterations of many metabolic pathways described in current literature some alterations were expected though our results were surprising as these changes were strongly visible on 1D-PAGE separated gels. Separation of membrane proteins was less successful (Figure 3-3). This is most likely due to contaminants in the sample such as lipids from phospholipid bilayer and other contaminants. This can be avoided with use of precipitation and de-salting methods. Though we have used acetone precipitation of protein samples for 2D-PAGE, this was omitted in 1D-PAGE. It is however clear that further decontamination of samples might be necessary before carrying out separation of complex protein mixtures. This is further supported by the MS/MS data from 1D-PAGE gels. The protein bands which were most heavily expressed in gel turned out to be albumin and haemoglobin derived from blood. This is perhaps due to high vasculature of the brain as well as tumour surrounding area. Because samples were flash frozen after surgery, a lot of blood has remained in the protein lysates. High expression of albumin and haemoglobin could have potentially masked expression of other significant proteins. Immunoprecipitation of these proteins would be beneficial for further investigations and should come into common practice when working with brain tissue samples as same proteins were detected in PFC control samples though at lower concentration. Albumin and haemoglobin, though not indicative of unique GBM proteome, could possibly point towards high vasculature of the tumour tissue caused by increased angiogenesis.

In addition to total protein stain we have used phospho-specific dye (Pro-Q diamond) to detect phosphoproteins. We were again able to detect global phosphorylation of proteins in cytosolic and nuclear fraction (Figure 3-4, 3-5) though due to previously mentioned problems; membrane phosphoproteins were not detected (Figure 3-6). Pro-Q diamond serves as a useful tool for in gel

detection of phosphoproteomic changes though several aspects need to be optimised. The signal of the imaging equipment was not sensitive enough to detect a strong signal though even with reduced sensitivity we were able to detect a noticeable signal in cytosolic and nuclear fraction. With use of phosphospecific stains such as Pro-Q diamond we have noticed general phosphorylation changes in all GBM tissues which confirm the highly heterogenous nature of GBM phospho-proteome and global phosphorylation of many proteins in the brain. Our results indicate that phosphorylation in GBM tissues confer minor and major changes and are often specific to certain protein regions. However, more specific investigations are necessary to elucidate the phosphorylated proteins involved in tumorigenesis and abnormal signalling.

We have further resolved samples with use of 2D-PAGE to separate proteins by their isoelectric point and denatured molecular weight. 2D-PAGE. We have compared different GBM regions and were able to identify more changes in expression as compared to 1D-PAGE. We have also noticed changes in specific areas of 2D gels that could correspond to PTM proteins though further analysis of these regions by more specific methods should be used to identify specific proteins and their PTM. Immunoprecipitation of specific proteins can serve as a useful method in assessing various isomers and protein modifications of these specific proteins. The extent of available options when using when using 1D- and 2D-PAGE for proteomic discovery is very robust and can be tailored to specific tasks and experiments. Because of this versatility it remains as one of the most commonly used method in proteomic research.

We also compared detection of two total protein stains on our large 2D-PAGE gels. We used silver stain and colloidal blue which vary in sensitivity with silver stain being approximately 30-fold more detectable sensitivity. Silver stain was much more sensitive and detected almost twice as many proteins than colloidal blue in both gels. Colloidal blue was a more cost-efficient way to detect the proteins highly expressed in GBM though silver stain was able to detect less abundant proteins with lower expression. The methods used here were very useful at comparing differences in global proteomic expression of GBM tumour samples and PFC controls. These methods are a good first step in quantifying

total protein expression but should also be used conjuncture with more specific protein identification methods such as western blotting or mass spectrometry.

Narrowing down specificity of methodology used we have investigated a range of important proteins involved in various metabolic processes. With western blotting analysis we were able to assess explicit changes in expression of certain proteins and semi-quantitatively assess differences in their abundance. Though not all antibodies have worked and the detection of proteins through western blotting can be a cumbersome and a lengthy process it is still one of the more versatile and useful techniques in identification of protein expression and content. We were able to assess a wide range of proteins and discovered various proteins such as catalase, SOD1, GAPDH, HDAC6, PIMT, acetylated α -tubulin, MAP2, ERK1/2 to be differentially expressed in our GBM tumour samples. Through quantification of blotting data, we were able to find significant differences between normal brain tissue and GBM tissue.

Along the old and tested methods, we were able to use some new and advanced technology such as Milliplex. With a single assay we had the ability to investigate a wide range of protein phosphorylation and found major differences between expression of key signalling kinases and transcription factors including p38, Akt, CREB and STAT3/5. It is a highly useful tool in mapping wide range of pathways and cellular regulators though it's very expensive to run. However, it is highly informative in assessment of kinases and various signalling pathways.

4.2 Role of Energy Metabolism Enzyme & Use of Housekeeping Protein GAPDH in GBM

GAPDH is considered as one of the key enzymes involved in energy metabolism and ATP production. It maintains catalytic conversion of glyceraldehyde-3-phosphate (G3P) to 1,3-biophosphoglycerate in presence of nicotinamide (NAD⁺) and an inorganic phosphate, an important step of glycolysis in the cytoplasm. Due to its high abundance in many cells and highly expressed mRNA levels, it has been commonly assigned a status of a 'housekeeping protein'. However, the function of GAPDH has been further

recognised in a plethora of cellular processes and several studies have implicated altered expression of GAPDH to numerous diseases including neurodegenerative disease and cancer (Butera et al., 2019; Zhang et al., 2015). These studies suggest that post-translational modifications of GAPDH have a direct role in the specialisation and function of GAPDH and are particularly dependent on the subcellular re-distribution of this enzyme (Tristan et al., 2011). Several studies have shown upregulation of GAPDH in various cancers and its possible role in cell proliferation. One of the hypotheses for the preferential selection of glycolytic pathway is the increase in glycolysis reactions enhancing energy production and enabling proliferation (Hao et al., 2015; Lau et al., 2000; Vilà et al., 2000).

In our study we have investigated GAPDH expression in four GBM patients and in three distinct regions; tumour core, tumour rim and invasive margin. We have observed variability in both, different tumours but also in different tumour areas. In few cases, there was visible reduction of expression of GAPDH and absence of one band suggesting either no expression of GAPDH or low abundance of protein below detectable threshold. The absence of GAPDH mostly matched the necrotic areas of the tumour and could perhaps be explained by lower turnover of protein production in highly necrotic areas as well as lack of nutrients such as glucose necessary for glycolysis. It needs to be further investigated whether down-regulation or lack of GAPDH has occurred due to low concentration of glucose and glycolysis or characteristic for GBM tumour necrosis and cell apoptosis in the necrotic core. Because of variable expression of GAPDH we have used total protein as an alternative mean of protein normalisation. Changes in various regions of GBM tumour could result in lower or abnormal expression of some housekeeping proteins and our study has presented this. Few samples have displayed a possibly higher expression (Figure 3-10, 'a', lane: 38.1, 39.1, 39.4, 40.5, 58.2) which generally coincides with tumour rim (apart from lane 58.2 which corresponds to tumour core) though statistical analysis revealed no statistical difference between this region and control. Most of the GAPDH levels were decreased in most areas of the tumour compared to healthy brain. Very few studies have investigated the suitability of GAPDH as housekeeping protein in GBM as most focus on mRNA expression rather than

protein expression though some have found mRNA levels to be altered in GBM (Madhuri G. S. Aithal and Rajeswari, 2015). The GAPDH have been noted to be altered in cancers and few studies show up-regulation of this glycolytic enzyme to be beneficial for cancer progression.

Hao and colleagues (2015) investigated expression of GAPDH in lung and oesophageal squamous cell carcinomas using variety of proteomic methods including 2D-PAGE, western blotting, mass spectrometry, tissue microarrays and immunohistochemistry. Their results indicate that GAPDH is highly expressed in tumour tissue. In addition, *in-vitro* and *in-vivo* investigations revealed that knockdown of GAPDH with siRNA (small-interfering RNA) in cells and mice leads to inhibited proliferation and reduced tumour size as compared to non-transfected controls. Study by Li and others (2014) have suggest acetylation of GAPDH at lysine 254 (K254) increases its catalytic activity consecutively promoting cell proliferation and growth. The increased expression of GAPDH often correlates with poor survival and high malignancy of a tumour (Wang et al., 2013). Evidence suggests that acetylation of GAPDH directs its nuclear translocation (Ventura et al., 2010). The nuclear GAPDH can have a variety of functions which could be determined through its binding to certain complexes. Cytoplasmic GAPDH phosphorylated by activated AMPK leads to GAPDH nuclear translocation and interaction with Sirt1 leading to autophagy (D. Zhang et al., 2015). Oxidation of GAPDH at cysteine residue (C152) leads to amyloid-like aggregation and nuclear translocation where it induces cell death (Nakajima et al., 2009). These studies highlight the importance of GAPDH in cancer as well as localisation its PTMs are vital in defining its function.

Additionally, transcription of GAPDH has been observed to be upregulated in hypoxic states of certain cancers including breast cancers through hypoxia related regulators such as HIF-1 α (Higashimura et al., 2011). However, in GBM tumours, studies show that GAPDH is not upregulated as a response to hypoxia and its suggested that GAPDH transcription levels remain constant even under hypoxic conditions (Said et al., 2009). However there is conflicting evidence on GAPDH expression in GBM as some studies have shown varied mRNA expression suggesting it as not suitable for a role of reference protein (Madhuri G S Aithal

and Rajeswari, 2015; Valente et al., 2014). These studies do in fact focus on the mRNA expression and do not consider the regional localisation of the protein across various tumour sites.

In our study, we would like to report GAPDH to be inconsistently expressed in four GBM tumours and across three different regions including tumour core, tumour rim and invasive margin (Figure 3-10). It is our suggestion that a different reference protein or total protein should be used for normalisation and quantification of GBM protein expression studies in various regions. This is somewhat supported by variability of GAPDH in mRNA expression studies though it would be useful to carry out qPCR analysis of samples examined in our study (Madhuri G. S. Aithal and Rajeswari, 2015; Valente et al., 2014). In our experiments, expression of tumour core and invasive margin was lower than that of normal brain and tumour rim resembled normal brain expression though with greater deviation from the mean. Although the differences were not significant, the variability of these samples should demonstrate enough evidence to suggest that cytosolic GAPDH should not be used as a reference protein for regional expression studies. Also, considering that expression of cytosolic GAPDH appeared lower in both tumour core and invasive margin, perhaps the GAPDH expression in tumour rim was in fact upregulated when compared with other areas of the tumour. One of the possible explanations could be an influx of glucose and other nutrients close to normoxic areas of the tumour rim leading to increased requirement for metabolic enzymes. However, this does not explain low expression at the invasive margin. We have also noticed that in three out of four tumours, cytosolic expression of GAPDH has been lowest or visually absent in the tumour core which could further suggest that the enzyme is not upregulated by the hypoxic conditions. To add to our current findings, further investigation of GAPDH expression in GBM would be beneficial with regards to its cellular localisation, modification and regulation at various tumour regions.

4.3 Cytoskeletal Associated Proteins in GBM

Structural integrity of a cell is maintained by a variety of organisational proteins such as microtubules and microfilaments. Highly dynamic structures such as microtubules are involved in cell motility, protein trafficking and cell division. Because of their structure and variety of microtubule isomers they contain positive and a negative ends allowing them, through protein rearrangement, to change cellular polarity (Oriolo et al., 2007). Maintaining proper cellular polarity makes sure that tissues are properly organised and appropriate architecture is preserved. However there is growing evidence that loss of polarity leads to uncontrolled cell growth and highly unregular organisation of tissue, which are both hallmarks of cancer (Royer and Lu, 2011). Study by Shuchen Gu and colleagues (2016) has observed reduced acetylated α -tubulin to be a key factor in epithelial to mesenchymal transition in epithelial and myoblast cell lines. Microtubules' dynamics serve as an important mechanism in cellular migration through reorganisation and depolarisation of the cytoskeleton. Association of various proteins such as microtubule associated proteins (MAP) act on regulation of these microtubule changes either through expression or PTMs of filaments (Dehmelt and Halpain, 2004). MAPs have also been shown to be involved in tumour invasion. MAP-2 isoform containing exon 13 (MAP-2e) can be expressed in paediatric and adult brain tumours containing glial features, including GBM (Suzuki et al., 2002). Expression of this isomer has been suggested to aid neoplastic infiltration and branching of cancer cells into adjacent healthy brain tissue. Conversely, transcriptional upregulation of normal MAP2 leads to inhibition of glioma cell invasion suggesting the role of this MAP in suppression of oncogenic invasion (Zhou et al., 2015).

In this study we have assessed acetylation of α -tubulin and investigated various proteins responsible for modification of microtubules which include HDAC6 and MAP2. We have found acetylated α -tubulin to be significantly downregulated along with MAP2. Whether de-acetylation of α -tubulin was associated with HDAC6 expression is not clear as there was differential expression of this enzyme in most GBM tissues and PFC. Nevertheless, HDAC6 had a higher expression in tumour rim of GBM samples whereas acetylation of α -

tubulin was significantly decreased in GBM tissue. Acetylation of tubulin has been suggested to have stabilising and neuroprotective function in brain preventing the microtubules from depolarisation and from acquiring harmful or destabilising PTMs (Mao et al., 2017; Portran et al., 2017). Furthermore acetylation of α -tubulin has been shown increase in response to cytotoxic brain damage and natural brain ageing (Labisso et al., 2018). Whether acetylation mechanisms of tubulins have stabilising effect in GBM or ageing brains needs to be further established. However, reduction of MAP2 with conjunction of other dysregulated pathways, as shown in this study, may result in more unstable microtubular phenotype and acquisition of a number of defects.

4.4 Redox Response & Repair Enzymes

In our study we have assessed cytosolic total carboxylation of proteins to determine general oxidative cytosolic damage which we followed by assessment of various redox and repair enzymes. With the Oxyblot we have observed potential changes in total oxidation though more interesting was carbonylation status of specific protein regions. We have found several regions of proteins to be specifically carbonylated in GBM tumours and in various regions of the tumour. Oxidation of proteins induced by increased concertation of ROS plays an important role in cancer progression. It has been suggested that specific proteins are oxidised in cancer often leading to their loss of function, a process which might benefit cancerous cells (Aryal and Rao, 2018). Although we were not able to find significant change in total oxidation between GBM regions and PFC tissue we have observed specific carbonylation of certain protein regions. Because our results have not reached optimal resolution of carbonylated proteins in all samples, we suggest that these experiments should be repeated as there is evidence to suggest selective carbonylation in GBM tissue as compared with PFC tissue.

Our findings of SOD1 expression showed global downregulation of SOD1 across all GBM tumour samples confirming previous findings by Aggarwal et al.

(2006). To add to the current finding, the SOD1 expression was collectively downregulated across all distinct tumour sites suggesting that downregulation of the SOD1 enzyme might be universal across GBM tumour regions. SOD1 is responsible for elimination of peroxides and reduction of its expression could in turn result in net increase of peroxides and sustained oxidative damage caused by ROS. In a study on SOD1 effects on U118 glioma cell lines, Li et al., (2000) suggested that increased activity of SOD1 inhibited growth rates and elongated cell doubling time in most SOD1 overexpressing clones. This suggests that SOD1 could act as tumour suppressor in GBM and lowered expression might be associated with GBM's fast growth and increased proliferation. In addition, downregulation of SOD1 might result in subsequent net accumulation of superoxides and lead to sustained oxidative damage. ROS accumulation can also result in higher rates of DNA damage and protein modifications resulting in dysregulation of signalling pathways and acquisition of somatic mutations favourable to cancer sub-populations. Study by Suh et al. (1999) suggested that sustained exposure to ROS in NIH3T3 cells was able to transform them and create aggressive tumours in athymic mice. It has also been suggested that ROS have a crucial function in activation and regulation of key signalling pathways (Huo et al., 2009).

We have also found that PIMT was completely absent in expression across all GBM tissue though it was uniformly expressed in PFC samples. These correlates with previous studies on PIMT expression where PIMT has been shown to be significantly downregulated in astrocytomas and gliomas and supports previous findings that PIMT is generally dysregulated in brain tumours (Lapointe et al., 2005). Dysregulation of repair activity of PIMT through reduction of expression could lead to abnormal protein modification and neurodegeneration. Downregulation of PIMT in human hippocampal regions is accompanied by accumulation of damaged proteins such as β -tubulin (Lapointe et al., 2005). Abnormal aspartyl residues accumulate in tubulin monomers during stage progression of gliomas could disrupt cytoskeletal protein structure, leading to improper microtubule polymerization or interaction with microtubule-associated proteins, which could favour carcinogenesis. Additionally, studies in knock-down of PIMT in neuroblastoma cell line, showed increased formation of

amyloid- β through reduction of α -disintegrating and metalloprotease 10 and 17 (ADAM10 and ADAM17). Amyloid aggregation and accumulation have been commonly associated with neurodegenerative disease however, evidence suggests that amyloid- β can be upregulated in GBM and also produced in glioma cell lines (Bae et al., 2011; Culicchia et al., 2008). Whether the possible pathway of amyloid- β accumulation could be caused by reduction of PIMT needs to be further addressed. However study by Siney and colleagues.(2017) suggests that ADAM10 and ADAM17 are upregulated in GBM, therefore formation of amyloid- β is not perhaps regulated by PIMT reduction in GBM. However, the same study has found that inhibition of ADAM10 and ADAM17 can promote migration and invasion of glioma stem cells from the tumorigenic niche into the surrounding parenchyma. Significant downregulation of PIMT might have major downstream effects whether it's maintenance of protein repair or regulation of other proteins' expression.

There is very limited data available on isoaspartyl formation in GBM tumours. The levels of L-isoaspartyl and D-aspartyl residues and proteins affected by these modifications need to be further investigated in GBM as dysregulation of PIMT could result in higher concentration of altered proteins. Histones and predominantly H2B has been shown to exhibit propensity for isoaspartyl formation (Young et al., 2001). Modification of H2B in such manner, affiliated with lack of PIMT enzyme responsible for its repair, results in beyond normal levels of isoaspartyl formation that can have profound effects on transcription of genes as well as DNA stability. Certain isoforms from family of protein arginine methyltransferases (PRMT) have been found to regulate transcription and contribute to oncogenic expression in GBM. For example PRMT1, PRMT2 and PRMT5 are highly expressed in GBM tissue leading to increased stem cell self-renewal and tumour growth (Dong et al., 2018; Han et al., 2014; Wang et al., 2012).Studies in expression of these proteins suggests that dysregulation of methylation patterns most likely contribute to the epigenetic heterogeneity of GBM as well as selective methylation and consecutive altered transcription of promoter regions. PIMT is generally highly expressed in human and rat brains therefore its absence could have significant neurodegenerative effects. Increase in proteins carrying abnormal isoaspartyl modifications could

lead to various biochemical changes and because of its association with microtubules it might be considered to have an effect on brain plasticity(Desrosiers and Fanélus, 2011). Accumulation of abnormal proteins could also contribute to loss of function of many signalling pathways and progressive neurodegeneration. Our findings on PIMT expression are certainly interesting though they lead towards further investigations of PIMTs deficiency role in malignant formation of GBM tumours. Whether increased rate of abnormal proteins is beneficial for invasion, growth or acquisition of somatic mutations in various areas of the brain is yet unknown and should be further investigated.

Because of the major loss of PIMT in GBM we wanted to investigate whether the increase of SAM necessary for methylation of various substrates would be effective in reduction of GBM proliferation in cells. Use of SAM as a compound to methylate certain promoter region has been shown to be successful in a number of studies proposing its antiproliferative effects on cancer cells (Hussain et al., 2013; Schmidt et al., 2016). However, we were only able to formulate the dose response curve which suggests that high doses are necessary for reduction of proliferation. This however does not suggest the mode of action or viability to use SAM as a therapeutic agent for cancer and methylation assessment of various promoter regions and proteins would be necessary to fully evaluate its efficacy

4.5 Transcription Factors

Involvement of transcription factors greatly contributes to oncogenic growth and tumour progression. There is vast amount of research from cell lines, murine models and human tissue implicating transcription factors in oncogenesis. These transcription factors are the culmination of cascade of signalling events and integrate the cytokine and growth factor signals to elicit response such as growth, proliferation, survival and motility.

In our study we have found few transcription factors to be altered in various GBM tumour regions. CREB, STAT3 and 5 have been differentially expressed in various regions. We have found STAT3 to be most significantly

upregulated in tumour rim and invasive margin. STAT5 however was significantly downregulated in the tumour rim but no other region.

STATs are a family of transcription factors with pleiotropic downstream effects often associated with canonical JAK/STAT signalling pathway responsible for plethora of cellular events as a response to extracellular signals (Rawlings et al., 2004). After ligand binding to a receptor JAK is activated and auto-phosphorylates STAT substrates causing them to dimerize and translocate to the nucleus. Presence of dimerized STATs in the nucleus leads to binding of the dimer to specific sequences directly affecting transcription by either activation or repression of certain genes. Aberrations of STAT3 and to some degree STAT5 has been confirmed in GBMs (Swiatek-machado and Kaminska, 2013). Phosphorylation of STAT3 has been identified as a therapeutic target in GBM due to being a downstream effector of several signalling pathways (Ouédraogo et al., 2017). Mutation *EGFRvIII* as well as amplification of EGFR has been frequently connected to persistent activation of STAT3 and STAT5 in GBM (Fan et al., 2013). EGFR phosphorylation has also been connected to downstream activation of Akt and ERK1/2 kinases which we have also found to be significantly upregulated in various regions of GBM tumours. Because of frequent amplifications and mutations of EGFR it is entirely possible that four samples analysed in this study could also exhibit these alterations and more extensive proteomic profiling of RTKs would be beneficial. Our results suggest that STAT3 is strongly expressed in all regions of GBM tumours and because of its pleiotropic function and transcription of various genes it could elicit different cell properties in different GBM regions. RNA studies of STAT3 transcription suggested its responsibility in activation of cell cycle regulation, extracellular matrix remodelling and downregulation of hypoxia response (Ganguly et al., 2018). STAT3 is therefore an important transcription factor in oncogenic progression and our results suggest that high overexpression of it might be highly conserved across all regions of GBM tumour.

Transcription factor CREB has also been significantly unregulated in tumour rim and invasive margin. It is a proto-oncogenic transcription factor that promotes tumorigenesis in many cancers and has been found to be upregulated

in glioma tumours (Tan et al., 2012). It has been shown that CREB phosphorylation is necessary in regulation of GBM proliferation mediated via PI3K and ERK1/2 pathways (Daniel et al., 2014). Similarly, to STAT3, it can be constitutively activated and highly expressed in glioma tissue. Our findings agree with previously mentioned studies that CREB is highly expressed in GBM tissue though perhaps it is mainly activated in areas surrounding the tumour core acting as a modulator of tumour growth and invasion.

4.6 CBD Treatment

Our study of CBD as a potential therapeutic showed promising results in reducing U87 cell proliferation at low doses. Our results showed IC₅₀ for cellular proliferation to be 14 μ M for 24-hour treatment and 11 μ M for 48-hour treatment. This is in a way similar to the results obtained Solinas et al (2013) study where they have achieved IC₅₀ of 11 μ M after 24 hours. However, their assessment involved invasion using a Matrigel and perhaps lesser concentration was needed for inhibition of movement across the surface. In addition, we have calculated a wider range of concentration and estimate of IC₅₀ might be more accurate. It would be useful, however, to expand our results into assessment of precise mode of action of CBD. We have touched upon possible mechanism and have achieved indicative results suggesting 5-HT_{1A} and GPR55 to be potential modulators for efficacy of cannabidiol. This is supported by a group of studies suggesting that GPR55 and 5-HT_{1A} might contain transient receptor viable for CBDs modulation (Dumitru et al., 2018). However, our results are only suggestive as the variability of the data has been extensive for the treatment with CBD in the antagonist study performed here.

5 Conclusion

In this study several proteomic methods have been used to assess proteomic changes that happen in various GBM regions. From simple preparation and simple quantification methods to more multidimensional methods of 2D-PAGE and complex MAP multiplex technology, we were able to create a more comprehensive image of possible protein alterations in GBM brain tumour. Each proteomic method has provided a plethora of information for analysis and further investigations of this malignant tumour and with each consequent step in analysis of the GBM tissue and normal brain tissue certain pieces started to paint a better picture of the disease. Though due to the scale of the possible proteome and implications of the highly heterogenous disease that is cancer, we were only able to scratch the surface and further proteomic investigations are required to uncover the full picture.

Through our assessment of the GBM proteome, we have uncovered profound changes in expression of important metabolic, cytoskeletal, redox, transcription and signalling proteins and enzymes. This change was not only perceived between tumour and normal tissue but also between various regions of the tumour. It is well established that tumour is a multi-layered disease that bestows a multifaceted genomic, transcriptomic and proteomic changes across the malignant tissue (Hambardzumyan and Bergers, 2015; Laplane et al., 2018; Persano et al., 2011b). For optimal treatment and application of therapeutics, the crosstalk between various areas needs to be closely examined as the communication between various subpopulation niches of cancer cells in tumour is one of the leading factors of high heterogeneity of this disease. With our study, we have observed some of this crosstalk and have discovered global changes as well as changes specific to tumour regions. This perhaps illustrates the need of the tumour to respond differentially to several metabolic and environmental changes which is governed by the continually changing proteomic landscape and expression and transcription pattern. Though many discoveries have been achieved through genomic screening of the GBM tumours, there is ever growing

necessity to delineate GBM tumours in terms of their active proteome. We have used methods which have been optimised and perfected over decades to investigate proteomic changes and they remain as relevant as ever in proteomic discovery. We have also used a more recent technologies such as Milliplex and MS/MS to assess various protein changes and these were also extremely useful in mapping changes in expression across various tumour regions. For most accurate assessment of proteomic changes in health and disease a conjuncture of various proteomic methods is most useful in outlining specific changes in cells and tissues We have evaluated this process and achieved thought-provoking results which can be further investigated and used in defining widespread alterations in GBM tumours. However, even with various investigations carried out in this study we were only able to touch upon the vast changes that occur in GBM which only signifies the intricate nature of cancer.

Glioblastoma is a complex and perplexing disease. It is one of the deadliest of brain tumours and despite significant advances in molecular and proteomic research there are still gaps which remain to be uncovered that could help in treatment of GBM. The genome and transcriptome have been extensively studied in hopes to delineate the progression, evolution and aggressiveness that drive GBM malignancy, yet the survival rates for patients remain low. In wake of genomic knowledge that is now widely available, further steps need to be taken to try and better understand GBM pathophysiology.

6 References

- Aggarwal, S., Subberwal, M., Kumar, S., Sharma, M., 2006. Brain tumor and role of beta-carotene, a-tocopherol, superoxide dismutase and glutathione peroxidase. *J. Cancer Res. Ther.* 2, 24–7. <https://doi.org/10.4103/0973-1482.19771>
- Aithal, Madhuri G. S., Rajeswari, N., 2015. Validation of Housekeeping Genes for Gene Expression Analysis in Glioblastoma Using Quantitative Real-Time Polymerase Chain Reaction. *Brain Tumor Res. Treat.* 3, 24. <https://doi.org/10.14791/btrt.2015.3.1.24>
- Aithal, Madhuri G S, Rajeswari, N., 2015. Validation of housekeeping genes for gene expression analysis in glioblastoma using quantitative real-time polymerase chain reaction. *Brain tumor Res. Treat.* 3, 24–9. <https://doi.org/10.14791/btrt.2015.3.1.24>
- Alfadda, A.A., Sallam, R.M., 2012. Reactive Oxygen Species in Health and Disease 2012. <https://doi.org/10.1155/2012/936486>
- Aryal, B., Rao, V.A., 2018. Specific protein carbonylation in human breast cancer tissue compared to adjacent healthy epithelial tissue. *PLoS One* 13, e0194164. <https://doi.org/10.1371/journal.pone.0194164>
- Bae, N., Byeon, S.E., Song, J., Lee, S., Kwon, M., Mook-jung, I., Cho, J.Y., 2011. Knock-down of protein L -isoaspartyl O -methyltransferase increases β -amyloid production by decreasing ADAM10 and ADAM17 levels. *Nat. Publ. Gr.* 32, 288–294. <https://doi.org/10.1038/aps.2010.228>
- Bai, J., Rodriguez, A.M., Melendez, J.A., Cederbaum, A.I., 1999. Overexpression of catalase in cytosolic or mitochondrial compartment protects HepG2 cells against oxidative injury. *J. Biol. Chem.* 274, 26217–24. <https://doi.org/10.1074/jbc.274.37.26217>
- Biernat, W., Kleihues, P., Yonekawa, Y., Ohgaki, H., 1997. Amplification and

- overexpression of MDM2 in primary (de novo) glioblastomas. *J. Neuropathol. Exp. Neurol.* 56, 180–5.
- Bocklandt, S., Lin, W., Sehl, M.E., Sánchez, F.J., Sinsheimer, J.S., Horvath, S., Vilain, E., 2011. Epigenetic predictor of age. *PLoS One* 6, e14821.
<https://doi.org/10.1371/journal.pone.0014821>
- Bray, F., Ferlay, J., Soerjomataram, I., Siegel, R., Torre, L., Jemal, A., 2018. Global cancer statistics 2018: GLOBOCAN estimates of incidence and mortality worldwide for 36 cancers in 185 countries. *CA A J. Clin.* 00, 1–31.
<https://doi.org/10.3322/caac.21492>.
- Butera, G., Mullappilly, N., Masetto, F., Palmieri, M., Scupoli, M.T., Pacchiana, R., Donadelli, M., 2019. Regulation of Autophagy by Nuclear GAPDH and Its Aggregates in Cancer and Neurodegenerative Disorders. *Int. J. Mol. Sci.* 20.
<https://doi.org/10.3390/ijms20092062>
- Campian, J., Gutmann, D.H., 2017. CNS Tumors in Neurofibromatosis. *J. Clin. Oncol.* 35, 2378–2385. <https://doi.org/10.1200/JCO.2016.71.7199>
- Cancer Research UK, 2018. Cancer mortality by Age [WWW Document]. Most common causes cancer death by age males/females, by Age, UK. URL <http://www.cancerresearchuk.org/health-professional/cancer-statistics/statistics-by-cancer-type/oral-cancer/mortality#heading-One> (accessed 8.20.07).
- Carrozza, M.J., Utley, R.T., Workman, J.L., Côté, J., 2003. The diverse functions of histone acetyltransferase complexes. *Trends Genet.* 19, 321–329.
[https://doi.org/10.1016/S0168-9525\(03\)00115-X](https://doi.org/10.1016/S0168-9525(03)00115-X)
- Castro-Castro, A., Janke, C., Montagnac, G., Paul-Gilloteaux, P., Chavrier, P., 2012. ATAT1/MEC-17 acetyltransferase and HDAC6 deacetylase control a balance of acetylation of alpha-tubulin and cortactin and regulate MT1-MMP trafficking and breast tumor cell invasion. *Eur. J. Cell Biol.* 91, 950–960. <https://doi.org/10.1016/j.ejcb.2012.07.001>
- Choudhary, C., Kumar, C., Gnäd, F., Nielsen, M.L., Rehman, M., Walther, T.C., Olsen, J. V., Mann, M., 2009. Lysine Acetylation Targets Protein Complexes

- and Co-Regulates Major Cellular Functions. *Science* (80-.). 325, 834–840.
<https://doi.org/10.1126/science.1175371>
- Chuang, Y.-H., Paul, K.C., Bronstein, J.M., Bordelon, Y., Horvath, S., Ritz, B., 2017. Parkinson's disease is associated with DNA methylation levels in human blood and saliva. *Genome Med.* 9, 76. <https://doi.org/10.1186/s13073-017-0466-5>
- Culicchia, F., Cui, J.-G., Li, Y.Y., Lukiw, W.J., 2008. Upregulation of beta-amyloid precursor protein expression in glioblastoma multiforme. *Neuroreport* 19, 981–5. <https://doi.org/10.1097/WNR.0b013e328302f139>
- Daniel, P., Filiz, G., Brown, D. V, Hollande, F., Gonzales, M., D'Abaco, G., Papalexis, N., Phillips, W.A., Malaterre, J., Ramsay, R.G., Mantamadiotis, T., 2014. Selective CREB-dependent cyclin expression mediated by the PI3K and MAPK pathways supports glioma cell proliferation. *Oncogenesis* 3, e108–e108. <https://doi.org/10.1038/oncsis.2014.21>
- Dasuri, K., Zhang, L., Keller, J.N., 2013. Oxidative stress, neurodegeneration, and the balance of protein degradation and protein synthesis. *Free Radic. Biol. Med.* 62, 170–185. <https://doi.org/10.1016/j.freeradbiomed.2012.09.016>
- De Bonis, P., Anile, C., Pompucci, A., Fiorentino, A., Balducci, M., Chiesa, S., Lauriola, L., Maira, G., Mangiola, A., 2013. The influence of surgery on recurrence pattern of glioblastoma. *Clin. Neurol. Neurosurg.* 115, 37–43. <https://doi.org/10.1016/j.clineuro.2012.04.005>
- De Jesús, M.L., Hostalot, C., Garibi, J.M., Sallés, J., Meana, J.J., Callado, L.F., 2010. Opposite changes in cannabinoid CB1 and CB2 receptor expression in human gliomas. *Neurochem. Int.* 56, 829–833. <https://doi.org/10.1016/j.neuint.2010.03.007>
- De Petrocellis, L., Melck, D., Palmisano, A., Bisogno, T., Laezza, C., Bifulco, M., Di Marzo, V., 1998. The endogenous cannabinoid anandamide inhibits human breast cancer cell proliferation. *Proc. Natl. Acad. Sci. U. S. A.* 95, 8375–80. <https://doi.org/10.1073/pnas.95.14.8375>
- de Souza, C.F., Sabedot, T.S., Malta, T.M., Stetson, L., Morozova, O., Sokolov, A.,

- Laird, P.W., Wiznerowicz, M., Iavarone, A., Snyder, J., deCarvalho, A., Sanborn, Z., McDonald, K.L., Friedman, W.A., Tirapelli, D., Poisson, L., Mikkelsen, T., Carlotti, C.G., Kalkanis, S., Zenklusen, J., Salama, S.R., Barnholtz-Sloan, J.S., Noushmehr, H., 2018. A Distinct DNA Methylation Shift in a Subset of Glioma CpG Island Methylator Phenotypes during Tumor Recurrence. *Cell Rep.* 23, 637–651.
<https://doi.org/10.1016/j.celrep.2018.03.107>
- Deaton, A.M., Bird, A., 2011. CpG islands and the regulation of transcription. *Genes Dev.* 25, 1010–22. <https://doi.org/10.1101/gad.2037511>
- Debevec, T., Millet, G.P., Pialoux, V., 2017. Hypoxia-Induced Oxidative Stress Modulation with Physical Activity. *Front. Physiol.* 8, 84.
<https://doi.org/10.3389/fphys.2017.00084>
- Dehmelt, L., Halpain, S., 2004. Actin and microtubules in neurite initiation: Are MAPs the missing link? *J. Neurobiol.* 58, 18–33.
<https://doi.org/10.1002/neu.10284>
- Del Vecchio, C.A., Giacomini, C.P., Vogel, H., Jensen, K.C., Florio, T., Merlo, A., Pollack, J.R., Wong, A.J., 2013. EGFRvIII gene rearrangement is an early event in glioblastoma tumorigenesis and expression defines a hierarchy modulated by epigenetic mechanisms. *Oncogene* 32, 2670–2681.
<https://doi.org/10.1038/onc.2012.280>
- Demuth, T., Berens, M.E., 2004. Molecular Mechanisms of Glioma Cell Migration and Invasion. *J. Neurooncol.* 70, 217–228.
<https://doi.org/10.1007/s11060-004-2751-6>
- Desrosiers, R.R., Fanéus, I., 2011. Damaged Proteins Bearing L-Isoaspartyl Residues and Aging : A Dynamic Equilibrium Between Generation of Isomerized Forms and Repair by PIMT 8–18.
- Dimitrijevic, A., Qin, Z., Aswad, D.W., 2014. Isoaspartyl Formation in Creatine Kinase B Is Associated with Loss of Enzymatic Activity; Implications for the Linkage of Isoaspartate Accumulation and Neurological Dysfunction in the PIMT Knockout Mouse. *PLoS One* 9, e100622.

<https://doi.org/10.1371/journal.pone.0100622>

- Dinavahi, R., Falkner, B., 2004. Relationship of Homocysteine With Cardiovascular Disease and Blood Pressure 494–500.
- Dittel, B.N., 2008. Direct suppression of autoreactive lymphocytes in the central nervous system via the CB 2 receptor. *Br. J. Pharmacol.* 153, 271–276. <https://doi.org/10.1038/sj.bjp.0707493>
- Doherty, G.H., 2007. Homocysteine: More than just a matter of life and death. *Exp. Neurol.* 205, 5–8. <https://doi.org/10.1016/J.EXPNEUROL.2007.02.012>
- Dong, F., Li, Q., Yang, C., Huo, D., Wang, X., Ai, C., Kong, Y., Sun, X., Wang, W., Zhou, Y., Liu, X., Li, W., Gao, W., Liu, W., Kang, C., Wu, X., 2018. PRMT2 links histone H3R8 asymmetric dimethylation to oncogenic activation and tumorigenesis of glioblastoma. *Nat. Commun.* 9, 4552. <https://doi.org/10.1038/s41467-018-06968-7>
- Dulbecco, R., 1986. Sequencing the Human Genome. *Science* (80-.). 231, 1055–1056. <https://doi.org/10.1126/science.3945817>
- Dumitru, C.A., Sandalcioğlu, I.E., Karsak, M., 2018. Cannabinoids in Glioblastoma Therapy: New Applications for Old Drugs. *Front. Mol. Neurosci.* 11, 159. <https://doi.org/10.3389/fnmol.2018.00159>
- Dunn, I.F., Heese, O., Black, P.M., 2000. Growth factors in glioma angiogenesis: FGFs, PDGF, EGF, and TGFs. *J. Neurooncol.* 50, 121–37.
- Easwaran, H., Johnstone, S.E., Van Neste, L., Ohm, J., Mosbrugger, T., Wang, Q., Aryee, M.J., Joyce, P., Ahuja, N., Weisenberger, D., Collisson, E., Zhu, J., Yegnasubramanian, S., Matsui, W., Baylin, S.B., 2012. A DNA hypermethylation module for the stem/progenitor cell signature of cancer. *Genome Res.* 22, 837–49. <https://doi.org/10.1101/gr.131169.111>
- Eaton, S.L., Roche, S.L., Llaverro Hurtado, M., Oldknow, K.J., Farquharson, C., Gillingwater, T.H., Wishart, T.M., 2013. Total Protein Analysis as a Reliable Loading Control for Quantitative Fluorescent Western Blotting. *PLoS One* 8, 1–9. <https://doi.org/10.1371/journal.pone.0072457>

- Ebner, R., Derynck, R., 1991. Epidermal growth factor and transforming growth factor- α : differential intracellular routing and processing of ligand-receptor complexes. *Cell Regul.* 2, 599–612.
<https://doi.org/10.1091/MBC.2.8.599>
- Ellert-Miklaszewska, A., Ciechomska, I., Kaminska, B., 2013. Cannabinoid Signaling in Glioma Cells, in: *Advances in Experimental Medicine and Biology*. pp. 209–220. https://doi.org/10.1007/978-94-007-4719-7_11
- England, B., Huang, T., Karsy, M., 2013. Current understanding of the role and targeting of tumor suppressor p53 in glioblastoma multiforme. *Tumor Biol.* 34, 2063–2074. <https://doi.org/10.1007/s13277-013-0871-3>
- Estécio, M.R.H., Issa, J.-P.J., 2011. Dissecting DNA hypermethylation in cancer. *FEBS Lett.* 585, 2078–86. <https://doi.org/10.1016/j.febslet.2010.12.001>
- Etcheverry, A., Aubry, M., Tayrac, M. DE, Vauleon, E., Boniface, R., Guenot, F., Saikali, S., Hamlat, A., Riffaud, L., Menei, P., Quillien, V., Mosser, J., 2010. DNA methylation in glioblastoma: impact on gene expression and clinical outcome. *BMC Genomics* 11, 701. <https://doi.org/10.1186/1471-2164-11-701>
- Fan, Q.-W., Cheng, C.K., Gustafson, W.C., Charron, E., Zipper, P., Wong, R.A., Chen, J., Lau, J., Knobbe-Thomsen, C., Weller, M., Jura, N., Reifemberger, G., Shokat, K.M., Weiss, W.A., 2013. EGFR phosphorylates tumor-derived EGFRvIII driving STAT3/5 and progression in glioblastoma. *Cancer Cell* 24, 438–49. <https://doi.org/10.1016/j.ccr.2013.09.004>
- Fan, Q.W., Cheng, C.K., Gustafson, W.C., Charron, E., Zipper, P., Wong, R.A., Chen, J., Lau, J., Knobbe-Thomsen, C., Weller, M., Jura, N., Reifemberger, G., Shokat, K.M., Weiss, W.A., 2013. EGFR Phosphorylates Tumor-Derived EGFRvIII Driving STAT3/5 and Progression in Glioblastoma. *Cancer Cell* 24, 438–449. <https://doi.org/10.1016/j.ccr.2013.09.004>
- Fife, C.M., McCarroll, J.A., Kavallaris, M., 2014. Movers and shakers: cell cytoskeleton in cancer metastasis. *Br. J. Pharmacol.* 171, 5507–5523. <https://doi.org/10.1111/bph.12704>

- Fredriksson, L., Li, H., Eriksson, U., 2004. The PDGF family: four gene products form five dimeric isoforms. *Cytokine Growth Factor Rev.* 15, 197–204. <https://doi.org/10.1016/j.cytogfr.2004.03.007>
- Gan, H.K., Cvrljevic, A.N., Johns, T.G., 2013. The epidermal growth factor receptor variant III (EGFRvIII): where wild things are altered. *FEBS J.* 280, 5350–5370. <https://doi.org/10.1111/febs.12393>
- Ganguly, D., Fan, M., Yang, C.H., Zbytek, B., Finkelstein, D., Roussel, M.F., Pfeffer, L.M., 2018. The critical role that STAT3 plays in glioma-initiating cells: STAT3 addiction in glioma. *Oncotarget* 9, 22095. <https://doi.org/10.18632/ONCOTARGET.25188>
- Garcia, A., Zanibbi, K., 2004. Homocysteine and cognitive function in elderly people 171, 897–904.
- Gimenez, M., Marie, S.K.N., Oba-Shinjo, S., Uno, M., Izumi, C., Oliveira, J.B., Rosa, J.C., 2015. Quantitative proteomic analysis shows differentially expressed HSPB1 in glioblastoma as a discriminating short from long survival factor and NOVA1 as a differentiation factor between low-grade astrocytoma and oligodendroglioma. *BMC Cancer* 15, 481. <https://doi.org/10.1186/s12885-015-1473-9>
- Glorieux, C., Zamocky, M., Sandoval, J.M., Verrax, J., Calderon, P.B., 2015. Regulation of catalase expression in healthy and cancerous cells. *Free Radic. Biol. Med.* 87, 84–97. <https://doi.org/10.1016/J.FREERADBIOMED.2015.06.017>
- Gómez del Pulgar, T., de Ceballos, M.L., Guzmán, M., Velasco, G., 2002. Cannabinoids Protect Astrocytes from Ceramide-induced Apoptosis through the Phosphatidylinositol 3-Kinase/Protein Kinase B Pathway. *J. Biol. Chem.* 277, 36527–36533. <https://doi.org/10.1074/jbc.M205797200>
- Gu, S., Liu, Y., Zhu, B., Ding, K., Yao, T.P., Chen, F., Zhan, L., Xu, P., Ehrlich, M., Liang, T., Lin, X., Feng, X.H., 2016. Loss of α -tubulin acetylation is associated with TGF- β -induced epithelial-mesenchymal transition. *J. Biol. Chem.* 291, 5396–5405. <https://doi.org/10.1074/jbc.M115.713123>

- GW Pharmaceuticals, 2017. GW Pharmaceuticals Achieves Positive Results in Phase 2 Proof of Concept Study in Glioma | GW Pharmaceuticals, plc [WWW Document]. URL <https://www.gwpharm.com/about/news/gw-pharmaceuticals-achieves-positive-results-phase-2-proof-concept-study-glioma> (accessed 8.20.18).
- Hambardzumyan, D., Bergers, G., 2015. Glioblastoma: Defining Tumor Niches. *Trends in Cancer*. <https://doi.org/10.1016/j.trecan.2015.10.009>
- Hambardzumyan, D., Gutmann, D.H., Kettenmann, H., 2016. The role of microglia and macrophages in glioma maintenance and progression. *Nat. Neurosci.* 19, 20–7. <https://doi.org/10.1038/nn.4185>
- Han, X., Li, R., Zhang, W., Yang, X., Wheeler, C.G., Friedman, G.K., Province, P., Ding, Q., You, Z., Fathallah-Shaykh, H.M., Gillespie, G.Y., Zhao, X., King, P.H., Nabors, L.B., 2014. Expression of PRMT5 correlates with malignant grade in gliomas and plays a pivotal role in tumor growth in vitro. *J. Neurooncol.* 118, 61–72. <https://doi.org/10.1007/s11060-014-1419-0>
- Handy, D.E., Zhang, Y., Loscalzo, J., 2005. Homocysteine down-regulates cellular glutathione peroxidase (GPx1) by decreasing translation. *J. Biol. Chem.* 280, 15518–25. <https://doi.org/10.1074/jbc.M501452200>
- Hao, L., Zhou, X., Liu, S., Sun, M., Song, Y., Du, S., Sun, B., Guo, C., Gong, L., Hu, J., Guan, H., Shao, S., 2015. Elevated GAPDH expression is associated with the proliferation and invasion of lung and esophageal squamous cell carcinomas. *Proteomics* 15, 3087–3100. <https://doi.org/10.1002/pmic.201400577>
- Hardiany, N.S., Sadikin, M., Siregar, N., Wanandi, S.I., Indonesia, U., 2017. The suppression of manganese superoxide dismutase decreased the survival of human glioblastoma multiforme T98G cells. *Basic Medical Research glioblastoma multiforme T98G cells*. <https://doi.org/10.13181/mji.v26i1.1511>
- Hartsel, J.A., Eades, J., Hickory, B., Makriyannis, A., 2016. Cannabis sativa and Hemp. *Nutraceuticals* 735–754. <https://doi.org/10.1016/B978-0-12->

- Hashmi, O., 2011. Vitamin B deficiency may increase risk of lung cancer. *Thorax* 66, 73–73. <https://doi.org/10.1136/thx.2010.150235>
- Hatanpaa, K.J., Burma, S., Zhao, D., Habib, A.A., 2010. Epidermal growth factor receptor in glioma: signal transduction, neuropathology, imaging, and radioresistance. *Neoplasia* 12, 675–84.
- Hegi, M.E., Diserens, A.-C., Gorlia, T., Hamou, M.-F., de Tribolet, N., Weller, M., Kros, J.M., Hainfellner, J.A., Mason, W., Mariani, L., Bromberg, J.E.C., Hau, P., Mirimanoff, R.O., Cairncross, J.G., Janzer, R.C., Stupp, R., 2005. *MGMT* Gene Silencing and Benefit from Temozolomide in Glioblastoma. *N. Engl. J. Med.* 352, 997–1003. <https://doi.org/10.1056/NEJMoa043331>
- Heldin, C.-H., 2012a. Autocrine PDGF stimulation in malignancies. *Ups. J. Med. Sci.* 117, 83–91. <https://doi.org/10.3109/03009734.2012.658119>
- Heldin, C.-H., 2012b. Autocrine PDGF stimulation in malignancies. *Ups. J. Med. Sci.* 117, 83–91. <https://doi.org/10.3109/03009734.2012.658119>
- Hibbert, S.A., Ozols, M., Griffiths, C.E.M., Watson, R.E.B., Bell, M., Sherratt, M.J., 2018. Defining tissue proteomes by systematic literature review. *Sci. Rep.* 1–10. <https://doi.org/10.1038/s41598-017-18699-8>
- Higashimura, Y., Nakajima, Y., Yamaji, R., Harada, N., Shibasaki, F., Nakano, Y., Inui, H., 2011. Up-regulation of glyceraldehyde-3-phosphate dehydrogenase gene expression by HIF-1 activity depending on Sp1 in hypoxic breast cancer cells. *Arch. Biochem. Biophys.* 509, 1–8. <https://doi.org/10.1016/j.abb.2011.02.011>
- Holland, E.C., Celestino, J., Dai, C., Schaefer, L., Sawaya, R.E., Fuller, G.N., 2000. Combined activation of Ras and Akt in neural progenitors induces glioblastoma formation in mice. *Nat. Genet.* 25, 55–57. <https://doi.org/10.1038/75596>
- Hong, J.-D., Wang, X., Peng, Y.-P., Peng, J.-H., Wang, J., Dong, Y.-P., He, D., Peng, Z.-Z., Tu, Q.-S., Sheng, L.-F., Zhong, M.-Z., Duan, C.-J., 2017. Silencing platelet-

- derived growth factor receptor- β enhances the radiosensitivity of C6 glioma cells in vitro and in vivo. *Oncol. Lett.* 14, 329–336.
<https://doi.org/10.3892/ol.2017.6143>
- Hood, L., Rowen, L., 2013. The Human Genome Project: big science transforms biology and medicine. *Genome Med.* 5, 79. <https://doi.org/10.1186/gm483>
- Horvath, S., Ritz, B.R., 2015. Increased epigenetic age and granulocyte counts in the blood of Parkinson's disease patients. *Aging (Albany, NY)*. 7, 1130–1142. <https://doi.org/10.18632/aging.100859>
- Huang, L., Ramirez, J.C., Frampton, G.A., Golden, L.E., Quinn, M.A., Pae, H.Y., Horvat, D., Liang, L., DeMorrow, S., 2011. Anandamide exerts its antiproliferative actions on cholangiocarcinoma by activation of the GPR55 receptor. *Lab. Investig.* 91, 1007–1017.
<https://doi.org/10.1038/labinvest.2011.62>
- Huang, Q., Zhang, Q. Bin, Dong, J., Wu, Y.Y., Shen, Y.T., Zhao, Y.D., Zhu, Y. De, Diao, Y., Wang, A.D., Lan, Q., 2008. Glioma stem cells are more aggressive in recurrent tumors with malignant progression than in the primary tumor, and both can be maintained long-term in vitro. *BMC Cancer* 8, 1–11.
<https://doi.org/10.1186/1471-2407-8-304>
- Huo, Y., Qiu, W.-Y., Pan, Q., Yao, Y.-F., Xing, K., Lou, M.F., 2009. Reactive oxygen species (ROS) are essential mediators in epidermal growth factor (EGF)-stimulated corneal epithelial cell proliferation, adhesion, migration, and wound healing. *Exp. Eye Res.* 89, 876–886.
<https://doi.org/10.1016/j.exer.2009.07.012>
- Hussain, Z., Khan, M.I., Shahid, M., Almajhdi, F.N., 2013. S-adenosylmethionine, a methyl donor, up regulates tissue inhibitor of metalloproteinase-2 in colorectal cancer. *Genet. Mol. Res.* 12, 1106–1118.
<https://doi.org/10.4238/2013.April.10.6>
- Invitrogen, 2010. Pro-Q ® Diamond Phosphoprotein Gel Stain 1–12.
- Janke, C., Montagnac, G., 2017. Causes and Consequences of Microtubule Acetylation. *Curr. Biol.* 27, R1287–R1292.

<https://doi.org/10.1016/J.CUB.2017.10.044>

- Karmali, R.N., Jones, N.M., Levine, A.D., 2010. Towards a knowledge-based Human Protein Atlas 28, 12–14. <https://doi.org/10.1038/nbt1210-1248>
- Kaur, B., Khwaja, F.W., Severson, E.A., Matheny, S.L., Brat, D.J., Van Meir, E.G., 2005. Hypoxia and the hypoxia-inducible-factor pathway in glioma growth and angiogenesis. *Neuro. Oncol.* 7, 134–153. <https://doi.org/10.1215/S1152851704001115>
- Kaut, O., Schmitt, I., Wüllner, U., 2012. Genome-scale methylation analysis of Parkinson's disease patients' brains reveals DNA hypomethylation and increased mRNA expression of cytochrome P450 2E1. *Neurogenetics* 13, 87–91. <https://doi.org/10.1007/s10048-011-0308-3>
- Khan, M.A., Tania, M., Zhang, D.Z., Chen, H.C., 2010. Antioxidant enzymes and cancer. *Chinese J. Cancer Res.* 22, 87–92. <https://doi.org/10.1007/s11670-010-0087-7>
- Kim, M.-S., Pinto, S.M., Getnet, D., Nirujogi, R.S., Manda, S.S., Chaerkady, R., Madugundu, A.K., Kelkar, D.S., Isserlin, R., Jain, S., Thomas, J.K., Muthusamy, B., Leal-Rojas, P., Kumar, P., Sahasrabudde, N.A., Balakrishnan, L., Advani, J., George, B., Renuse, S., Selvan, L.D.N., Patil, A.H., Nanjappa, V., Radhakrishnan, A., Prasad, S., Subbannayya, T., Raju, R., Kumar, M., Sreenivasamurthy, S.K., Marimuthu, A., Sathe, G.J., Chavan, S., Datta, K.K., Subbannayya, Y., Sahu, A., Yelamanchi, S.D., Jayaram, S., Rajagopalan, P., Sharma, J., Murthy, K.R., Syed, N., Goel, R., Khan, A.A., Ahmad, S., Dey, G., Mudgal, K., Chatterjee, A., Huang, T.-C., Zhong, J., Wu, X., Shaw, P.G., Freed, D., Zahari, M.S., Mukherjee, K.K., Shankar, S., Mahadevan, A., Lam, H., Mitchell, C.J., Shankar, S.K., Satishchandra, P., Schroeder, J.T., Sirdeshmukh, R., Maitra, A., Leach, S.D., Drake, C.G., Halushka, M.K., Prasad, T.S.K., Hruban, R.H., Kerr, C.L., Bader, G.D., Iacobuzio-Donahue, C.A., Gowda, H., Pandey, A., 2014. A draft map of the human proteome. *Nature* 509, 575–581. <https://doi.org/10.1038/nature13302>
- Kim, S.C., Sprung, R., Chen, Y., Xu, Y., Ball, H., Pei, J., Cheng, T., Kho, Y., Xiao, H., Xiao, L., Grishin, N. V., White, M., Yang, X.-J., Zhao, Y., 2006. Substrate and

- Functional Diversity of Lysine Acetylation Revealed by a Proteomics Survey. *Mol. Cell* 23, 607–618.
<https://doi.org/10.1016/j.molcel.2006.06.026>
- Koul, D., 2008. PTEN signaling pathways in glioblastoma. *Cancer Biol. Ther.* 7, 1321–5.
- Kowanetz, M., Ferrara, N., 2006. Vascular endothelial growth factor signaling pathways: therapeutic perspective. *Clin. Cancer Res.* 12, 5018–22.
<https://doi.org/10.1158/1078-0432.CCR-06-1520>
- Krex, D., Mohr, B., Appelt, H., Schackert, H.K., Schackert, G., 2003. Genetic analysis of a multifocal glioblastoma multiforme: a suitable tool to gain new aspects in glioma development. *Neurosurgery* 53, 1377–84; discussion 1384. <https://doi.org/10.1227/01.neu.0000093426.29236.86>
- Krock, B.L., Skuli, N., Simon, M.C., 2011. Hypoxia-induced angiogenesis: good and evil. *Genes Cancer* 2, 1117–33.
<https://doi.org/10.1177/1947601911423654>
- Kushwaha, D., Ramakrishnan, V., Ng, K., Steed, T., Nguyen, T., Futral, D., Akers, J.C., Sarkaria, J., Jiang, T., Chowdhury, D., Carter, B.S., Chen, C.C., 2014. A genome-wide miRNA screen revealed miR-603 as a MGMT-regulating miRNA in glioblastomas. *Oncotarget* 5, 4026–39.
<https://doi.org/10.18632/oncotarget.1974>
- Labisso, W.L., Raulin, A.-C., Nwidi, L.L., Kocon, A., Wayne, D., Erdozain, A.M., Morentin, B., Schwendener, D., Allen, G., Enticott, J., Gerdes, H.K., Johnson, L., Grzeskowiak, J., Drizou, F., Tarbox, R., Osna, N.A., Kharbanda, K.K., Callado, L.F., Carter, W.G., 2018. The loss of α - and β -tubulin proteins are a pathological hallmark of chronic alcohol consumption and natural brain ageing. *Brain Sci.* 8. <https://doi.org/10.3390/brainsci8090175>
- Laplane, L., Duluc, D., Larmonier, N., Pradeu, T., Bikfalvi, A., 2018. The Multiple Layers of the Tumor Environment. *Trends in cancer* 4, 802–809.
<https://doi.org/10.1016/j.trecan.2018.10.002>
- Lapointe, M., Lanthier, J., Moumdjian, R., Régina, A., Desrosiers, R.R., 2005.

- Expression and activity of L-isoaspartyl methyltransferase decrease in stage progression of human astrocytic tumors. *Mol. Brain Res.* 135, 93–103. <https://doi.org/10.1016/j.molbrainres.2004.12.008>
- Lau, W.Y., Lai, P.B., Leung, M.F., Leung, B.C., Wong, N., Chen, G., Leung, T.W., Liew, C.T., 2000. Differential gene expression of hepatocellular carcinoma using cDNA microarray analysis. *Oncol. Res.* 12, 59–69.
- Lee, S.Y., 2018. Current knowledge for the western blot normalization . 3, 3–6.
- Li, S., Yan, T., Yang, J.Q., Oberley, T.D., Oberley, L.W., 2000. The role of cellular glutathione peroxidase redox regulation in the suppression of tumor cell growth by manganese superoxide dismutase. *Cancer Res.* 60, 3927–39.
- Li, T., Liu, M., Feng, X., Wang, Z., Das, I., Xu, Y., Zhou, X., Sun, Y., Guan, K.-L., Xiong, Y., Lei, Q.-Y., 2014. Glyceraldehyde-3-phosphate dehydrogenase is activated by lysine 254 acetylation in response to glucose signal. *J. Biol. Chem.* 289, 3775–85. <https://doi.org/10.1074/jbc.M113.531640>
- Li, T., Zhang, C., Hassan, S., Liu, X., Song, F., Chen, K., Zhang, W., Yang, J., 2018. Histone deacetylase 6 in cancer. *J. Hematol. Oncol.* 11, 111. <https://doi.org/10.1186/s13045-018-0654-9>
- Liberti, M. V., Locasale, J.W., 2016. The Warburg Effect: How Does it Benefit Cancer Cells? *Trends Biochem. Sci.* 41, 211–218. <https://doi.org/10.1016/j.tibs.2015.12.001>
- Liu, G., Yuan, X., Zeng, Z., Tunici, P., Ng, H., Abdulkadir, I.R., Lu, L., Irvin, D., Black, K.L., Yu, J.S., 2006. Analysis of gene expression and chemoresistance of CD133+ cancer stem cells in glioblastoma. *Mol. Cancer* 5, 67. <https://doi.org/10.1186/1476-4598-5-67>
- Louis, D.N., 2012. The next step in brain tumor classification: “Let us now praise famous men” ... or molecules? *Acta Neuropathol.* 124, 761–762. <https://doi.org/10.1007/s00401-012-1067-4>
- Louis, D.N., Ohgaki, H., Wiestler, O.D., Cavenee, W.K., Burger, P.C., Jouvett, A., Scheithauer, B.W., Kleihues, P., 2007. The 2007 WHO Classification of

Tumours of the Central Nervous System 97–109.

<https://doi.org/10.1007/s00401-007-0243-4>

Louis, D.N., Perry, A., Reifenberger, G., von Deimling, A., Figarella-Branger, D., Cavenee, W.K., Ohgaki, H., Wiestler, O.D., Kleihues, P., Ellison, D.W., 2016. The 2016 World Health Organization Classification of Tumors of the Central Nervous System: a summary. *Acta Neuropathol.* 131, 803–820. <https://doi.org/10.1007/s00401-016-1545-1>

Lowry et al., 1951. Protein Measurement with the Folin Phenol Reagent. *Readings* 193, 265–275. [https://doi.org/10.1016/0304-3894\(92\)87011-4](https://doi.org/10.1016/0304-3894(92)87011-4)

Lubanska, D., Porter, L., 2017. Revisiting CDK Inhibitors for Treatment of Glioblastoma Multiforme. *Drugs R. D.* 17, 255–263. <https://doi.org/10.1007/s40268-017-0180-1>

Mahmood, N., Cheishvili, D., Arakelian, A., Tanvir, I., Khan, H.A., Pépin, A.-S., Szyf, M., Rabbani, S.A., 2018. Methyl donor S-adenosylmethionine (SAM) supplementation attenuates breast cancer growth, invasion, and metastasis in vivo; therapeutic and chemopreventive applications. *Oncotarget* 9, 5169–5183. <https://doi.org/10.18632/oncotarget.23704>

Mao, C.-X., Wen, X., Jin, S., Zhang, Y.Q., 2017. Increased acetylation of microtubules rescues human tau-induced microtubule defects and neuromuscular junction abnormalities in *Drosophila*. *Dis. Model. Mech.* 10, 1245–1252. <https://doi.org/10.1242/dmm.028316>

Mao, H., LeBrun, D.G., Yang, J., Zhu, V.F., Li, M., 2013. Deregulated Signaling Pathways in Glioblastoma Multiforme: Molecular Mechanisms and Therapeutic Targets. *Cancer Invest.* 30, 48–56. <https://doi.org/10.3109/07357907.2011.630050>.Deregulated

Marioni, R.E., Shah, S., McRae, A.F., Ritchie, S.J., Muniz-Terrera, G., Harris, S.E., Gibson, J., Redmond, P., Cox, S.R., Pattie, A., Corley, J., Taylor, A., Murphy, L., Starr, J.M., Horvath, S., Visscher, P.M., Wray, N.R., Deary, I.J., 2015. The epigenetic clock is correlated with physical and cognitive fitness in the Lothian Birth Cohort 1936. *Int. J. Epidemiol.* 44, 1388–1396.

<https://doi.org/10.1093/ije/dyu277>

Martín-Bernabé, A., Balcells, C., Tarragó-Celada, J., Foguet, C., Bourgoïn-Voillard, S., Seve, M., Cascante, M., 2017. The importance of post-translational modifications in systems biology approaches to identify therapeutic targets in cancer metabolism. *Curr. Opin. Syst. Biol.* 3, 161–169.
<https://doi.org/10.1016/j.coisb.2017.05.011>

McDonald, F.E., Ironside, J.W., Gregor, A., Wyatt, B., Stewart, M., Rye, R., Adams, J., Potts, H.W.W., 2002. The prognostic influence of bcl-2 in malignant glioma. *Br. J. Cancer* 86, 1899–904.
<https://doi.org/10.1038/sj.bjc.6600217>

Mrugala, M.M., 2013. Advances and challenges in the treatment of glioblastoma: a clinician's perspective. *Discov. Med.* 15, 221–30.

Nakajima, H., Amano, W., Kubo, T., Fukuhara, A., Ihara, H., Azuma, Y.-T., Tajima, H., Inui, T., Sawa, A., Takeuchi, T., 2009. Glyceraldehyde-3-phosphate dehydrogenase aggregate formation participates in oxidative stress-induced cell death. *J. Biol. Chem.* 284, 34331–41.
<https://doi.org/10.1074/jbc.M109.027698>

National Cancer Institute, 2018. Cancer Trends Progress Report. NIH.

Nishikawa, R., Ji, X.D., Harmon, R.C., Lazar, C.S., Gill, G.N., Cavennee, W.K., Huang, H.J., 1994. A mutant epidermal growth factor receptor common in human glioma confers enhanced tumorigenicity. *Proc. Natl. Acad. Sci.* 91, 7727–7731. <https://doi.org/10.1073/pnas.91.16.7727>

Nogueira, L., Ruiz-Ontañón, P., Vazquez-Barquero, A., Moris, F., Fernandez-Luna, J.L., 2011. The NFκB pathway: a therapeutic target in glioblastoma. *Oncotarget* 2, 646–53.
<https://doi.org/10.18632/oncotarget.322>

Noushmehr, H., Weisenberger, D.J., Diefes, K., Phillips, H.S., Pujara, K., Berman, B.P., Pan, F., Pelloski, C.E., Sulman, E.P., Bhat, K.P., Verhaak, R.G.W., Hoadley, K.A., Hayes, D.N., Perou, C.M., Schmidt, H.K., Ding, L., Wilson, R.K., Van Den Berg, D., Shen, H., Bengtsson, H., Neuvial, P., Cope, L.M., Buckley, J., Herman,

- J.G., Baylin, S.B., Laird, P.W., Aldape, K., 2010. Identification of a CpG Island Methylator Phenotype that Defines a Distinct Subgroup of Glioma. *Cancer Cell* 17, 510–522. <https://doi.org/10.1016/j.ccr.2010.03.017>
- Ohgaki, H., Kleihues, P., 2013. The Definition of Primary and Secondary Glioblastoma 19, 764–773. <https://doi.org/10.1158/1078-0432.CCR-12-3002>
- Olow, A., Chen, Z., Niedner, R.H., Wolf, D.M., Yau, C., Pankov, A., Lee, E.P.R., Brown-Swigart, L., van 't Veer, L.J., Coppé, J.-P., 2016. An Atlas of the Human Kinome Reveals the Mutational Landscape Underlying Dysregulated Phosphorylation Cascades in Cancer. *Cancer Res.* 76, 1733–45. <https://doi.org/10.1158/0008-5472.CAN-15-2325-T>
- Oriolo, A.S., Wald, F.A., Ramsauer, V.P., Salas, P.J.I., 2007. Intermediate filaments: a role in epithelial polarity. *Exp. Cell Res.* 313, 2255–64. <https://doi.org/10.1016/j.yexcr.2007.02.030>
- Ouédraogo, Z.G., Biau, J., Kemeny, J.-L., Morel, L., Verrelle, P., Chautard, E., 2017. Role of STAT3 in Genesis and Progression of Human Malignant Gliomas. *Mol. Neurobiol.* 54, 5780–5797. <https://doi.org/10.1007/s12035-016-0103-0>
- Ozaki, T., Nakagawara, A., 2011. Role of p53 in Cell Death and Human Cancers. *Cancers (Basel)*. 3, 994–1013. <https://doi.org/10.3390/cancers3010994>
- Özkan, Y., Yardim-Akaydin, S., Firat, H., Çalışkan-Can, E., Ardiç, S., Şimşek, B., 2007. Usefulness of homocysteine as a cancer marker: Total thiol compounds and folate levels in untreated lung cancer patients. *Anticancer Res.* 27, 1185–1189.
- Papa, L., Manfredi, G., Germain, D., 2014. SOD1, an unexpected novel target for cancer therapy. *Genes Cancer* 5, 15. <https://doi.org/10.18632/GENESANDCANCER.4>
- Paugh, B.S., Zhu, X., Qu, C., Endersby, R., Diaz, A.K., Zhang, Junyuan, Bax, D.A., Carvalho, D., Reis, R.M., Onar-Thomas, A., Broniscer, A., Wetmore, C., Zhang, Jinghui, Jones, C., Ellison, D.W., Baker, S.J., 2013. Novel oncogenic PDGFRA

- mutations in pediatric high-grade gliomas. *Cancer Res.* 73, 6219–29.
<https://doi.org/10.1158/0008-5472.CAN-13-1491>
- Pegg, A.E., 1990. Mammalian O6-alkylguanine-DNA alkyltransferase: regulation and importance in response to alkylating carcinogenic and therapeutic agents. *Cancer Res.* 50, 6119–29.
- Persano, L., Rampazzo, E., Della Puppa, A., Pistollato, F., Basso, G., 2011a. The Three-Layer Concentric Model of Glioblastoma: Cancer Stem Cells, Microenvironmental Regulation, and Therapeutic Implications. *Sci. World J.* 11, 1829–1841. <https://doi.org/10.1100/2011/736480>
- Persano, L., Rampazzo, E., Della Puppa, A., Pistollato, F., Basso, G., 2011b. The Three-Layer Concentric Model of Glioblastoma: Cancer Stem Cells, Microenvironmental Regulation, and Therapeutic Implications. *Sci. World J.* 11, 1829–1841. <https://doi.org/10.1100/2011/736480>
- Phillips, H.S., Kharbanda, S., Chen, R., Forrest, W.F., Soriano, R.H., Wu, T.D., Misra, A., Nigro, J.M., Colman, H., Soroceanu, L., Williams, P.M., Modrusan, Z., Feuerstein, B.G., Aldape, K., 2006. Molecular subclasses of high-grade glioma predict prognosis , delineate a pattern of disease progression , and resemble stages in neurogenesis 157–173.
<https://doi.org/10.1016/j.ccr.2006.02.019>
- Phillips, J.J., Aranda, D., Ellison, D.W., Judkins, A.R., Croul, S.E., Brat, D.J., Ligon, K.L., Horbinski, C., Venneti, S., Zadeh, G., Santi, M., Zhou, S., Appin, C.L., Sioletic, S., Sullivan, L.M., Martinez-Lage, M., Robinson, A.E., Yong, W.H., Cloughesy, T., Lai, A., Phillips, H.S., Marshall, R., Mueller, S., Haas-Kogan, D.A., Molinaro, A.M., Perry, A., 2013. PDGFRA amplification is common in pediatric and adult high-grade astrocytomas and identifies a poor prognostic group in IDH1 mutant glioblastoma. *Brain Pathol.* 23, 565–73.
<https://doi.org/10.1111/bpa.12043>
- Portran, D., Schaedel, L., Xu, Z., Théry, M., Nachury, M.V., 2017. Tubulin acetylation protects long-lived microtubules against mechanical ageing. *Nat. Cell Biol.* 19, 391–398. <https://doi.org/10.1038/ncb3481>

- Preusser, M., Bienkowski, M., Birner, P., 2016. BRAF inhibitors in BRAF-V600 mutated primary neuroepithelial brain tumors. *Expert Opin. Investig. Drugs* 25, 7–14. <https://doi.org/10.1517/13543784.2016.1110143>
- Raica, M., Cimpean, A.M., 2010. Platelet-Derived Growth Factor (PDGF)/PDGF Receptors (PDGFR) Axis as Target for Antitumor and Antiangiogenic Therapy. *Pharmaceuticals (Basel)*. 3, 572–599. <https://doi.org/10.3390/ph3030572>
- Rajalingam, K., Schreck, R., Rapp, U.R., Albert, Š., 2007. Ras oncogenes and their downstream targets. *Biochim. Biophys. Acta - Mol. Cell Res.* 1773, 1177–1195. <https://doi.org/10.1016/j.bbamcr.2007.01.012>
- Rawlings, J.S., Rosler, K.M., Harrison, D.A., 2004. The JAK/STAT signaling pathway. *J. Cell Sci.* 117, 1281–3. <https://doi.org/10.1242/jcs.00963>
- Reardon, D.A., Wen, P.Y., Desjardins, A., Batchelor, T.T., Vredenburgh, J.J., 2008. Glioblastoma multiforme: an emerging paradigm of anti-VEGF therapy. *Expert Opin. Biol. Ther.* 8, 541–53. <https://doi.org/10.1517/14712598.8.4.541>
- Reay, J.L., Smith, M.A., Riby, L.M., 2013. B vitamins and cognitive performance in older adults: review. *ISRN Nutr.* 2013, 650983. <https://doi.org/10.5402/2013/650983>
- Ren, T., Lin, S., Wang, Z., Shang, A., 2016. Differential proteomics analysis of low- and high-grade of astrocytoma using iTRAQ quantification. *Onco. Targets. Ther.* 9, 5883–5895. <https://doi.org/10.2147/OTT.S111103>
- Riemenschneider, M.J., Betensky, R.A., Pasedag, S.M., Louis, D.N., 2006. AKT activation in human glioblastomas enhances proliferation via TSC2 and S6 kinase signaling. *Cancer Res.* 66, 5618–5623. <https://doi.org/10.1158/0008-5472.CAN-06-0364>
- Rinaldi, M., Caffo, M., Minutoli, L., Marini, H., Abbritti, R.V., Squadrito, F., Trichilo, V., Valenti, A., Barresi, V., Altavilla, D., Passalacqua, M., Caruso, G., 2016. ROS and brain gliomas: An overview of potential and innovative therapeutic strategies. *Int. J. Mol. Sci.* 17. <https://doi.org/10.3390/ijms17060984>

- Riss, T.L., Moravec, R.A., Niles, A.L., Duellman, S., Benink, H.A., Worzella, T.J., Minor, L., 2004. Cell Viability Assays. *Assay Guid. Man.* 740, 33–43.
<https://doi.org/10.1016/j.acthis.2012.01.006>
- Rocha, F.C.M., dos Santos Júnior, J.G., Stefano, S.C., da Silveira, D.X., 2014. Systematic review of the literature on clinical and experimental trials on the antitumor effects of cannabinoids in gliomas. *J. Neurooncol.* 116, 11–24.
<https://doi.org/10.1007/s11060-013-1277-1>
- Rong, Y., Durden, D.L., Van Meir, E.G., Brat, D.J., 2006. “Pseudopalisading” necrosis in glioblastoma: a familiar morphologic feature that links vascular pathology, hypoxia, and angiogenesis. *J. Neuropathol. Exp. Neurol.* 65, 529–39.
- Royer, C., Lu, X., 2011. Epithelial cell polarity: a major gatekeeper against cancer? *Cell Death Differ.* 18, 1470–7.
<https://doi.org/10.1038/cdd.2011.60>
- Said, H.M., Polat, B., Hagemann, C., Anacker, J., Flentje, M., Vordermark, D., 2009. Absence of GAPDH regulation in tumor-cells of different origin under hypoxic conditions in - vitro. *BMC Res. Notes* 2, 8.
<https://doi.org/10.1186/1756-0500-2-8>
- Saito, K., Mukasa, A., Narita, Y., Tabei, Y., Shinoura, N., Shibui, S., Saito, N., 2014. Toxicity and outcome of radiotherapy with concomitant and adjuvant temozolomide in elderly patients with glioblastoma: a retrospective study. *Neurol. Med. Chir. (Tokyo).* 54, 272–9.
<https://doi.org/10.2176/NMC.OA2012-0441>
- Sánchez, A.J., García-Merino, A., 2012. Neuroprotective agents: Cannabinoids. *Clin. Immunol.* 142, 57–67. <https://doi.org/10.1016/j.clim.2011.02.010>
- Sánchez, C., Díaz-Nido, J., Avila, J., 2000. Phosphorylation of microtubule-associated protein 2 (MAP2) and its relevance for the regulation of the neuronal cytoskeleton function. *Prog. Neurobiol.* 61, 133–68.
- Schley, M., Ständer, S., Kerner, J., Vajkoczy, P., Schüpfer, G., Dusch, M., Schmelz, M., Konrad, C., 2009. Predominant CB2 receptor expression in endothelial

- cells of glioblastoma in humans. *Brain Res. Bull.* 79, 333–337.
<https://doi.org/10.1016/j.brainresbull.2009.01.011>
- Schmidt, T., Leha, A., Salinas-Riester, G., 2016. Treatment of prostate cancer cells with S-adenosylmethionine leads to genome-wide alterations in transcription profiles. *Gene* 595, 161–167.
<https://doi.org/10.1016/J.GENE.2016.09.032>
- Setién-Suero, E., Suárez-Pinilla, M., Suárez-Pinilla, P., Crespo-Facorro, B., Ayesa-Arriola, R., 2016. Homocysteine and cognition: A systematic review of 111 studies. *Neurosci. Biobehav. Rev.* 69, 280–298.
<https://doi.org/10.1016/J.NEUBIOREV.2016.08.014>
- Shchemelinin, I., Šefc, L., Necas, E., 2006. Protein Kinases, Their Function and Implication in Cancer and Other Diseases. Stránka 81.
- Shwetha, S.D., Shastry, A.H., Arivazhagan, A., Santosh, V., 2016. Manganese superoxide dismutase (MnSOD) is a malignant astrocytoma specific biomarker and associated with adverse prognosis in p53 expressing glioblastoma. *Pathol. - Res. Pract.* 212, 17–23.
<https://doi.org/10.1016/J.PRP.2015.11.002>
- Siney, E.J., Holden, A., Casselden, E., Bulstrode, H., Thomas, G.J., Willaime-Morawek, S., 2017. Metalloproteinases ADAM10 and ADAM17 Mediate Migration and Differentiation in Glioblastoma Sphere-Forming Cells. *Mol. Neurobiol.* 54, 3893–3905. <https://doi.org/10.1007/s12035-016-0053-6>
- Škovierová, H., Vidomanová, E., Mahmood, S., Sopková, J., Drgová, A., Červeňová, T., Halašová, E., Lehotský, J., 2016. The Molecular and Cellular Effect of Homocysteine Metabolism Imbalance on Human Health. *Int. J. Mol. Sci.* 17.
<https://doi.org/10.3390/ijms17101733>
- Smith, A.D., Refsum, H., 2016. Homocysteine , B Vitamins , and Cognitive Impairment. *Annu. Rev. Nutr.* 211–39. <https://doi.org/10.1146/annurev-nutr-071715-050947>
- Snuderl, M., Fazlollahi, L., Le, L.P., Nitta, M., Zhelyazkova, B.H., Davidson, C.J., Akhavanfard, S., Cahill, D.P., Aldape, K.D., Betensky, R.A., Louis, D.N., Iafrate,

- A.J., 2011. Mosaic Amplification of Multiple Receptor Tyrosine Kinase Genes in Glioblastoma. *Cancer Cell* 20, 810–817.
<https://doi.org/10.1016/j.ccr.2011.11.005>
- Soeda, A., Hara, A., Kunisada, T., Yoshimura, S., Iwama, T., Park, D.M., 2015. The evidence of glioblastoma heterogeneity. *Sci. Rep.* 5, 7979.
<https://doi.org/10.1038/srep07979>
- Solinas, M., Massi, P., Cinquina, V., Valenti, M., Bolognini, D., Gariboldi, M., Monti, E., Rubino, T., Parolaro, D., 2013. Cannabidiol, a non-psychoactive cannabinoid compound, inhibits proliferation and invasion in U87-MG and T98G glioma cells through a multitarget effect. *PLoS One* 8, e76918.
<https://doi.org/10.1371/journal.pone.0076918>
- Sottoriva, A., Spiteri, I., Piccirillo, S.G.M., Touloumis, A., Collins, V.P., Marioni, J.C., Curtis, C., Watts, C., Tavaré, S., 2013. Intratumor heterogeneity in human glioblastoma reflects cancer evolutionary dynamics. *Proc. Natl. Acad. Sci.* 110, 4009–4014. <https://doi.org/10.1073/pnas.1219747110>
- Srivastava, A., Creek, D.J., 2018. Discovery and Validation of Clinical Biomarkers of Cancer: A Review Combining Metabolomics and Proteomics. *Proteomics* 1700448, 1–9. <https://doi.org/10.1002/pmic.201700448>
- Stanger, O., Pietrzik, K., Huemer, M., Haschke, E., 2009. Homocysteine, folate and vitamin B 12 in neuropsychiatric diseases : review and treatment recommendations 1393–1412.
- Stratton, M.R., Campbell, P.J., Futreal, P.A., 2009. The cancer genome. *Nature* 458, 719–24. <https://doi.org/10.1038/nature07943>
- Suh, Y.-A., Arnold, R.S., Lassegue, B., Shi, J., Xu, X., Sorescu, D., Chung, A.B., Griendling, K.K., Lambeth, J.D., 1999. Cell transformation by the superoxide-generating oxidase Mox1. *Nature* 401, 79–82.
<https://doi.org/10.1038/43459>
- Suzuki, S.O., Kitai, R., Llana, J., Lee, S.C., Goldman, J.E., Shafit-Zagardo, B., 2002. MAP-2e, a Novel MAP-2 Isoform, Is Expressed in Gliomas and Delineates Tumor Architecture and Patterns of Infiltration. *J. Neuropathol. Exp.*

- Neurol. 61, 403–412. <https://doi.org/10.1093/jnen/61.5.403>
- Swiatek-machado, K., Kaminska, B., 2013. STAT Signaling in Glioma Cells 189–208. <https://doi.org/10.1007/978-94-007-4719-7>
- Talasila, K.M., Soentgerath, A., Euskirchen, P., Rosland, G. V, Wang, J., Huszthy, P.C., Prestegarden, L., Skaftnesmo, K.O., Sakariassen, P.Ø., Eskilsson, E., Stieber, D., Keunen, O., Brekka, N., Moen, I., Nigro, J.M., Vintermyr, O.K., Lund-Johansen, M., Niclou, S., Mørk, S.J., Enger, P.O., Bjerkvig, R., Miletic, H., 2013. EGFR wild-type amplification and activation promote invasion and development of glioblastoma independent of angiogenesis. *Acta Neuropathol.* 125, 683–98. <https://doi.org/10.1007/s00401-013-1101-1>
- Tan, X., Wang, S., Zhu, L., Wu, C., Yin, B., Zhao, J., Yuan, J., Qiang, B., Peng, X., 2012. cAMP response element-binding protein promotes gliomagenesis by modulating the expression of oncogenic microRNA-23a. *Proc. Natl. Acad. Sci. U. S. A.* 109, 15805–10. <https://doi.org/10.1073/pnas.1207787109>
- Taylor, S.C., Posch, A., 2014. The design of a quantitative western blot experiment. *Biomed Res. Int.* 2014. <https://doi.org/10.1155/2014/361590>
- Taylor, T.E., Furnari, F.B., Cavenee, W.K., 2012. Targeting EGFR for treatment of glioblastoma: molecular basis to overcome resistance. *Curr. Cancer Drug Targets* 12, 197–209.
- TCGA Research Network, 2008. Comprehensive genomic characterization defines human glioblastoma genes and core pathways. *Nature* 455, 1061–1068. <https://doi.org/10.1038/nature07385>
- Testa, J.R., Tschlis, P.N., 2005. AKT signaling in normal and malignant cells. *Oncogene* 24, 7391–7393. <https://doi.org/10.1038/sj.onc.1209100>
- ThermoFisher Scientific, n.d. Phosphorylation - UK [WWW Document]. URL <https://www.thermofisher.com/uk/en/home/life-science/protein-biology/protein-biology-learning-center/protein-biology-resource-library/pierce-protein-methods/phosphorylation.html> (accessed 10.24.18).

- Tristan, C., Shahani, N., Sedlak, T.W., Sawa, A., 2011. The diverse functions of GAPDH: views from different subcellular compartments. *Cell. Signal.* 23, 317–23. <https://doi.org/10.1016/j.cellsig.2010.08.003>
- Turcan, S., Rohle, D., Goenka, A., Walsh, L.A., Fang, F., Yilmaz, E., Campos, C., Fabius, A.W.M., Lu, C., Ward, P.S., Thompson, C.B., Kaufman, A., Guryanova, O., Levine, R., Heguy, A., Viale, A., Morris, L.G.T., Huse, J.T., Mellinghoff, I.K., Chan, T.A., 2012. IDH1 mutation is sufficient to establish the glioma hypermethylator phenotype. *Nature* 483, 479–83. <https://doi.org/10.1038/nature10866>
- Uhrbom, L., Hesselager, G., Nistér, M., Westermarck, B., 1998. Induction of brain tumors in mice using a recombinant platelet-derived growth factor B-chain retrovirus. *Cancer Res.* 58, 5275–9.
- UniProtKB/Swiss-Prot [WWW Document], 2019. URL <https://www.uniprot.org/statistics/Swiss-Prot> (accessed 6.12.19).
- Valente, V., Teixeira, S.A., Neder, L., Okamoto, O.K., Oba-Shinjo, S.M., Marie, S.K., Scrideli, C.A., Paçó-Larson, M.L., Carlotti, C.G., 2014. Selection of suitable housekeeping genes for expression analysis in glioblastoma using quantitative RT-PCR. *Ann. Neurosci.* 21, 62–3. <https://doi.org/10.5214/ans.0972.7531.210207>
- Ventura, M., Mateo, F., Serratos, J., Salaet, I., Carujo, S., Bachs, O., Pujol, M.J., 2010. Nuclear translocation of glyceraldehyde-3-phosphate dehydrogenase is regulated by acetylation. *Int. J. Biochem. Cell Biol.* 42, 1672–1680. <https://doi.org/10.1016/j.biocel.2010.06.014>
- Verhaak, R.G.W., Hoadley, K.A., Purdom, E., Wang, V., Qi, Y., Wilkerson, M.D., Miller, C.R., Ding, L., Golub, T., Mesirov, J.P., Alexe, G., Lawrence, M., O’Kelly, M., Tamayo, P., Weir, B.A., Gabriel, S., Winckler, W., Gupta, S., Jakkula, L., Feiler, H.S., Hodgson, J.G., James, C.D., Sarkaria, J.N., Brennan, C., Kahn, A., Spellman, P.T., Wilson, R.K., Speed, T.P., Gray, J.W., Meyerson, M., Getz, G., Perou, C.M., Hayes, D.N., Cancer Genome Atlas Research Network, T.C.G.A.R., 2010. Integrated genomic analysis identifies clinically relevant subtypes of glioblastoma characterized by abnormalities in PDGFRA, IDH1,

- EGFR, and NF1. *Cancer Cell* 17, 98–110.
<https://doi.org/10.1016/j.ccr.2009.12.020>
- Verma, M., 2009. Cancer Epidemiology, *Cancer Epidemiology Vol 2 Modifiable Factors*. <https://doi.org/10.1007/978-1-60327-492-0>
- Vilà, M.R., Nicolás, A., Morote, J., de, I., Meseguer, A., 2000. Increased glyceraldehyde-3-phosphate dehydrogenase expression in renal cell carcinoma identified by RNA-based, arbitrarily primed polymerase chain reaction. *Cancer* 89, 152–64.
- Villanueva-Meyer, J.E., Han, S.J., Cha, S., Butowski, N.A., 2017. Early tumor growth between initial resection and radiotherapy of glioblastoma: incidence and impact on clinical outcomes. *J. Neurooncol.* 134, 213–219.
<https://doi.org/10.1007/s11060-017-2511-z>
- Wagih, O., Bader, G.D., 2013. The mutational landscape of phosphorylation signaling in cancer. <https://doi.org/10.1038/srep02651>
- Wang, D., Moothart, D.R., Lowy, D.R., Qian, X., 2013. The expression of glyceraldehyde-3-phosphate dehydrogenase associated cell cycle (GACC) genes correlates with cancer stage and poor survival in patients with solid tumors. *PLoS One* 8, e61262.
<https://doi.org/10.1371/journal.pone.0061262>
- Wang, Q., Hu, B., Hu, X., Kim, H., Squatrito, M., Scarpance, L., deCarvalho, A.C., Lyu, S., Li, P., Li, Y., Barthel, F., Cho, H.J., Lin, Y.-H., Satani, N., Martinez-Ledesma, E., Zheng, S., Chang, E., Sauv  , C.-E.G., Olar, A., Lan, Z.D., Finocchiaro, G., Phillips, J.J., Berger, M.S., Gabrusiewicz, K.R., Wang, G., Eskilsson, E., Hu, J., Mikkelsen, T., DePinho, R.A., Muller, F., Heimberger, A.B., Sulman, E.P., Nam, D.-H., Verhaak, R.G.W., 2017a. Tumor Evolution of Glioma-Intrinsic Gene Expression Subtypes Associates with Immunological Changes in the Microenvironment. *Cancer Cell* 32, 42-56.e6.
<https://doi.org/10.1016/j.ccell.2017.06.003>
- Wang, Q., Hu, B., Hu, X., Kim, H., Squatrito, M., Scarpance, L., deCarvalho, A.C., Lyu, S., Li, P., Li, Y., Barthel, F., Cho, H.J., Lin, Y.H., Satani, N., Martinez-Ledesma,

- E., Zheng, S., Chang, E., Sauv , C.E.G., Olar, A., Lan, Z.D., Finocchiaro, G., Phillips, J.J., Berger, M.S., Gabrusiewicz, K.R., Wang, G., Eskilsson, E., Hu, J., Mikkelsen, T., DePinho, R.A., Muller, F., Heimberger, A.B., Sulman, E.P., Nam, D.H., Verhaak, R.G.W., 2017b. Tumor Evolution of Glioma-Intrinsic Gene Expression Subtypes Associates with Immunological Changes in the Microenvironment. *Cancer Cell* 32, 42-56.e6.
<https://doi.org/10.1016/j.ccell.2017.06.003>
- Wang, S., Tan, X., Yang, B., Yin, B., Yuan, J., Qiang, B., Peng, X., 2012. The role of protein arginine-methyltransferase 1 in gliomagenesis. *BMB Rep.* 45, 470–475. <https://doi.org/10.5483/BMBRep.2012.45.8.022>
- Wang, Y., Sun, Z., Szyf, M., 2017. S-adenosyl-methionine (SAM) alters the transcriptome and methylome and specifically blocks growth and invasiveness of liver cancer cells 8, 111866–111881.
- Warburg, O., 1956. On the Origin of Cancer Cells. *Science* (80-.).
<https://doi.org/10.2307/1750066>
- Weir, D.G., Molloy, A.M., Keating, J.N., Young, P.B., Kennedy, S., Kennedy, D.G., Scott, J.M., 1992. Correlation of the ratio of S-adenosyl-L-methionine to S-adenosyl-L-homocysteine in the brain and cerebrospinal fluid of the pig: implications for the determination of this methylation ratio in human brain. *Clin. Sci. (Lond)*. 82, 93–7. <https://doi.org/10.1042/CS0820093>
- Wilhelm, M., Schlegl, J., Hahne, H., Gholami, A.M., Lieberenz, M., Savitski, M.M., Ziegler, E., Butzmann, L., Gessulat, S., Marx, H., Mathieson, T., Lemeer, S., Schnatbaum, K., Reimer, U., Wenschuh, H., Mollenhauer, M., Slotta-Huspenina, J., Boese, J.-H., Bantscheff, M., Gerstmair, A., Faerber, F., Kuster, B., 2014. Mass-spectrometry-based draft of the human proteome. *Nature* 509, 582–587. <https://doi.org/10.1038/nature13319>
- Witsch, E., Sela, M., Yarden, Y., 2010. Roles for Growth Factors in Cancer Progression. *Physiology* 25, 85–101.
<https://doi.org/10.1152/physiol.00045.2009>
- Wu, X., Han, L., Zhang, X., Li, L., Jiang, C., Qiu, Y., Huang, R., Xie, B., Lin, Z., Ren, J.,

- Fu, J., 2012. Alteration of endocannabinoid system in human gliomas. *J. Neurochem.* 120, 842–849. <https://doi.org/10.1111/j.1471-4159.2011.07625.x>
- Wüllner, U., Kaut, O., deBoni, L., Piston, D., Schmitt, I., 2016. DNA methylation in Parkinson's disease. *J. Neurochem.* 139, 108–120. <https://doi.org/10.1111/jnc.13646>
- Yang, P., Zhang, W., Wang, Y., Peng, X., Chen, B., Qiu, X., Li, G., Li, S., Wu, C., Yao, K., Li, W., Yan, W., Li, J., You, Y., Chen, C.C., Jiang, T., 2015. IDH mutation and MGMT promoter methylation in glioblastoma: results of a prospective registry. *Oncotarget* 6, 40896–906. <https://doi.org/10.18632/oncotarget.5683>
- Yang, W., Liu, Y., Gao, R., Yu, H., Sun, T., 2018. HDAC6 inhibition induces glioma stem cells differentiation and enhances cellular radiation sensitivity through the SHH/Gli1 signaling pathway. *Cancer Lett.* 415, 164–176. <https://doi.org/10.1016/j.canlet.2017.12.005>
- Young, A.L., Carter, W.G., Doyle, H.A., Mamula, M.J., Aswad, D.W., 2001. Structural Integrity of Histone H2B in Vivo Requires the Activity of Protein L-Isoaspartate O-Methyltransferase, a Putative Protein Repair Enzyme. *J. Biol. Chem.* 276, 37161–37165. <https://doi.org/10.1074/jbc.M106682200>
- Zhang, D., Shen, H., Chang, C., Su, H., Zhang, D., Wang, Y., Shen, Q., Liu, B., Huang, R., Zhou, T., 2015. AMPK-Dependent Phosphorylation of GAPDH Triggers Sirt1 Activation and Is Necessary for Autophagy upon Glucose Starvation Article AMPK-Dependent Phosphorylation of GAPDH Triggers Sirt1 Activation and Is Necessary for Autophagy upon Glucose Starvation. *Mol. Cell* 60, 930–940. <https://doi.org/10.1016/j.molcel.2015.10.037>
- Zhang, J., Zhang, F., Hong, C., Giuliano, A.E., Cui, X., Zhou, G., 2015. Critical protein GAPDH and its regulatory mechanisms in cancer cells. *Cancer Biol Med* 12, 10–22. <https://doi.org/10.7497/j.issn.2095-3941.2014.0019>
- Zhao, Y.-H., Wang, Z.-F., Cao, C.-J., Weng, H., Xu, C.-S., Li, K., Li, J.-L., Lan, J., Zeng, X.-T., Li, Z.-Q., 2018. The Clinical Significance of O6-Methylguanine-DNA

Methyltransferase Promoter Methylation Status in Adult Patients With Glioblastoma: A Meta-analysis. *Front. Neurol.* 9, 127.
<https://doi.org/10.3389/fneur.2018.00127>

Zheng, H., Ying, H., Yan, H., Kimmelman, A.C., Hiller, D.J., Chen, A.-J., Perry, S.R., Tonon, G., Chu, G.C., Ding, Z., Stommel, J.M., Dunn, K.L., Wiedemeyer, R., You, M.J., Brennan, C., Wang, Y.A., Ligon, K.L., Wong, W.H., Chin, L., DePinho, R.A., 2008. p53 and Pten control neural and glioma stem/progenitor cell renewal and differentiation. *Nature* 455, 1129–33.
<https://doi.org/10.1038/nature07443>

Zheng, J., 2012. Energy metabolism of cancer: Glycolysis versus oxidative phosphorylation (Review). *Oncol. Lett.* 4, 1151–1157.
<https://doi.org/10.3892/ol.2012.928>

Zhou, Y., Wu, S., Liang, C., Lin, Y., Zou, Y., Li, K., Lu, B., Shu, M., Huang, Y., Zhu, W., Kang, Z., Xu, D., Hu, J., Yan, G., 2015. Transcriptional upregulation of microtubule-associated protein 2 is involved in the protein kinase A-induced decrease in the invasiveness of glioma cells. *Neuro. Oncol.* 17, 1578–1588. <https://doi.org/10.1093/neuonc/nov060>

Ziello, J.E., Jovin, I.S., Huang, Y., 2007. Hypoxia-Inducible Factor (HIF)-1 regulatory pathway and its potential for therapeutic intervention in malignancy and ischemia. *Yale J. Biol. Med.* 80, 51–60.

7 Appendix

| Tissue ID | Tissue weight (g) | Dissected sample weight (g) | Cut by |
|-----------|-------------------|-----------------------------|--------|
| 29.1 | 0.2 | 0.05 | AK |
| 29.2 | 0.16 | 0.04 | AK |
| 29.3 | 0.12 | 0.04 | AK |
| 29.4 | 0.25 | 0.03 | AK |
| 29.5 | 0.07 | 0.02 | AK |
| 38.1 | 0.36 | 0.05 | AK |
| 38.2 | 0.43 | 0.06 | AK |
| 38.3 | 0.38 | 0.06 | AK |
| 38.4 | 0.57 | 0.05 | AK |
| 38.5 | 0.59 | 0.05 | AK |
| 39.1 | 0.11 | 0.05 | AK |
| 39.2 | 0.23 | 0.05 | AK |
| 39.3 | 0.32 | 0.06 | AK |
| 39.4 | 0.49 | 0.08 | AK |
| 39.5 | 0.38 | 0.06 | AK |
| 40.1 | 0.22 | 0.05 | AK |
| 40.2 | 0.21 | 0.06 | AK |
| 40.3 | 0.23 | 0.05 | AK |
| 40.4 | 0.41 | 0.06 | AK |
| 40.5 | 0.52 | 0.07 | AK |
| 58.1 | 1.29 | 0.05 | MD |
| 58.2 | 0.93 | 0.06 | MD |
| 58.3 | 1.01 | 0.07 | MD/AK |
| 58.3 (2) | 1.14 | 0.06 | AK |
| 58.4 | 1.35 | 0.05 | AK |
| 58.5 | 0.65 | 0.07 | AK |

Table 7-1/ Showing amount of dissected tissue acquired from CBTRC and how much was taken for experiments performed in this study.

Table 7-1 is showing the amount of tissue dissected described in Section 2.2. Weighted GBM tissue has been cut to approx. 50mg and remainder has been stored for future experiments.

| Sample ID. | Cellular Fraction (conc. mg/ml) | | |
|------------|---------------------------------|--------------|--------------|
| | Membrane | Cytosol | Nuclear |
| 38.1 | 6.307 | 3.461 | 7.992 |
| 38.2 | 5.926 | 3.733 | 8.831 |
| 38.3 | 7.143 | 3.880 | 8.176 |
| 38.4 | 6.067 | 3.572 | 8.031 |
| 38.5 | 6.387 | 3.641 | 7.865 |
| | | | |
| 39.1 | 6.201 | 4.053 | 6.696 |
| 39.2 | 5.820 | 4.020 | 6.433 |
| 39.3 | 6.238 | 4.363 | 6.606 |
| 39.4 | 6.528 | 4.562 | 7.357 |
| 39.5 | 6.458 | 3.840 | 7.248 |
| | | | |
| 40.1 | 6.953 | 3.846 | 6.654 |
| 40.2 | 6.303 | 3.809 | 7.519 |
| 40.3 | 6.480 | 3.869 | 6.834 |
| 40.4 | 7.278 | 4.054 | 7.198 |
| 40.5 | 6.849 | 3.313 | 8.160 |
| | | | |
| 58.1 | 5.730 | 4.978 | 5.666 |
| 58.2 | 6.051 | 5.673 | 5.892 |
| 58.3 | 5.743 | 5.381 | 5.258 |
| 58.4 | 5.760 | 5.565 | 5.904 |
| 58.5 | 6.042 | 5.958 | 7.019 |
| | | | |
| CTRL1 | 5.354 | 3.729 | 7.757 |
| CTRL2 | 6.101 | 3.799 | 7.596 |
| CTRL3 | 4.857 | 3.817 | 6.830 |
| CTRL4 | 5.923 | 3.852 | 7.021 |

Table 7-2| Protein quantification of each sample and their fractionated protein content. Results obtained from modified Lowry protein quantification.

Quantification of all samples using a modified Lowry method described in section 2.5. Samples have been quantified for all fractions including cytosolic, nuclear and membrane fractions and values from Table 7-2 were used for all experiments.